ABSTRACT

Zhou, Wei. Application of Affinity Chromatography Combined with Capillary Electrophoresis or Mass Spectrometry in the Biochemical Analysis. (Under the direction of Dr. Morteza G. Khaledi.)

The focus of the research has been to develop combined techniques, such as affinity chromatography combined with capillary electrophoresis or mass spectrometry, for the structural analysis of biologically important proteins. In the first part of the research, a method that allows the direct analysis the peptides affinity-bound to the immobilized metal ion media by matrix assisted laser desorption/ionization mass spectrometry (MALDI/MS) has been developed and applied to detect sequence errors of recombinant proteins occuring at the N-terminus and to locate phosphorylation sites in proteins. This method allows the fast identification of two recombinant proteins with expression errors, one is proteins p24, a major capsid protein of human immunodeficiency virus (HIV), the other is Vif, a viral infectivity factor required for the efficient transmission of free virus. Phsophorylation sites on proteins p53 and p21 that are involved in determining cellular response to DNA damage are also detected using this method. Huge gain in terms of selectivity, sensitivity and structural information are achieved with minimal sample consumption.

In the second part of the research, affinity capillary electrophoresis (ACE) has been applied to evaluate biomolecular interactions, such as protein-drug and

antibody-antigen interactions, and to better understand the interaction. ACE with laser induced fluorescence detection (LIF) is used to systematically evaluate binding between phosphorothioate oligodeoxynucleotides (Sd, potential anti-HIV drugs) and viral envelope glycoprotein HIV-1 gp120. The results show that the interaction has a strong dependence on the sulfur phosphorothioate backbone. Chain length and the sequence of Sd also affect the ability of binding to gp120. The results may provide useful information to clinical trial. ACE is also used to examine the effect of each residue of the epitope of HIV-1 capsid protein p24 on their affinity to an anti-p24 monoclonal antibody. Each amino acid within epitope is successively substituted by alanine, and the effect of the substitutes on their affinity for the antibody is examined by ACE. We are able to determine the relative importance of each amino acid within the epitope to the binding affinity of the peptide. The results provide a better understanding of these interactions. High separation power and ease of automation of ACE offer an effective and rapid means to study of these types of biological interaction.

Application of Affinity Chromatography Combined with Capillary Electrophoresis or Mass Spectrometry in the Biochemical Analysis

By

Wei Zhou

A dissertation submitted to the Graduate Faculty of North Carolina State University in partial fulfillment of the requirement for the Degree of Doctor of Philosophy in Chemistry

Department of Chemistry

Raleigh

2000

Approved by:

Charles B. Boss	Edmond F. Bowden
Bill Switzer	Kenneth B. Tomer

Morteza G. Khaledi, Chair of Advisory Committee

Dedicated to my husband and parents for their love and support.

Biography

The author was born in Jinan, P. R. China on October 7, 1969. She received her B.S. in Chemistry from the Shandong Teachers' University in 1991. Then she went to the Beijing Institute of Technology where she obtained her M.S. in Chemical Engineering in 1994. With the thirst for knowledge and the passion for adventure, she went to the United States to further her education. Shortly after she went to the University of Kansas in 1994, she married Mr. Yu Cui and transferred to the North Carolina State University in 1995 to be with her husband. She majored in Analytical Chemistry under the direction of Professor Morteza G. Khaledi. During her Ph.D. study, she also worked as a Guest Researcher at the National Institute of Environmental Health Science/National Institutes of Health under the direction of Dr. Kenneth B. Tomer.

Acknowledgements

First, I would like to acknowledge my advisors Dr. Morteza G. Khaledi and Dr. Kenneth B. Tomer for their guidance, encouragement and inspiration throughout my years of study. My training under these two great scientists is not only invaluable to my career, but also gives me confidence and courage to take on any scientific challenges. I would like to extend my acknowledgement to everyone in my advisory committee, for their constructive advice and helpful discussions. In addition, I would also like to thank the members of both research groups, present and past, for their helps and friendship, especially Dr. Leesa J. Deterding, Dr. Xiaohong Qian, Dr. Xuegong Zhu, Dr. Christopher Borchers, Dr. B. Alexander Merrick and Ms. Jocelyn Mckeon.

I wish to reserve the second paragraph of this acknowledgement to my family, although my gratitude to them is far beyond any language can reach. I would like to thank my parents for their unconditional support, emotional and financial. Finally, I would like to thank my husband for his love, his steadfast support and for being resourceful whenever I need his help. I cannot get even close to where I am without him.

Table of Contents

List of Tables

Page

List of Figures

Page

Chapter 3

Chapter 4

Chapter 5

Chapter 6

Appendix

Chapter 1

INTRODUCTION

Background and Significance of the Research

A thorough understanding of diseases on a molecular basis will help to elucidate the cause and progression of diseases, and thus, provides useful information for diagnosis and treatment of patients. Due to the extreme complexity of many biological samples, a method which provides high sensitivity and selectivity, great resolving power, rapid analysis and increased structural information is necessary for significant progress in biomedical analysis.

Over the years, affinity techniques have occupied a unique place in bioanalytical application [1,2]. Affinity based methods allow purification of biomolecules on the basis of their biological function or individual structure. Since the techniques became routinely available more than thirty years ago [2], their applications have developed rapidly. Separations that are time-consuming, difficult, or even impossible using other techniques, can be readily achieved using affinity techniques. Most useful and powerful areas of application include: (1) isolation and purification of target macromolecules; (2) capture and detection of molecules of interest for analytical purposes; and (3) selective removal of undesirable contaminants from process stream.

Affinity methods are also easily combined with a variety of other techniques, such as mass spectrometry (MS) or capillary electrophoresis (CE), to further characterize the structure or biochemical functions of the molecule. Huge gain in terms of selectivity, sensitivity and structural information can be realized. The focus of this research is, therefore, to develop combined techniques for the analysis of biologically important proteins, including human immunodeficiency virus (HIV) related proteins, such as the viral envelope glycoprotein gp120, viral capsid protein p24 and proteins involved in determining cellular response to DNA damage, such as whether the cell undergo apoptosis or repair, such as p53 and p21.

1. Matrix Assisted Laser Desorption/Ionization Mass Spectrometry

In the past decade, matrix assisted laser desorption/ionization mass spectrometry (MALDI/MS) has developed substantially as an analytical tool [3-6]. The major advantages of this technique include: generation of unfragmented protonated molecules; the ability to accurately determine the molecular weight of proteins up to and exceeding 100 kDa; detection limits at the low-picomole level; and its compatibility with a variety of commonly used biological salts and buffers.

(1) MALDI/MS Instrumentation

In the late 1980s, it was discovered that desorption/ionization of large, nonvolatile molecules, such as proteins, can be obtained when samples are light irradiated after being co-deposited with a large molar excess of an energy-

absorbing “matrix” material. Absorption of energy by the matrix initiates a phase change of the analyte from a solid to a gas while also inducing preformed ions, even if the analyte does not strongly absorb at the wavelength of the laser radiation. Nitrogen (337 nm) and Nd-YAG (355 nm) lasers have frequently been used as the irradiation sources. Despite a lack of an established ionization mechanism, the dependence on the matrix material in the desorption/ionization process gave rise to the terminology matrix assisted laser desorption/ionization (MALDI).

Among hundreds of different organic compounds that absorb light at the commonly employed laser wavelengths (337 or 355 nm), only a few are widely applicable, examples are α-cyano-4-hydroxycinnamic acid, sinapinic and 2,5-dihydroxybenzonic acid [7-9]. The effect of the matrix composition is not the same for different classes of macromolecules. Changing the matrix or including a matrix additive can often yield better results if when signals are detected using the initial sample-matrix combination [10].

The mass analyzer used for MALDI is the time-of-flight (TOF) analyzer [11-13]. TOF is characterized by a nearly unlimited mass range and by high sensitivity. Additional advantages of TOF are its simplicity and low cost. However, until the recent development of delayed extraction technology, TOF/MS has been characterized by the low mass resolution. This has limited its ability to detect certain protein modification or sequence variations, especially at

higher masses. In spite of this, the molecular mass of peptides and proteins in the mass range of 1 to 40 kDa can be routinely determined with an accuracy of 0.1% (and as low as 0.01%).

A schematic diagram of a MALDI/TOF/MS is shown in Figure 1-1 [5]. The laser beam is focused onto the sample target to induce ionization. The ions formed are accelerated by the electric field in the ion source through the flight tube toward the detector. The time required for ions to travel through the flight tube depends on their masses and is described by the equation:

$$TOF=L/v=L(m/2zeV)^{1/2}$$

where L is the length of the flight tube, v is the ion velocity, m is the mass of the ion, z is the charge state of the ion, and V is the acceleration potential. Thus, low mass ions have a shorter flight time than heavier ions. The laser pulse also triggers the clock in the transient recorder that measures the time-of-flight for the different ions. Time-to-mass conversion is achieved by incorporating the TOF of ions of known mass (from internal or external standards) into a calibration file from which mass value of unknown ions can be calculated.

(2) Applications of MALDI/MS

A. Characterization of Recombinant Proteins with His-tag

In addition to molecular weight determination, MALDI/MS is also used intensively to obtain more structural information from proteins [14-20]. MALDI/MS has been used to rapidly map the mass of protein digests for sequence

confirmation, often without requiring peptide fractionation [14-15]. Using a combination of chemical and enzymatic reactions of the analyte prior to MALDI/MS analysis, posttranslational modifications, such as phosphorylation and glycosylation can also be identified and localized [16-20].

Among several different approaches for the direct sequencing of peptides and proteins of unknown structure, affinity chromatography (AC) coupled to MALDI/MS for the isolation and detection of specific molecules from complex biological matrices has been developed rapidly in the past few years [21,22]. The high specificity of AC combined with the advantages provided by MS, such as rapid analysis, high sensitivity and structural information, makes this hyperated technique very attractive in protein structural analysis. Analytes have been analyzed directly from affinity media using MALDI/MS to obtain accurate molecular weight information [23]. Consecutive enzymatic reactions have been carried out on the analytes affinity-bound to immobilized antibodies with subsequent direct analysis of the products by MALDI//MS for accurate amino acid sequencing of an epitope. This method has been applied to the determination of epitopes on large proteins, such as HIV-1 p26 and HIV-1 gp120 [24-26].

Introduced by Porath, et al. [27], immobilized metal ion affinity chromatography (IMAC) is an affinity technique that takes advantage of the specific interaction between an analyte and an immobilized metal ion.

Immobilized metal ions, such as Ni^{2+}, Co^{2+}, Zn^{2+}, or Mn^{2+}, have been shown to bind proteins containing adjacent histidine residues [28-30]. IMAC has been used extensively in the purification of recombinant proteins in which a histidine affinity tag (His-tag, MRGSHHHHHHGS) is incorporated into the expression system [31,32]. One problem encountered, however, in protein expression systems is incorrect expression of the desired protein [33,34]. It has been reported that a small elongation or deletion of up to three N-terminal amino acids can dramatically change the binding properties of the protein, possibly affecting the biological and/or especially therapeutic properties of the recombinant protein [35]. It is, therefore, important to verify the sequence of expressed proteins to assure the quality of production. Due to the similarity in physical characteristics between the intact and error proteins, however, they can not be easily detected or separated using standard purification techniques. Development of an effective and convenient method that combines the high specificity of IMAC with the increased structural information provided by MALDI/MS to confirm the sequence of recombinant proteins is highly desired.

B. Identification of Phosphorylation Sites

Protein phosphorylation has become a focus of attention in cell biology and biochemical sciences because it plays a central role in signaling pathways by providing a means for transducting extracellular signals and coordinating intracellular events. It is involved in major regulatory pathways for gene expression, protein synthesis, and/or cell growth, division, differentiation and

death [36-38]. In order to better understand the molecular basis of these regulatory pathway, it is necessary to identify phosphorylation sites.

Protein phosphorylation is catalyzed by a class of enzymes called protein kinases, while removal of phosphates is controlled by specific phosphatases [39,40]. Typical phosphorylation acceptors are mainly serine, threonine, and tyrosine residues. There is no simple sequence motif for the occurrence of protein phosphorylation, though charged amino acids are frequently found near the phosphorylation sites. Therefore, there is no simple way to predict phosphorylation sites on proteins.

A number of techniques have been used to identify phosphorylation sites on proteins [40]. The detection of protein phosphorylation is facilitated by the incorporation of radioactive [^{32}P] phosphate into the target protein, with the labeled phosphoproteins being separated and detected by gel electrophoresis [41-43]. An alternative to radiolabeling is immunoblotting. Antibodies have been used to immunoblot phosphoproteins that contain serine, threonine, and tyrosine as part of the recognition epitopes [44-45]. Identification of phosphorylation sites often employs reversed-phase high performance liquid chromatography (rp-HPLC), gel electrophoresis, and Edman sequencing [41,42]. Identification of phosphorylation sites by conventional methods, however, is often difficult for several reasons, such as the instability of the phosphoamino acids under the Edman degradation conditions, and steric hindrance within the recognition site.

Mass spectrometry has proven to be very useful in mapping posttranslational modifications of proteins [16-20]. In the MS analysis of protein digests, however, components can not always be detected due either to suppression effects or to low ionization efficiency [10,46,47]. The suppression effect means that the existence of one or more ions can suppress the signal of other ions due either to dynamic range or to difference in ionization efficiency. The ionization efficiency is particularly problematic when phosphopeptides are present, because phosphorylated peptides usually exhibit low response in MS in the positive ion mode due to the negative charges associated with phosphate group. The negative charge interference in detection becomes even worse when multiple phosphate groups are clustered in one peptide. In order to reduce suppression effects and to enhance the detectability of these components, the digests can be subjected to HPLC separation prior to MS analysis. The HPLC separation, however, is laborious, and the loss of sample during the HPLC separation makes the analysis of phosphoproteins present in cells at very low concentrations more difficult.

Immobilized metal ions, such as Fe^{3+}, Ga^{3+} and Al^{3+} have been known to bind phosphoproteins and phosphopeptides with high specificity [48-50]. The use of immobilized metal ion affinity chromatography (IMAC) to isolate peptides of interest from mixture has been shown to be useful in structural studies of phosphoproteins. By enriching phosphopeptides using metal ions before MS

analysis, suppression effects are greatly reduced. This technique has been used successfully with both on-line and off-line coupling to MS analysis [23,51-55]. Most of the applications reported so far have involved the elution of the phosphopeptides from the metal ion column before MS analysis. As a result, loss of sample during the elution procedure can hinder the MS detection of low level phospopeptides. In addition, the problem of low sensitivity of phoshopeptides in MS detection should be addressed. It is necessary, therefore, to develop a method that minimizes the interference of the phosphate group on MS detection and enables direct analysis of phosphopeptides from the protein digest with minimum sample loss.

2. Affinity Capillary Electrophoresis

The popularity of capillary electrophoresis (CE) has expanded tremendously in the past few years. The major advantages of CE include high efficiency, ease of automation, short analysis time and low sample consumption. In addition, the flexibility of incorporating various separation mechanisms has greatly expanded the scope of application of this technique to a variety of compounds, from small molecules to very large proteins [56-58].

(1) Instrumentation of CE-LIF

Since its introduction in 1981 [59], CE has undergone phenomenal growth. In CE separation, a capillary is filled with buffer. The sample is introduced into the capillary by either hydrodynamic injection or by electrokinetic injection. After

the introduction of the sample, a high voltage is applied along the capillary. As a result, electroosmotic flow (EOF) moves both solvent and solutes to the detection window. Solutes are separated based on their differences in charge to size ratios.

The use of CE is widespread, in part, because of the ease of coupling to various detectors. The most commonly used detectors are UV-VIS, MS, and electrochemistry [60,61]. Laser-induced fluorescence detection (LIF) is a detection technique that offers high sensitivity, with detection limits in the range of attomoles to zeptomoles [62,63]. Even single molecule detection is possible with CE-LIF [64]. Following the pioneering CE-LIF work of Zare [65], a number of studies have been reported due to the availability of a wide variety of fluorescent tags and lasers [62,63]. A typical experimental set up is shown in Figure 1-2. A laser beam is focused by a pair of mirrors. It travels through a chopper that is also connected with a lock-in-amplifier to filter the noise from the signal. The modulated light then enters the microscope which focuses the light onto the capillary detection window. The excitation and emission light travels through a series of filters before entering the current-to-voltage preamplifier and lock-in-amplifier. The output of the signal is recorded by computer [62].

(2) Applications of ACE-LIF

A. Determination of Protein-Drug Binding Constants

The characterization of binding constants is essential for the understanding of biomolecular interactions. Over the years, numerous methods have been developed to qualitatively and quantitatively evaluate molecular association, including spectroscopy, separations, calorimetry and potentiometry [66,67]. In the past few years, the popularity of affinity capillary electrophoresis (ACE) as a powerful probe for molecular interactions has expanded tremendously [68-71]. The criteria that need to be met for the application of ACE to the study of biomolecular interaction are as follows. First, unbound molecules must have mobilities that differ from the complex. Second, one of the reactants must be detectable and quantifiable. In cases where the binding constants are greater than 10^6 M^{-1}, a highly sensitive detection technique, such as LIF can be used to obtain accurate measurements. Binding constants derived from ACE studies reflect the native interactions between molecules because complications related to phase-dependent behavior, such as the bioactivity changes caused by the covalent immobilization of protein, are minimized. Furthermore, the relative ease of automation and the potential for array detection enables simultaneous analysis of the affinity of a large number of compounds for a specific molecule, thus, making it a promising tool for screening large combinatorial libraries [72].

Despite reports of studies on the interaction between HIV viral envelope glycoprotein gp120 and phosphorothioate oligonucleotides, which are potential anti-HIV drugs, using traditional biological binding assays [73-75], accurate measurements of binding constants between gp120 and phosphorothioate

oligonucleotides have not been reported. In addition, research conducted so far requires either radiolabeling or covalent immobilization of the protein. Besides being tedious, conformational changes of the protein caused by immobilization of the protein can lead to inaccurate results. Development of a rapid and accurate technique, such as ACE with LIF detection, to further probe the binding between potential anti-HIV drugs and gp120, therefore, can provide useful information for potential clinical trials.

B. Evaluation of Antibody-antigen Interactions

ACE can also be used as an alternative to immunoassay for studies of antibody-antigen interactions [76,77]. Proteins present the most abundant and diverse class of antigens, and anti-protein antibodies are everyday tools in biochemical research. The regions of proteins to which antibodies binds are called antigenic determinants or epitopes. Defining the structure of epitopes is important in the development of vaccines as well as in furthering our basic understanding of how antibodies and antigens interact.

Over the years, epitopes have been analyzed using a variety of experimental techniques, including X-ray crystallography, nuclear magnetic resonance spectroscopy (NMR), site directed mutagenesis, proteolytic footprinting combined with mass spectrometry (MS), and rapid screening of the cross-reactivity of synthetic peptides from combinatorial libraries with anti-protein antibodies [79-81]. ACE has also recently been used to investigate the fine

structure of epitopes [78]. Although ACE has a number of inherent advantages for studying monoclonal antibody and antigen interactions, experimentally, ACE faces many challenges. Among them is adsorption of analytes onto the capillary wall, which has been a notorious problem for CE analyses in general. The use of buffers extremes pHs (pH<4 or pH>9) to suppress solute adsorption might not be applicable in many cases, because such conditions can affect the formation and stability of antigen-antibody complexes. The use of coated capillaries or buffer additives may be necessary to minimize adsorption [82]. However, these separation conditions may not work equally well for all cases. The other major concern is that the determination of antibody-antigen interactions is based on the measurement of changes in either the peak area or the mobility of antibody. The separation of bound from unbound antibody, however, is not trivial. The poor separation often observed can be attributed to the fact that binding of the antigen to its antibody does not always significantly alter the electrophoretic mobility of the complexed antibody due to the size of antibody.

In spite of these difficulties, ACE has been used for the study of a number of antigen-antibody interactions [76-78]. Electrophoretic separation conditions are carefully chosen to achieve satisfactory performance. For example, ACE has been used to investigate the epitope on the HIV capsid protein p24 recognized by a monoclonal antibody. In this study, the affinity of a series of peptides with N- and C-terminal truncations of the previously determined epitope sequence was studied by ACE [78]. The experiments showed that the antibody recognized an

eleven amino acid peptide with highest affinity. Further evaluating of the relative contribution of each amino acid side chain in the epitope to its binding with the antibody may provide a better understanding of these interactions.

Human Immunodeficiency Virus (HIVs) and Cancer Related Proteins

During the past decade, the discovery of the human immunodeficiency virus (HIV) triggered the detailed study of its structure, replication and pathogenic properties [83]. Understanding the biological interactions of the virus will give new insights and will lead to many new opportunities for antiviral intervention. Among different strains of the virus, HIV-1 is probably the most intensely studied virus, for which we have very detailed knowledge on a molecular basis [84]. It currently serves as the prototypical retrovirus. The core viral particle is composed of the p24 capsid protein (gag), viral RNA and enzymes, and other proteins that directly regulate viral gene expression, such as a viral infectivity factor protein (Vif). A large glycoprotein, gp160, is found on the surface of the virus and can be cleaved intracellularly into gp120 and gp41.

It is now well known that the entrance of the virus into a cell is initiated by the interaction of the surface glycoprotein gp120 with cellular receptors [85-88]. This interaction leads to conformational changes and membrane fusion between the virus and the target cell. Therefore, drugs designed to block the interaction between the viral envelope glycoprotein and its coreceptors may prevent the progression of the disease. Systematically studies of the binding between

potential anti-HIV drugs and the viral envelope protein gp120, therefore, are of great interest.

Antibodies to the viral capsid protein p24 are among the first antibodies to appear in individuals infected by the HIV [89,90]. The presence of antibodies to this protein is used as a preliminary diagnosis of infection by HIV and as a screen for blood supplies [91,92]. Although a number of epitopes on p24 recognized by various monoclonal antibodies have been reported [93], a thorough investigation of the relative contribution of each amino acid to binding has significant potential application to the improvement of diagnostic approaches and to the generation of prototype vaccines.

Cancer is a heterogeneous disease. An in-depth understanding of its molecular composition will be very important in the treatment of cancer patients. Despite the enormous variation in tumor types, a common feature of cancer is that normal cell proliferation controls are lost at the level of cell signaling, cell-cycle arrest, differentiation, or apoptotic cell death [94]. The analysis of proteins involved in any of these processes, therefore, should help to elucidate the cause and progression of specific tumor type.

Two proliferation control proteins have recently drawn researchers' attention. One is the tumor suppressor protein p53, and the other is the protein p21, a cyclin-kinase inhibitor important in mediating p53-dependent cell-cycle

arrest [95-97]. Protein p53 has been revealed to play a key role in suppressing the development of cancer. Under normal conditions, p53 is usually expressed at low levels due to a short half-life, and this low level of expression does not interfere with cell proliferation. When, however, the cell is exposed to a DNA-damaging agent, such as ultraviolet light, ionizing radiation or certain chemicals, at excessive levels, DNA damage overwhelms the threshold of its repair system, and the level of p53 increases in response to this damage. This increase, in turn, leads to suppression of cell growth or to apoptosis that prevents damaged cells from replicating [98-102]. In other words, p53 plays a possible role in the safeguarding system controlling the integrity of the genome.

The increase in the amount of p53 also results in transcriptional activation of the *p21* gene due to the increase in the sequence-specific DNA-binding activity of activated p53 [103]. As a result, the level of p21 is increased. Studies have also shown the presence of other pathways that increase p21 expression that are totally independent of p53, such as high levels of toxic oxygen species, vitamin D, etc. [104, 105]. Expression of high levels of p21 in response to both p53-dependent and p53 independent signals is believed to mediate cell-cycle arrest and differentiation through inhibition of cyclin-dependent kinases (Cdks), a group of kinases that control cell cycle progression. Though the exact function remains to be elucidated, a suggested mechanism for the cellular decision to arrest or die is related to the ratio of p53:p21 protein levels [95, 106-108].

Given the fact that p53 and p21 are phosphoproteins and that the modification of proteins through phosphorylation is believed to be an important means of regulation for many proteins, studying phosphorylation sites on p53 and p21 is important in understanding the biological activity of the protein.

Research Objective

The goal of this research is to develop and to apply affinity techniques combined with mass spectrometry and capillary electrophoresis for biochemical analysis. A method that is effective and convenient for detecting protein sequence errors occuring at the N-terminus with minimal sample manipulation has been developed. It combines IMAC with MALDI/MS. Recombinant proteins were first isolated by IMAC. Direct analysis of recombinant proteins affinity-bound to the IMAC media by MALDI/MS provides accurate molecular weight information. Consecutive enzymatic reactions could be carried out on the affinity-bound analytes. Subsequent direct analysis of the products by MALDI/MS could further accurately define the amino acid sequences of the bound peptides, thus, providing a rapid and powerful means of confirming the sequence of recombinant proteins. The application of this method to the analysis of HIV related recombinant proteins, such as p24 and vif $_{IIIB,}$ is addressed in chapter 2.

We also have developed a method that allows the direct analysis of phosphopeptides affinity-bound to the IMAC media. As shown in Figure 1-3, agarose loaded with either Fe^{3+} or Ga^{3+} can be used to isolate phosphopeptides

from a protein digest. The affinity-bound phosphopeptides are then analyzed directly by MALDI/MS. Consecutive enzymatic digestion was performed to locate phosphorylation sites on the bound phosphopeptides. IMAC combined with MALDI/MS enables the direct analysis of phosphopeptides from the protein digest without any HPLC separation. Furthermore, this method allows the detection of phosphopeptides with multiple phosphate groups. The significance of this method and its application to the analysis of cancer related phosphoproteins, such as p53 and p21, is the focus of chapters 3 and 4.

Affinity capillary electrophoresis has been applied in the evaluation of biomolecular interactions, such as protein-drug and antibody-antigen interactions. The high separation power, small sample consumption, short analysis time and the ability to analyze the interactions of proteins in their native states make this method very attractive. The results obtained in chapters 5 and 6 provide information that may be useful in clinical trials.

REFERENCES:

1. Hermanson, G. T., Mallia A. K., Smith P. K. in Immobilized Affinity Ligand Techniques, pp.317-417, Academic Press, San Diego, **1992**.
2. Axen, R., Porath, J., Ernback, S. Chemical Couple of Peptides and Proteins to Polysaccharides by Means of Cyanogen Halides. *Nature*, **1967,** *214,* 1302-1304.
3. Karas, M., Bahr, U., Giessman, U. Matrix-assisted Laser Desorption Ionization Mass Spectrometry*. Mass Spectrom. Rev*., **1991,***10*, 359-451.
4. Hillenkamp, F., Karas, M., Beavis, R. C., Chait, B. T. Matrix-assisted Laser Desorption/Ionization Mass Spectrometry of Biopolymers*. Anal. Chem*., **1991,** *63*, 1193A-1203A.
5. Zaluzec, E. J., Gage, D. A., Watson, J. T. Matrix-assisted Laser Desorption Ionization Mass Spectrometry: Application in Peptide and Protein Characterization. *Protein Expression Purif*., **1995,***6*, 109-123.
6. Nelson, R. W. The Use of Bioreactive Probes in Protein Characterization. *Mass Spectrom. Rev*., **1997**, *16,* 353-376.
7. Beavis, R. C., Chait, B. T. Cinnamic Acid Derivatives as Matrices for Ultraviolet Laser Desorption Mass Spectrometry of Proteins. *Rapid Commun. Mass Spectrom*., **1989,** *3*, 432-435.
8. Strupat, K., Karas, M., Hillenkamp, F. 2,5-Dihydroxybenzoic Acid: A New Matrix for Laser Desorption-ionization Mass Spectrometry. *Int. J. Mass Spectrom. Ion Processes,* **1992,** *111,* 89-102.

9. Beavis, R. C., Chaudhary, T., Chait, B. T. α-Cyano-4-hydroxycinnamic Acid as a Matrix for Matrix-assisted Laser Desorption Mass Spectrometry. *Org. Mass Spectrom*., **1992,** *27*, 156-158.
10. Asara, J. M., Allison, J. Enhanced Detection of Phosphopeptides in Matrix-Assisted Laser Desorption/Ionization Mass Spectrometry Using Ammonium Salts. *J. Am. Soc. Mass Spectrom.,* **1999**, *10*, 35-44.
11. Guilhaus, M., Mlynski, V., Selby, D. Perfect Timing: Time-of-flight Mass Spectrometry. *Rapid Commun. in Mass Spectrom.,* **1997,** *11*, 951-962.
12. Cotter, R. J. Time-of-flight Mass Spectrometry for the Structure Analysis of Biological Molecules. *Anal. Chem*., **1992,** *64*, 1027A-1239A.
13. Cotter, R. J. Time-of-flight Mass Spectrometry: An Increasing Role in the Life Sciences. *Biomed. Environ. Mass Spectrom.,* **1989,***18*, 513-532.
14. Thiede, B., Wittmann-Liebold, B., Bienert, M., Krause, E. MALDI-MS for C-terminal Sequence Determination of Peptides and Proteins Degraded by Carboxypeptidase Y and P. *FEBS,* **1995**, *357*, 65-69.
15. Schilling, B. Fragmentation and Sequencing of Cyclic Peptides by Matrix-Assisted Laser Desorption/ionization Post-source Decay Mass Spectrometry. *Rapid Commun. Mass Spectrom.,* **1999**, 13, 2174-2179.
16. Zhang, W., Czernik, A. J., Yungwirth, T., Aebersold, R., Chait, B. T. Matrix-Assisted Laser Desorption Mass Spectrometry Peptide mapping of Proteins Separated by Two-dimensional Gel Electrophoresis: Determination of Phosphorylation in Synapsin I. *Protein Sci.,* **1994,** *3,* 677-686.

17. Annan, R. S., Carr. S. A. Phosphopeptide Analysis by Matrix-assisted Laser Desorption Time-of-flight Mass Spectrometry. *Anal. Chem.,* **1996**, *68*, 3413-3421.

18. Annan, R. S., Carr, S. A. The Essential Role of Mass Spectrometry in Characterizing Protein Structure: Mapping Posttranslational Modifications. *J. Protein Chem.,* **1997**, *16,* 391-402.

19. Qin, J., Chait, T. Identification and Characterization of Posttranslational Modifications of Proteins by MALDI Ion Trap Mass Spectrometry. *Anal. Chem.,* **1997,** *69*, 4002-4009.

20. Wu, J., Gage, D. A., Watson, J. T. A Strategy to Locate Cysteine Residues in Proteins by Specific Chemical Cleavage Followed by Matrix-assisted Laser Desorption/Ionization Time-of-flight Mass Spectrometry. *Anal. Biochem*., **1996,** *235,* 161-174.

21. Nelson, R. W., Krone, J. R., Bieber, A. L., Williams, P. Mass Spectrometric Immunoassay. *Anal. Chem.,* **1995**, *67,* 1153-1158.

22. Liang, X., Lubman, D. M., Rossi, D. T., Nordblom, G. D., Barksdale, C. M. On-probe Immunoaffinity Extraction by Matrix-Assisted Laser Desorption/Ionization Mass Spectrometry. *Anal. Chem.,* **1998**, *70*, 498-503.

23. Papac, D. I., Hoyes, J., Tomer, K. B. Direct Analysis of Affinity-Bound Analytes by MALDI/TOF MS. *Anal. Chem.,* **1994**, *66*, 2609-2613.

24. Parker, C. E., Papac D. I.,Trojak, S. K., Tomer, K. B. Epitope Mapping by Mass Spectrometry. *J. Immun.,* **1996**, *157*, 198-206.

25. Jeyarajah, S., Parker, C. E., Sumner, M. T., Tomer, K. B. Matrix-Assisted Laser Desorption Ionization/Mass Spectrometry Mapping of Human Immunodeficiency Virus-gp120 Epitopes Recognized by a Limited Polyclonal Antibody. *J. Am. Soc. Mass Spectrom.,* **1998**, *9*, 157-165.
26. Papac, D. I., Hoyes, J., Tomer, K. B. Epitope Mapping of the Gastrin-releasing Peptide/anti-bombesin Monoclonal Antibody Complex by Proteolysis Followed by Matrix-Assisted Laser Desorption Ionization Mass spectrometry. *Protein Science,* **1994**, *3*, 1485-1492.
27. Porath, J., Carlsson, J., Olsson, I., Belfrage, G. Metal Chelate Affinity Chromatography, a New Approach to Protein Fractionation. *Nature,* **1975**, *258*, 598-599.
28. Hochuli, E., Bannwaeth, W., Dobeli, H., Gentz, R., Stuber, D. Genetic Approach to Facilitate Purification of Recombinant Proteins with a Novel Metal Chelate Adsorbent. *BiolTechnology.,* **1988**, *6,* 1321-1325.
29. Bharath, M. M., Khadake, J. R., Rao, M. R. Expression of Rat Histone H 1d in *Escherchia coli* and its Purification. *Protein Expression Purif.,* **1998**, *12***,** 38-44.
30. Hutchens, I. W., Nelson, R. W., Li, C. M., Yip, T. T. Synthetic Metal-binding Protein Surface Domains for Metal Ion-dependent Interaction Chromatography. I. Analysis of Bound Metal Ions by Matrix-assisted UV Laser Desorption Time-of-flight Mass Spectrometry. *J. Chromatogr.,* **1992**, *604,* 133-141.

31. Bateson M., Devenish, R. J., Nagley, P., Prescott, M. Entrapment by Immobilized Metal Ion Affinity Chromatography of Assembled Yeast Mitochondrial ATP Synthase Containing Individual Subunits Tagged with Hexahistidine. *Anal. Biochem.,* **1996**, *238,*14-18.
32. Hochuli, E., Dobeli, H., Schacher, A. New Metal Chelate Adsorbent Selective for Proteins and Peptides Containing Neighbouring Histidine Residues. *J. Chromatogr*., **1987,** *411*, 177-184.
33. Kurland C. G., Gallant, J. Errors of Heterologous Protein Expression. *Curr-Opin-Biotechnol*., **1996**, *7*, 489-493.
34. Kurland C. G., Jorgensen, F. Processivity Errors of Gene Expression in *Escherichia coli*. *J. Mol. Biol.,* **1990**, *215*, 511-521.
35. Svoboda, M., Bauhofer, A., Schwind, P., Bade, E., Rasched, I., Przybyski, M. Structural Characterization and Biological activity of Recombinant Human Epidermal Growth Factor Proteins with Different N-terminal Sequences. *Biochimica et biophysica Acta,* **1994**,*1206*, 35-41.
36. Krebs, E. G. The Growth of Research on Protein Phosphorylation. *Trends Biol. Sci.,* **1994,** *19*, 439-439.
37. Posada, J., Cooper, J. A. Molecular Signal Integration: Interplay between Serine, Threonine, and Tyrosine Phosphorylation. *Mol. Biol. Cell*, **1992,** *3*, 583-592.
38. Kemp, B. E. Ed., *Peptides and Protein Phosphorylation*, CRC: Boca Raton, FL, 1990.

39. Hunter, T. Protein Kinases and Phosphatases: the Yin and Yang of Protein Phosphorylation and Signaling. *Cell*, **1995,** *80*, 225-236.

40. Yan, J. X., Packer, N. H., Gooley, A. A., Williams, K. L. Protein Phosphorylation: Technology for the Identification of Phosphoamino Acids. *J. Chromatogr.*, **1998**, *808*, 23-41.

41. Boyle, W. J., Geer, Van der P., Hunter, T. Phosphopeptide Mapping and Phosphoamino Acid Analysis by Two-Dimensional Separation on Thin-Layer Cellulose Plates. *Methods Enzymol*. **1991,** *201*, 110-149.

42. Aebersold, R., Watts, J. D., Morrison, H. D., Bures, E. Determination of the Site of Tyrosine Phosphorylation at the Low Picomole Level by Automated Solid-Phase Sequence Analysis. *Anal. Biochem.*, **1991,** *199*, 51-60.

43. Wettenhall, R. E. H., Aebersold, R., Hood, L. E. Solid-Phase Sequencing of ^{32}P-labeled Phosphopeptides at Picomole and Subpicomole Levels. *Methods Enzymol*., **1991,** *201*, 186-200.

44. Zhao, J. Y., Kuang, J., Adlakha, R. C., Rao, P. N. Threonine Phosphorylation is Associated with Mitosis in Hela Cells. F*EBS Lett.*, **1989,** *249*, 389-395.

45. Abu-lawi, K. I., Sultzer, B. M. Induction of Serine and Threonine Protein Phosphorylation by Endotoxin-Associated Protein in Murine Resident Peritoneal Macrophages. *Infect. Immun*., **1995,** *63*, 498-502.

46. Liao, P. C., Leykam, J., Andrews, P. C., Cage, D. A., Allison, J. An Approach to Locate Phosphorylation Sites in a Phosphoprotein: Mass Mapping by Combining Specific Enzymatic Degradation with Matrix-Assisted Laser Desorption/Ionization Mass Spectrometry. *Anal. Biochem.*, **1994**, *219*, 9-20.

47. Carr, S. A., Huddleston, M. J., Annan, R. S. Selective Detection and Sequencing of Phosphopeptides at the Femtomole Level by Mass Spectrometry. *Anal. Biochem.*, **1996,** *239*, 180-192.

48. Anderrsson, L., Porath, J. Isolation of Phosphoproteins by Immobilized Metal (Fe^{3+}) Affinity Chromatography. *Anal. Biochem.,* **1986,** *154*, 250-254.

49. Muszynska, G., Dobrowolska, G., Medin, A., Ekamn, P., Porath, J. O. Model Studies on Iron (III) Ion Affinity Chromatography II. Interaction of Immobilized Iron (III) Ions with Phosphorylated Amino Acids, Peptides and Proteins. *J. Chromatogr*., **1992,** *604*, 19-28.

50. Posewitz, M., Tempst, P. Immobilized Gallium (III) Affinity Chromatography of Phosphopeptides. *Anal. Chem.,* **1999,** *71,* 2883-2892.

51. Nuwaysir, L. M., Stults, J. T. Electrospray Ionization Mass Spectrometry of Phosphopeptides Isolated by On-Line Immobilized Metal-Ion Affinity Chromatography. *J. Am. Soc. Mass Spectrom.,* **1993,** *4*, 662-669.

52. Michel, H., Hunt, D. F., Shabanowitz, J., Bennett, J. Tandem Mass Spectrometry Reveals that Three Photosystem II Proteins of Spinach Chloroplasts Contain N-Acetyl-O-Phosphothreonine at Their NH_2 Termini. *J. Biol. Chem.,* **1988,** *263*, 1123-1130.

53. Hanger, D. P., Betts, J. C., Loviny, T. L. F., Blackstock, W. P., Anderton, B. H. New Phosphorylation Sites Identified in Hyperphosphorylated Tau (Paired Helical Filament-Tau) from Alzheimer's Disease Brain Using Nanoelectrospray Mass Spectrometry. *J. Neurochem.,* **1998,** *71*, 2465-2476.

54. Neville, D. C. A., Rozanas, C. R., Price, E. M., Gruis, D. B., Verkman, A. S., Townsend, R. R. Evidence for Phosphorylation of Serine 753 in CFTR using a Novel Metal-Ion Affinity Resin and Matrix-Assisted Laser Desorption Mass Spectrometry. *Protein Science*, **1997,** *6*, 2436-2445.

55. Li, S., Dass, C. Iron(III)-immobilized Metal ion Affinity Chromatography and Mass Spectrometry for the Purification and Characterization of Synthetic Phosphopeptides. *Anal. Biochem*., **1999**, *270*, 9-14.

56. Karger, B. L., Chu, Y. H., Foret, F. Capillary Electrophoresis of Proteins and Nucleic Acids. *Annu. Rev. Biophys. Biomol. Struct.,* **1995**, *24,* 579-610.

57. Khaledi, M. G. Characterization of Mixed Micellar Pseudostationary Phases in Electrokinetic Chromatography using Linear Solvation Energy Relationships. *J Chromatogr.,* **1998**, *802*, 35-47.

58. Honda, S. Separation of Neutral Carbohydrates by Capillary Electrophoresis. *J Chromatogr.,* **1996**, *720*, 337-351.

59. Beale, S. Capillary Electrophoresis. *Anal. Chem.,* **1998**, *70*, 279R-300R.

60. Bryant, B. R., Swanek, F. D., Ewing, A. G. in High Performance Capillary Electrophoresis: Theory, Techniques and Applications. pp.355-375, A Wiley-Interscience Publication, **1998**.

61. Tomer, K. B., Deterding, L. J., Parker, C. E. in High Performance Capillary Electrophoresis: Theory, Techniques and Applications. pp.405-449, A Wiley-Interscience Publication, **1998**.

62. Ward, V. L., Khaledi, M. G. Nonaqueous Capillary Electrophoresis with Laser Induced Fluorescence Detection. *J. Chromatogr. B Biomed. Sci. App.,* **1998,** *718,* 15-22.

63. MacTaylor, C. E., Ewing, A. G. Critical Review of Recent Developments in Fluorescence Detection for Capillary Electrophoresis. *Electrophoresis,* **1997,** *18*, 2279-2291.

64. Xian, J., Harrington, M. G., Davidson, E. H. DNA-protein Binding Assays from a Single Sea Urchin Egg: a High Sensitivity Capillary Electrophoresis Method. *Proc. Natl. Acad. Sci., USA*. **1996**, *93 (1)*, 86-90.

65. Gassamann, E., Kuo, J. E., Zare, R. N. Laser Chemical Analysis. *Science,* **1985,** *230*, 813-814.

66. Rose, N. J., Drago, R. S. *J. Amer. Chem. Soc.,* **1959**, *81,* 6138-6141.

67. Gelb, R. I., Schwartz, L. N., Johnson, R. F., Raufer, D. A. *J. Amer. Chem. Soc.,* **1979**, *101,* 1869-1874.

68. Liu, J., Volk, K. J., Lee, M. S., Kens, E. H., Rosenberg, I. E. Affinity Capillary Electrophoresis Applied to the Studies of Interaction of a Number of Heat Shock Protein Family with an Immunosuppressant. *J. Chromatogr.,* **1994**, *680*, 395-403.

69. Rippel, G., Corstjens, H., Billiet, H. A. H., Frank, J. Affinity Capillary Electrophoresis. *Electrophoresis*, **1997**, *18*, 2175-2183.

70. Liu, J., Abid, S., Hail, M. E., Lee, M. S., Hangeland, J., Zein, N. Use of Affinity Capillary Electrophoresis for the Study of Protein and Drug Interaction. *Analyst*, **1998**, *123*, 1455-1459.

71. Rundlett, K. L., Armstrong, D. W. Method for the Estimation of Binding Constants by Capillary Electrophoresis. *Electrophoresis*, **1997**, *18*, 2194-2202.

72. Chu, Y. H., Dunayevskiy, Y. M., Kirby, D. P., Vouros, P., Karger, B. L. Affinity Capillary Electrophoresis-Mass Spectrometry for Screening Combinatorial Libraries. *J. Am. Chem. Soc.,* **1996,** *118,* 7827-7835.

73. Wyatt, J. R., Vickers, T. A., Roberson, J. L., Buckheit, R. W., Jr., Klimkait, T., DeBates, E., Davis, P. W., Rayner, B., Imbach, J. L., Ecker, D. J. Combinatorially Selected Guanosine-Quarter Structure is a Potent Inhibitor of Human Immunodeficiency Virus Envelope-Mediated Cell Fusion. *Proc. Natl. Acad. Sci. USA,* **1994**, *91*, 1356-1360.

74. Lederman, S., Sullivan, G., Benimetskaya, L., Lowy, I., Land, K., Khaled, Z., Cleary, E. M., Yakubov, L., Stein, C. A. Polydeoxyguanine Motifs in a 12-mer Phosphorothioate Oligodeoxynucleotide Augment Binding to the V3 Loop of HIV-1 gp120 and Potency of HIV-1 Inhibition Independently of G-tetrad Formation. *Antisense & Nucleic Acid Drug Development,* **1996**, 6, 281-289.

75. Hotoda, H., Koizumi, M., Koga, R., Kaneko, M., Shimada, K. Biologically Active Oligodeoxyribonucleotides. 5,[1] 5'-End-Substituted d(TGGGAG) Possesses Anti-Human Immunodeficiency Virus Type 1 Activity by Forming a G-Quadruplex Structure. *J. Med. Chem*., **1998**, *41*, 3655-3663.

76. Heegard, N. H. H. Determination of Antigen-Antibody Affinity by Immuno-Capillary Electrophoresis. *J. Chromatogr.,* **1994**, *680*, 405-412.

77. Schmalzing, D., Nashabeh, W. Capillary Electrophoresis Based Immunoassays: a Critical Review. *Electrophoresis*, **1997**, *18*, 2184-2193.

78. Qian, X. H., Tomer, K. B. Affinity Capillary Electrophoresis Investigation of an Epitope on Human Immunodeficiency Virus Recognized by a Monoclonal Antibody. *Electrophoresis*, **1998**, *19*, 415-419.

79. Jemmerson, R., Paterson, Y. Mapping antigenic Sites on Proteins: Implications for the Design of Synthetic Vaccines. *Bio. Techniques*., **1986**, *4,* 18-31.

80. Paterson, J. Mapping Antibody Binding Sites on Protein Antigens. *Nature,* **1992,** *356,* 456-457.

81. Regenmortel, V., M. H. V. The Concept and Operational Definition of Protein Epitopes. *Philos. Trans. R. Soc. Lond. B,* **1989,** *323,* 451-466.

82. El Rassi, Z., Nashabeh, W., in Guzman, N. A. (Ed) Capillary Electrophoresis Technology, Marcel Dekker, Inc., New York, **1993,** 384-434.

83. Gallo, R. AIDS: the Process of Discovery. *Science,* **1997,** 275, 5297-5299.

84. Pavlakis, G. N. Structure and Function of the Human Immunodeficiency Virus Type 1. *Semin. Liver Dis.,* **1992,** *12,* 103-107.

85. McDougal, J. S., Kennedy, M. S., Sligh, J. M., Mawle, S. P., Nicholson, J. K. A. Binding of HTLV-III/LAV to $T4^+$ T Cells by a Complex of the 110K Viral Protein and the T4 Molecule. *Science*, **1985**, *231*, 382-385.

86. Dalgleish, A. G., Beverley, P. C. L., Clapham, P. R., Crawfors, D. H., Greaves, M. R., Weiss, R. A. The CD4 (T4) antigen is Essential Component of the receptor for the AIDS Retrovirus. *Nature*, **1984**, *312*, 763-767.

87. Picard, L., Simmons, G., Power, C. A., Meyer, A., Weiss, R. A., Clapham, P. R. Multiple Extracellular Domains of CCR-5 Contribute to Human Immunodeficiency Virus Type 1 Entry and Fusion. *J. Virol.,* **1997**, *71*, 5003-5011.

88. Feng, Y. C., Broder, C., Kennedy, P. E., Berger, E. HIV-1 Entry Cofactor: Functional cDNA Cloning of a Seven-Transmembrane, G Protein-Coupled Receptor. *Science*, **1996**, *272*, 872-877.

89. Janvier, B., Baillou, A., Archinard, P. Immune Response to a Major Epitope of p24 during HIV-1 Infection., Implication for Diagnosis and Prognosis. *J. Clin. Microbiol.,* **1991**, *29,* 488-492.

90. Gaines, H. Antibody Response in Primary Human Immunodeficiency Virus Infection. *Lancet,* **1987**, *5,* 1249-1253.

91. Weber, B., Fall, E. H., Berger, A., Doerr, H. W. Reduction of Diagnostic Window by New Forth-generation Human Immunodeficiency Virus Screening Assays. *J. Clin. Microbiol.,* **1998**, *36,* 2235-2239.

92. Hashida, S., Hashinaka, K., Ishikawa, S., Ishikawa, E. More Reliable Diagnosis of Infection with Human Immonodeficiency Virus Type 1 (HIV-1) by Detection of Antibody IgGs to Pol and Gag Proteins of HIV-1 and p24 Antigen of HIV-1 in Urine, Saliva, and/or Serum with Highly Sensitive and Specific Enzyme immunoassay: a Review. *J. Clin. Lab Anal*., **1997**, *11,* 267-286.

93. Langedijk, J. P., Schalken, J. J., Tersmette, M., Huisman, J. G., Meloen, R. H. Location of Epitopes on the Major Core Protein p24 of Human Immunodeficiency Virus. *J. Gen. Virol*., **1990,** *71*, 2609-2614.

94. Kernohan, N. M., Cox, L. S. Regulation of Apoptosis by Bc1-2 and its Related Protein: Immunochemical Challenges and Therapeutic Implications. *J. Pathol.,* **1996,** *179*, 1-3.

95. Cox, L. S. Multiple Pathways Control Cell Growth and Transformation: Overlapping and Independent Activities of p53 and p21 $^{Cip1/WAF1/Sdi1}$. *J. Pathol.,* **1997,** *183*, 134-140.

96. Nakayama, K., Nakayama, K. Cip/Kip Cyclin-Dependent Kinase Inhibitors: Brakes of the Cell Cycle Engine During Development. *BioAssay.,* **1998,** *20*, 1020-1029.

97. Giaccia, A. J., Kastan, M. B. The complexity of p53 Modulation: Emerging Patterns from Divergent Signals. *Genes & Dev*., **1998,** *12*, 2973-2983.

98. Lane, D. P., Benchimol, S. p53: Oncogene or Anti-Oncogene? *Genes & Dev*., **1990,** 4, 1-8.

99. Levine, A. J., Momand, J., Finlay, C. A. The p53 Tumor Suppressor Gene. *Nature*, **1991,** *351*, 453-456.

100. Maki, C. G., Howley, P. M. Ubiquitination of p53 and p21 is Differentially Affected by ionizing and UV Radiation. *Mol. Cell*. *Biol.,* **1997,** 17, 355-363.

101. Agarwal, M. L., Taylor, W, R., Chernov, M, V., Chernova, O. B., Stark, G. R. The p53 Network. *J. Biol. Chem*., **1998,** *273*, 1-4.

102. Levine, A. J. The Cellular Gatekeeper for Growth and Division. *Cell,* **1997,** *88*, 323-331.

103. El-Deiry, W., Tokino, T., Velculescu, V., Levy, D., Parsons, R., Trent, J., Lin, D., Mercer, W., Kinzler, K., Vogelstein, B. WAF1, a Potential Mediator of p53 Tumor Suppression. *Cell*, **1993,** *75*, 817-825.

104. Qiu, X., Forman, H. J., Schonthal, A. H., Cadenas, E. Induction of p21 Mediated by Reactive Oxygen Species Formed during the Metabolism of Aziridinylbenzoquinones by HCT116 Cells. *J. Biol. Chem*., **1996,** *271*, 31915-31921.

105. James, S. Y., Mackay, A. G., Colston, K. W. Effects of 1, 25-Dihydroxyvitamin D3 and its Analogues on Induction of Apoptosis in Breast Cancer Cells. *J. Steroid. BioChem. Mol. Biol*., **1996,** *58,* 395-401.

106. Gartel, A. L., Tyner, A. L. Transcriptional Regulation of the p21 Gene. *Experi. Cell. Res*., **1999**, *246*, 280-289.

107. Cox, L. S., Lane, D. P. Tumor Suppressors, Kinases and Clamps: How p53 Regulates the Cell Cycle in Response to DNA Damage. *BioEssays.,* **1995,** *17*, 501-508.

108. Sherr C. J., Roberts, J. M. Inhibitors of Mammalian G1 Cyclin-Dependent Kinases. *Genes & Dev*., **1995,** *9,* 1149-1163.

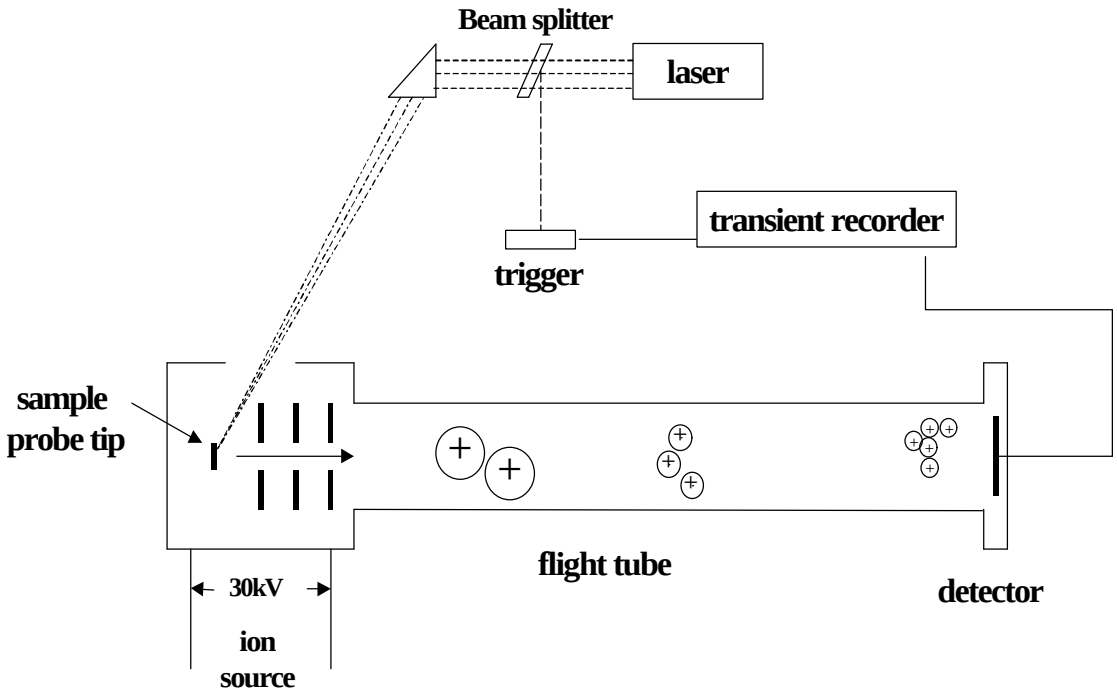

Figure 1-1: Matrix assisted laser desorption/ionization (MALDI) mass spectrometry with time of flight detection (TOF).

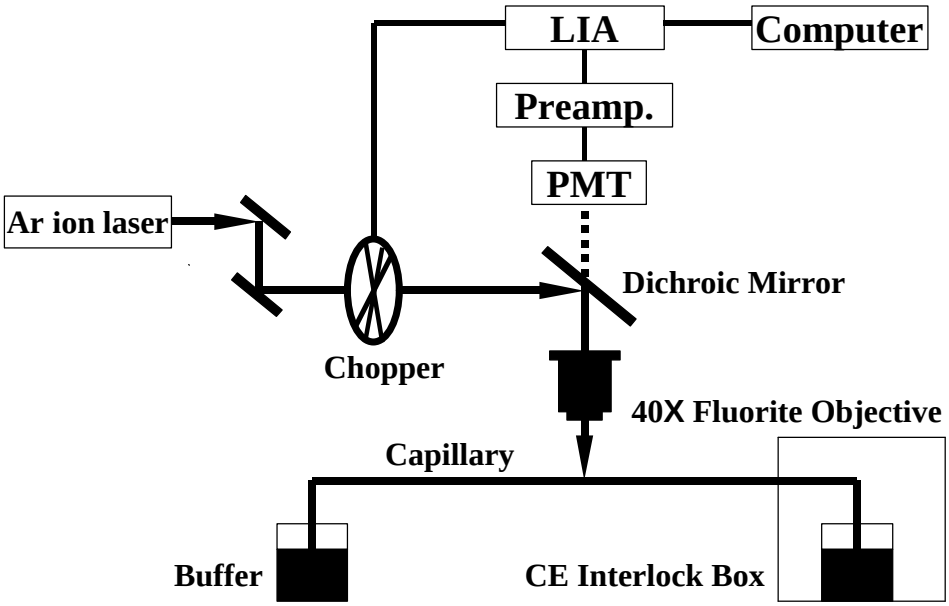

Figure 1-2: Capillary electrophoresis with laser induced fluorescence detection.

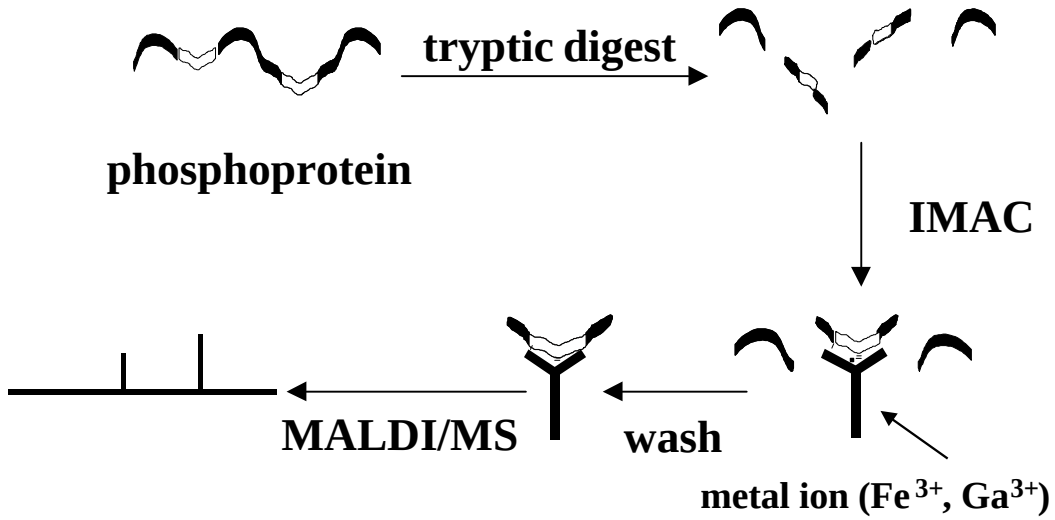

Figure 1-3: Identifying phosphorylation sites by IMAC/MALDI/TOF/MS.

Chapter 2

Direct Analysis of the Products of Sequential Cleavages of Peptides and Proteins Affinity-Bound to Immobilized Metal Ion Beads by Matrix-Assisted Laser Desorption/Ionization Mass Spectrometry

Wei Zhou, Xiaohong Qian, Morteza G. Khaledi, Kenneth B.Tomer

Anal. Biochem. **1999,** 274, 174-180.

ABSTRACT

Consecutive enzymatic reactions on analytes affinity-bound to immobilized metal ion beads with subsequent direct analysis of the products by matrix-assisted laser desorption/ionization time-of-flight mass spectrometry (MALDI/TOF/MS) have been used for detecting protein synthesis errors occuring at the N-terminus. The usefulness of this method was demonstrated by analyzing two commercially-available recombinant HIV proteins with affinity-tags at the N-terminus, and histatin-5, a peptide with multiple histidine residues. The high specificity, sensitivity, and speed of analysis make this method especially useful in obtaining N-terminal sequencing information of histidine-tagged recombinant proteins.

INTRODUCTION

Immobilized affinity techniques, especially affinity chromatography (AC), are widely used in the biochemical laboratory [1-3]. These techniques rely on the specific interactions between receptors and ligands rather than on differential partitioning to separate analytes. Because of the high specificity of the interaction, proteins are often expressed with a specific sequence or 'tag' that permits the use of AC for isolation and purification. For example, fusion proteins can be prepared by fusing the coding sequence of a protein of interest with the coding sequence of staphylococcal protein A together with the sequence of a specific cleavage site. Such proteins can be conveniently purified by immobilized IgG by taking advantage of the specific interaction of IgG and protein A [4]. The affinity tag can be easily removed at the designed cleavage site after purification.

Introduced by Porath, et al. [5], immobilized metal ion affinity chromatography (IMAC) is another affinity technique, in this case, one which takes advantage of the specific interaction between a ligand and an immobilized metal ion. Recently, IMAC has also been used extensively in the purification of recombinant proteins where amino acid residues that are expected to coordinate metal ions are introduced into the primary structure of a protein by expressing the modified gene. For example, by incorporating a histidine affinity tag (His-tag), usually consisting of a six histidine-residue sequence into the expression system, the expressed proteins can be effectively isolated by affinity chromatography based on immobilized metal ions such as Ni^{2+}, Co^{2+}, Zn^{2+}, or Mn^{2+}[6-10].

One problem sometimes encountered in protein expression systems is incorrect expression of the desired protein [11-14]. Mass spectrometry (MS) offers a rapid and sensitive approach to obtaining reliable qualitative sequence information about proteins. It is extremely sensitive, and provides molecular weight information with high accuracy. Significant gains in determining the sequence of recombinant proteins can be realized in terms of high specificity and volume of information when MS is combined with AC.

MS combined with AC for the isolation and detection of specific molecules from complex biological matrices has been developed dramatically in the past few years [16-18]. Our laboratory is currently involved in epitope determination by combining proteolytic footprinting of antigens bound to immobilized antibodies with MALDI/TOF/MS product identification [19-21]. In the development of our approach to this problem, we initially observed that bound analytes, including proteins such as human apotransferrin and phosphopeptides such as phosphokemptide, could be analyzed directly from an affinity matrix using MALDI/TOF/MS [22]. We also found that consecutive enzymatic reactions could be carried out on the analytes affinity-bound to immobilized antibodies with subsequent direct analysis of the products by MALDI/TOF/MS. For example, either aminopeptidase or carboxypeptidase digestion could be performed on the products of the tryptic digest of an affinity-bound protein to more accurately define the amino acid sequence of an epitope. We have applied this combination

to the fine-structure determination of epitopes on large proteins, such as HIV-1 p26 and HIV-1 gp120 [20-21].

In this paper, we demonstrate that the direct MALDI/TOF/MS analysis of affinity-bound analytes can also be used in combination with consecutive reactions of immobilized metal ion affinity-bound analytes. Two commercially-available recombinant proteins, their cleavage products, and a peptide, were analyzed without prior removal of the analytes from the affinity beads. Further structural information on immobilized analytes can be obtained with minimal sample manipulation. The results indicate that this method is effective and convenient in detecting protein sequence errors occuring at the N-terminus.

MATERIALS AND METHODS

Chemicals and Reagents. Ni-NTA agarose was purchased from QIAGEN Inc. (Chatsworth, CA, USA). Recombinant HIV-1 $p24_{H\times B2}$ and HIV-1 vif_{IIIB} were purchased from Bartels Division of Intracel Inc. (Issaquah, WA, USA). Carboxypeptidase Y was obtained from Sigma (St. Louis, MO, USA). Histatin 5 was acquired from BACHEM California (Torrance, CA, USA). Trypsin-TPCK was obtained from Worthington Biochemical Corp. (Freehold, NJ, USA). α-Cyano-4-hydroxycinnamic acid was purchased from Aldrich Chemical Co. (Milwaukee, WI, USA).

Methods

Ni-NTA IMAC. Binding of proteins or a peptide to the Ni-NTA chelating resin was accomplished by adding a 50% slurry of Ni-NTA resin (20 μL) to the sample solution and incubating at 37 °C for 30 min on a rotator. The mixed solution was then centrifuged twice at 14,000g for 3 min to pellet the resin. The supernatant was carefully removed and the resin was washed three times with 40 μL of a solution of 0.02 M dibasic sodium phosphate, 0.5 M sodium chloride and 0.02 M imidazole (pH=7.2) to remove non-specifically-bound analytes [23]. A 0.5 μL aliquot of the resin was placed directly onto the MALDI target followed by 0.5 μL aliquot of the matrix solution. The sample was then allowed to dry at room temperature before loading the target into the mass spectrometer.

On-bead Trypsin Digest. Tryptic digestion of the protein bound to the IMAC beads was carried out as follows: 40 μl of a 50 mM ammonium bicarbonate digestion buffer (pH=7.8) was added to approximately 2 μg of protein or peptide bound to an IMAC gel. A trypsin solution [4 μL (1μg/μL)] was then added (enzyme to protein ratio was 2:1 by weight). The mixture was incubated at 37 °C for 30 min on a rotator. The supernatant was discarded and the resin was washed three times with 40 μL of 0.02 M dibasic sodium phosphate, 0.5 M sodium chloride and 0.02 M imidazole (pH=7.2) to remove non-specifically-bound analytes. A 0.5 μL aliquot of the resin was spotted onto the MALDI target.

On-bead Carboxypeptidase Y Digest. Ni-NTA resin containing a bound peptide was dissolved in 40 μL digestion buffer (50 mM sodium citrate buffer, pH=6.0). Carboxypeptidase Y solution was then added (enzyme to peptide ratio is 2:1 by weight). The mixture was incubated at 37 °C on a rotator. The digestion course was monitored by removing the reaction mixture at specific times. The mixture was centrifuged and the supernatant was discarded. The resin was then washed three times with 40 μL of 0.1 M acetic acid to remove non-specifically-bound analytes and followed by MALDI/TOF/MS analysis.

MALDI/MS. Mass spectra were acquired on a Voyager-RP (PerSeptive Biosystem, Framingham, MA, USA) equipped with a nitrogen laser (λ=337nm). The accelerating voltage used was 30 kV. All spectra were recorded in the positive linear mode. A saturated solution, prepared fresh daily, of recrystallized α-cyano-4-hydroxycinnamic acid in ethanol:water:formic acid (45:45:10) was used as the MALDI matrix. The affinity beads on the target were held in place during the analysis by the crystallized matrix. The acidity and organic nature of the matrix are sufficient to release the affinity-bound analyte from the affinity media, although release due to the energy imparted by the laser has not been ruled out [22]. Mass calibration was carried out using cytochrome C $[M+H]^{+}$=12361.5 and $[M+3H]^{3+}$=4120.5 as an external standard. Although we have observed some decrease in mass accuracy for analytes directly released from affinity beads, when an external calibration is used, typical mass accuracies are 0.07%, even for m/z 1000 peptides. Although there may be mass errors that

can be attributed to surface inhomogeneities due to the presence of the affinity media and to differences in laser energy used between standards and analytes which require higher laser energy, this error is within the specifications of the instrument for externally calibrated samples (< 0.1%). This mass accuracy in the determination of mass differences between consecutive peaks is accurate enough to make an unambiguous amino acid sequence assignment (except for I/L and K/E).

RESULTS AND DISCUSSION

Histatin: Immobilized nickel ion affinity media have been shown to bind peptides and proteins containing adjacent histidine residues and to bind peptides containing two or more histidines in close proximity, such as H×H and H××H [16]. In order to see if carboxypeptidase Y can be used to obtain amino acid sequence data from immobilized metal affinity bound peptides, histatin-5 (Figure 2-1A), a 24-amino-acid peptide which contains two HH and two H×H/H××H sequences, was chosen as a model compound. The MALDI/TOF mass spectrum of histatin-5 affinity-bound to the IMAC media is shown in Figure 2-2A. In addition to the expected protonated molecule at m/z 3037, there are prominent impurity ions of m/z 3063, 2953 and 2903. Treatment of the affinity-bound histatin-5 with carboxypeptidase Y and direct MALDI/TOF/MS analysis of the products from the affinity beads gave the spectrum in Figure 2-2B. Peaks corresponding to ions due to loss of five C-terminal residues (Y, G, R, H, S) were observed. These data indicate that carboxypeptidase Y can cleave the C-terminus of IMAC-bound

peptides, and that it also can cleave a His that is part of an H×H sequence. A peak corresponding to an ion due to loss of Y from the m/z 2903 species is also observed, indicating that this impurity is the result of an N-terminal truncation. These results demonstrate that it is possible to identify and obtain the sequence information from a mixture of IMAC-bound truncated peptides by MALDI/TOF/MS.

We also probed IMAC-bound histatin with aminopeptidase enzymes, but no aminopeptidase cleavage was observed. Based on this observation, aminopeptidase enzymes, which require the presence of a metal, do not work well with IMAC-bound peptides. This may be due to the affinity media binding the metal ion required for activity of the aminopeptidase enzymes.

HIV-1 vif $_{IIIB}$: HIV-1 vif $_{IIIB}$ is a commercially available protein which was expressed by adding the tagging residues MRGSHHHHHHGS to the N-terminus of the protein. Figure 2-1B shows the amino acid sequence of this protein, a viral infectivity factor required for the efficient transmission of free virus in tissue culture. Although the calculated M_r is 23911, the MALDI/TOF mass spectrum (Figure 2-3A) of HIV-1 vif $_{IIIB}$ bound to the IMAC support shows an M_r 23737 indicating the presence of a truncation in the expressed sequence. Tryptic digestion of the affinity-bound protein, followed by intensive washing to remove non-specifically-bound analytes, yielded the spectrum shown in Figure 2-3B. Peaks corresponding to ions of m/z 1531, 1818, 2970 and 3257 are observed

which can be assigned, on the basis of their masses, to four tryptic fragments at the N-terminus (T2, T1-2, T2-3, T1-3) less 131±2 Da. These data indicate that there is an N-terminal truncation in HIV-1 vif $_{IIIB}$ and that residue M13, the first residue after the His-tag sequence, with a residue mass of 131, may be the missing amino acid.

In order to confirm this assumption, the still-affinity-bound fragments were treated with carboxypeptidase Y, and the reaction was monitored over a 23-hr time period. A typical spectrum is shown in Figure 2-3C. Peaks were observed which correspond to ions arising from sequential loss of amino acids from the two tryptic fragments at the N-terminus of this recombinant protein, T1-3 and T2-3. All residues from residue V19 to residue S12, which is part of His-tag, were observed, except for residue M13. These data identify the missing amino acid as M13.

HIV-1 p24$_{H\times B2}$: Recombinant truncated HIV-1 p24$_{H\times B2}$ (Figure 2-1C) is another commercially-available protein expressed with a His-tag sequence. It appeared to be relatively pure by MALDI/TOF/MS analysis which showed a protonated molecule with an M_r of 21253 in the spectrum. Direct MALDI/TOF/MS analysis of the IMAC bound protein (Figure 2-4A) also showed a molecular weight of 21267. This observed molecular mass is about 1300 Da lower than that calculated from the sequence provided by the manufacturer.

The MALDI/TOF mass spectrum of a tryptic digest of the truncated protein did not contain peaks due to tryptic fragments corresponding to T2 (m/z 4431), or T1-2 (m/z 4719), but did show an abundant peak corresponding to an ion of m/z 3413 with an unknown composition (data not shown). IMAC-bound truncated p24 was treated with trypsin followed by intensive washing to remove any non-specifically-bound analytes. MALDI/TOF/MS analysis of the remaining affinity-bound fragments also showed peaks due to the presence of two fragments, one of m/z 3416 and the other of m/z 3128, shown in Figure 2-4B. Although no matching tryptic fragment could be found based on the masses of these two ions, the mass difference between these two is the same as the predicted mass difference between T1-2 and T2. This means that T1 has the predicted molecular weight, and that the modification is in T2. The presence of peaks in the spectrum corresponding to these ions indicates that they are still affinity bound to the IMAC. This means that these fragments also contain the His-tag. Thus, the likely site of the unknown sequence modification is at the N-terminal of the protein.

Based on these MALDI/TOF/MS data, we postulated that the peak corresponding to the ion of m/z 3416 is the truncated tryptic fragment T1-2 of the protein. In addition, a peak corresponding to an ion due to oxidation of the m/z 3416 fragment was also observed, suggesting the possible presence of a methionine in the fragment. The second species, of m/z 3128, was postulated to correspond to the truncated tryptic fragment T2 which differs from truncated T1-2 by M and R at the N-terminus. The peak corresponding to oxidation of the tryptic

fragment of m/z 3128 is much less abundant than the peak corresponding to oxidation of the tryptic fragment of m/z 3416, this is consistent with M in the latter peptide, but not in the former. The mass difference between the calculated and observed molecular weights of the tryptic fragments T1 or T1-2 is 1302 $\pm$ 2 Da.

In order to obtain further structural information, the same strategy used for HIV-1 vif_{IIIB} was applied to HIV-1 $p24_{H\times B2}$. The still affinity-bound fragments were digested with carboxypeptidase Y, and the reaction was monitored over a 20-hr time period. Spectra are shown in Figure 2-5. Nine major peaks plus peaks due to oxidation were observed. They are postulated as the products of the carboxypeptidase Y cleavage of the T1-2 fragment. The m/z values of these peaks are: 3416, 2962, 2891, 2527, 2396, 2268, 1629, 1516, and 1419 Da. Another set of eight major peaks without accompanying peaks due to oxidation were also observed. The m/z values of these peaks are: 3128, 2676, 2604, 2110, 1982, 1342, 1229, and 1132 Da and are postulated as the products of the cleavage from the T2 fragment. If one adds 1302 Da (the difference in mass between the calculated and observed masses of the tryptic fragments) to each of these ions, the resulting masses match the predicted peptide sequence to residue P25 with a mass deviation of $\pm$ 2 Da. The ions of m/z 1419 and m/z 1132 correspond to the His-tag, MRGSHHHHHHGS, and the loss of M and R from the His-tag, respectively.

These data are consistent with the sequence error being at the N-terminus, and most likely due to omission of residues 13-24. The combined mass of these residues (1302 Da=DTGHSSQVSQNY) is consistent with the difference between the calculated and observed mass of the intact protein. The MS results were confirmed by Edman sequencing which indicated that residues 13-24 were not present.

CONCLUSIONS

Sequential enzymatic cleavages of peptides and proteins affinity-bound to immobilized metal ion beads combined with direct MALDI/TOF/MS analysis of the products has been shown to be a very promising technique. A MALDI/TOF mass spectrum of the resulting mixture yields molecular weight information corresponding to each truncated peptide affinity-bound to metal ion beads. The mass difference between consecutive peaks can be directly related to the mass of one or more amino acid residues. The order of occurrence defines the primary structure of the peptide.

We have used this methodology to successfully identify the truncation sites occuring at the N-terminus of two commercially available recombinant proteins. Carboxypeptidase Y has been reported to nonspecifically cleave all residues from the C-terminus, including proline [24]. The ability of C-terminal enzymatic sequencing using a time-dependent carboxypeptidase Y digestion coupled with MALDI/TOF/MS analysis of the resulting peptides ladders has also

been demonstrated [25-26]. In this study, we used caboxypeptidase Y to sequentially cleave all residues from the C-terminus of affinity-bound N-terminal peptides of recombinant proteins. The method offers a rapid and sensitive way for obtaining N-terminal sequence information on blocked recombinant proteins.

Because it has been reported that a small elongation or deletion of up to three N-terminal amino acids can dramatically change the binding properties of the protein, and thus may affect biological and especially therapeutic properties of the recombinant proteins [15], it is important to verify the sequence of expressed proteins. The present method allows the fast identification of protein expression errors occuring at the N-terminus. In addition, the femtomole sensitivity range of MALDI/TOF/MS makes this method extremely useful in providing sequence information from limited amount of sample, information which is not readily obtainable by other, more traditional techniques.

ACKNOWLEDGMENT

Support for the purchase of the MALDI/TOF instrument by the NIH, Office of AIDS Research is gratefully acknowledged.

REFERENCES:

1. Kawasaki, I., Kawasaki, N., Yamashina, I. Mannose/N-Acetylglucosamine-Binding Proteins from Mammalian Sera. in *Meth. Enzymol*., **1989**, *179*, 310-321.
2. Belew, M., Juntti, N., Larsson, A., Porath, J. A One-step Purification Method for Monoclonal Antibodies Based on Salt-promoted Adsorption Chromatography on a 'Thiophilic' Adsorbent. *J. Immunol. Meth.,* **1987**, *102*,173-182.
3. Hermanson, G. T., Mallia A. K., Smith P. K. in Immobilized Affinity Ligand Techniques, Academic Press, San Diego, **1992**, pp.317-417.
4. Moks, I., Abrahmsen, L., Oesterlof, B., Josephson, S., Oestling, M., Enfors, S. 0., Persson , I., Nilsson, B., Uhlen, M. Large-scale Affinity Purification of Human Insulin-like Growth Factor I from Culture Medium of E. *coil. Bio/Technology,* **1987**, *5,* 379-382.
5. Porath, J., Carlsson, J., Olsson, I., Belfrage, G. Metal Chelate Affinity Chromatography, a New Approach to Protein Fractionation. *Nature,* **1975**, *258*, 598-599.
6. Hochuli, E., Bannwaeth, W., Dobeli, H., Gentz, R., Stuber D. Genetic Approach to Facilitate Purification of Recombinant Proteins with a Novel Metal Chelate adsorbent. *BiolTechnology,* **1988**, *6,* 1321-1325.
7. Bharath, M. M., Khadake, J. R., Rao, M. R. Expression of Rat Histone H 1d in *Escherchia coli* and its Purification. *Protein Expression Purif.,* **1998**, *12***,** 38-44.

8. Hutchens, I. W., Nelson, R. W., Li, C. M., Yip, T. T. Synthetic Metal-Binding Protein Surface Domains for Metal Ion-Dependent Interaction Chromatography. I. Analysis of Bound Metal Ions by Matrix-Assisted UV Laser Desorption Time-of-Flight Mass Spectrometry. *J. Chromatogr.,* **1992**, *604,*133-141.
9. Bateson M., Devenish, R. J., Nagley, P., Prescott, M. Entrapment by Immobilized Metal Ion Affinity Chromatography of Assembled Yeast Mitochondrial ATP Synthase Containing Individual Subunits Tagged with Hexahistidine. *Anal. Biochem.,* **1996**, *238,*14-18.
10. Yip, T. I., Hutchens, T. W. Metal Ion Affinity Adsorption of Zn(II)-Transport Protein Present in Maternal Plasma during Lactation: Structural Characterization and Identification as Histidine-Rich Glycoprotein. *Protein Expression Purif.,* **1991**, *2,* 355-62.
11. Kurland C. G., Gallant, J. Errors of Heterologous Protein Expression. *Curr-Opin-Biotechnol*., **1996**, *7*, 489-493.
12. Kurland C. G., Jorgensen F. Processivity Errors of Gene Expression in *Escherichia coli*. *J. Mol. Biol.,* **1990**, *215*, 511-521.
13. Benhar, I., Miller, C., Engelberg-Kulka, H. Frameshifting in the Expression of *Escherichia coli trpR* Gene is Modulated by Translation Initiation. *J. Bacteriol*., **1993**, *175*, 3204-3207.
14. Lu, H. S., Rausset, P. R., Sotos, L. S., Clogston, C. L., Rohde, M. R., Stoney, K. S., Herman, A. C. Isolation and Characterization of Three Recombinant

Human Granulocyte Colony Stimulating Factor His→Gln Isoform Products in *Escherichia coli. Protein Expression Purif.,* **1993**, *4,* 465-472.

15. Svoboda, M., Bauhofer, A., Schwind, P., Bade, E., Rasched, I., Przybyski, M. Structural Characterization and Biological activity of Recombinant Human Epidermal Growth Factor Proteins with Different N-terminal Sequences. *Biochimica et biophysica Acta,* **1994**,*1206*, 35-41.
16. Volz, J., Bosch, R. U., Wunderlin M., Schuhmacher, M., Melchers, K., Bensch K., Steinhilber, W., Schafer K. P., Toth, G., Penke, B., Przybyski, M. Molecular Characterization of Metal-Binding Polypeptide Domains by Electrospay Ionization Mass Spectrometry and Metal Chelate Affinity Chromatography. *J. Chromatogr.,* **1998**, *800*, 29-37.
17. Nelson, R. W., Krone, J. R., Bieber, A. L., Williams, P. Mass Spectrometric Immunoassay. *Anal. Chem.,* **1995**, *67,* 1153-1158.
18. Liang, X., Lubman, D. M., Rossi, D. T., Nordblom, G. D., Barksdale, C. M. On-probe Immunoaffinity Extraction by Matrix-Assisted Laser Desorption/Ionization Mass Spectrometry. *Anal. Chem.,* **1998**, *70*, 498-503.
19. Papac, D. I., Hoyes, J., Tomer, K. B. Epitope Mapping of the Gastrin-releasing Peptide/anti-bombesin Monoclonal Antibody Complex by Proteolysis Followed by Matrix-Assisted Laser Desorption Ionization Mass spectrometry. *Protein Science,* **1994**, *3*, 1485-1492.
20. Parker, C. E., Papac D. I., Trojak, S. K., Tomer, K. B. Epitope Mapping by Mass Spectrometry. *J. Immun.,* **1996**, *157*, 198-206.

21. Jeyarajah, S., Parker, C. E., Sumner, M. T., Tomer, K. B. Matrix-Assisted Laser Desorption Ionization/Mass Spectrometry Mapping of Human Immunodeficiency Virus-gp120 Epitopes Recognized by a Limited Polyclonal Antibody. *J. Am. Soc. Mass Spectrom.,* **1998**, *9*, 157-165.
22. Papac, D. I., Hoyes, J.,Tomer, K. B. Direct Analysis of Affinity-Bound Analytes by MALDI/TOF MS. *Anal. Chem.,* **1994**, *66*, 2609-2613.
23. Yip, T.-T. H., I. W. in Methods in Molecular Biology (Donan, S., Eds.) 59 Protein Purification Protocols*,* Human Press, Inc., Totowa, NJ. **1996,** pp. 197-210.
24. Hayashi, R., in *Meth. Enzymol.,* **1977**, *47*, 84-93.
25. Thiede, B., Wittmann-Liebold, B., Bienert, M., Krause, E. MALDI-MS for C-terminal Sequence Determination of Peptides and Proteins Degraded by Carboxypeptidase Y and P. *FEBS lett.,* **1995**, *357*, 65-69.
26. Patterson, D. H., Tarr, G. E., Regnier, F. E., Martin, S. A. C-terminal Ladder Sequencing via Matrix-Assisted Laser Desorption Mass Spectrometry Coupled with Carboxypeptidase Y Time-Dependent and Concentration-Dependent Digestions. *Anal. Chem.,* **1995**, *67*, 3971-3978.

Figure 2-1. Primary structures of proteins and peptide analyzed.

(A) Histatin-5 and calculated m/z of the ions due to the sequential loss of one of the amino acids from the C-terminal, (B) HIV-1 vif $_{IIIB}$ and the predicted masses of the tryptic digestion products. (C) HIV-1 p24 $_{H\times B2}$ and predicted masses of the tryptic digestion products.

Figure 2-2. MALDI/TOF mass spectra of (A) Ni-NTA bound Histatin-5, (B) peptides bound to Ni-NTA after carboxypeptidase Y digest of Histatin-5 overnight. * are the impurities with m/z 2903 and an ion corresponding to the loss of Y from m/z 2903 species.

Figure 2-3. MALDI/TOF mass spectra of (A) Ni-NTA bound truncated HIV-1 vif $_{IIIB}$, (B) Ni-NTA bound tryptic digests from truncated HIV-1 vif $_{IIIB}$, (C) peptides bound to Ni-NTA after tryptic digest for 30 min followed by carboxypeptidase Y digest for 23 hours of truncated HIV-1 vif$_{IIIB}$. T1-3: MRGSHHHHHHGSMENRWQV, T2-3: GSHHHHHHGSMENRWQV.

Figure 2-4. MALDI/TOF mass spectra of (A) Ni-NTA bound truncated HIV p24 $_{H\times B2}$, (B) Ni-NTA bound tryptic digests from truncated HIV p24 $_{H\times B2}$.

Figure 2-5. MALDI/TOF mass spectra of peptides bound to Ni-NTA after tryptic digest for 30 min followed by carboxypeptidase Y digest for (A) 2 hours,

(B) 4 hours, (C) 20 hours of truncated HIV p24 $_{H\times B2}$. [DTGHSSQVSQNY] are the missing residues.

T1-2: MRGSHHHHHHGS[DTGHSSQVSQNY]PIVQNIQGQMVHQAISPR

T2: GSHHHHHHGS[DTGHSSQVSQNY] PIVQNIQGQMVHQAISPR

(A)

m/z |2437|2524|2661|2817|2874|3037

DSHAKRHHGYKRKFHEKH | H | S | H | R | G | Y

(B)

| T1(m/z 306) |T1-2 (m/z 1948) |T1-3(m/z 3389)

[1]MR| GSHHHHHH [11]GSMENR|WQVM [21]IVWQVDR| MRI

[31]RTWKSLVKHH [41]MYVSGKARGW [51]FYRHHYESPH [61]PRISSEVHIP

[71]LGDARLVITT [81]YWGLHTGERD [91]WHLGQGVSIE [101]WRKKRYSTQV

[111]DPELADQLIH [121]LYYFDCFSDS [131]AIRKALLGHI [141]VSPRCEYQAG

[151]HNKVGSLQYL [161]ALAALITPKK [171]IKPPLPSVTK [181]LTEDRWNKPQ

[191]KTKGHRGSHT [201]MNGH

(C)

|T1(m/z 306)

[1]MR| GSHHHHHH [11]GSDTGHSSQV [21]SQNYPIVQNI [31]QGQMVHQAIS

|T1-2 (m/z 4719)

[41]PR |TLNAWVKV [51]VEEKAFSPEV [61]IPMFSALSEG [71]ATPQDLNTML

[81]NTVGGHQAAM [91]QMLKETINEE [101]AAEWDRVHPV [111]HAGPIAPGQM

[121]REPRGSDIAG [131]TTSTLQEQIG [141]WMTNNPPIPV [151]GEIYKRWIIL

[161]GLNKLWRMYS [171]PTSILDIRQG [181]PKEPFRDYVD [191]RFYKTLRAEQ

[201]A

Figure 2-1

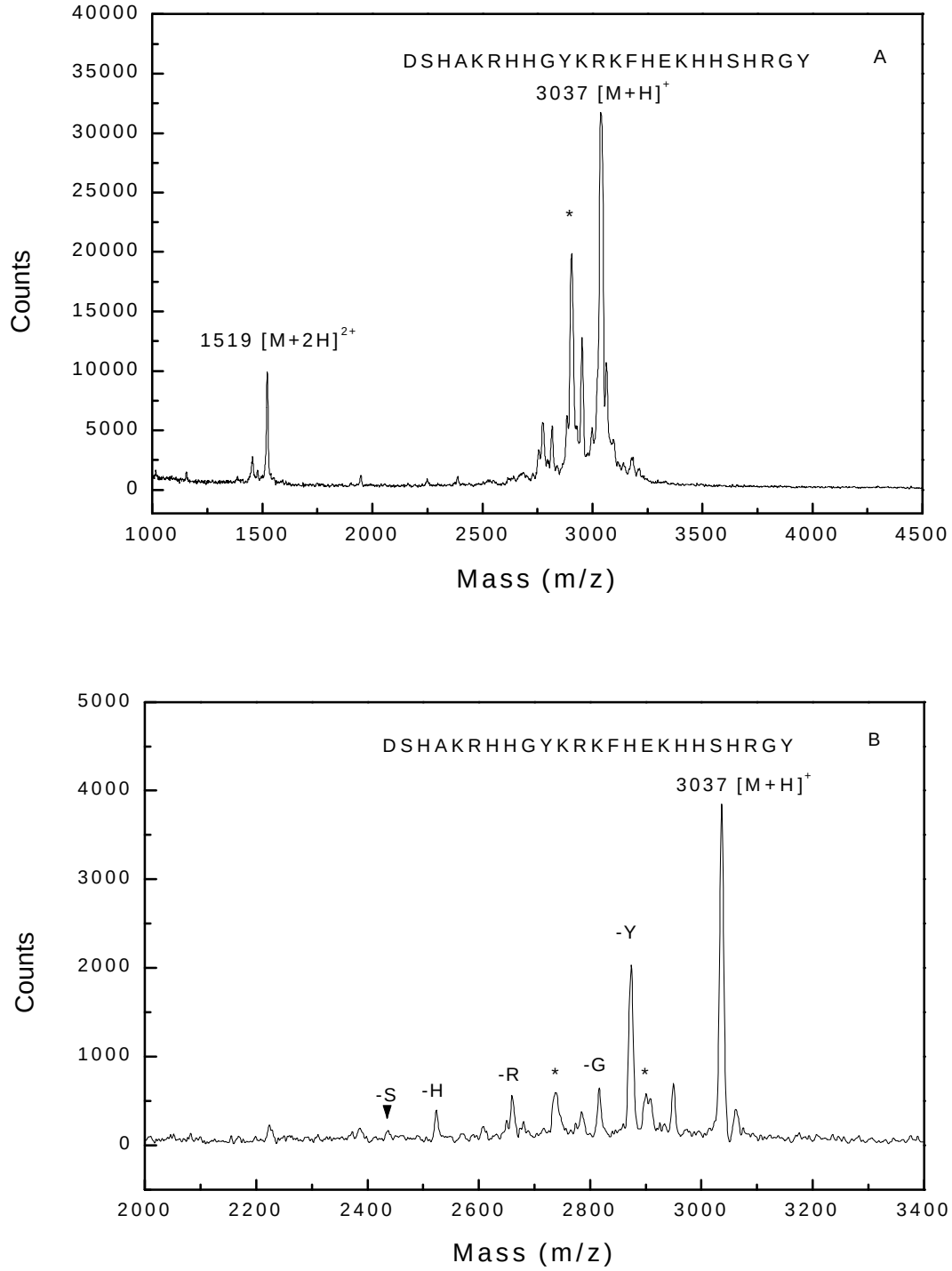
DSHAKRHHGYKRKFHEKHHSHRGY
A
3037 [M+H]+
*
1519 [M+2H]2+
Counts
Mass (m/z)
DSHAKRHHGYKRKFHEKHHSHRGY
B
3037 [M+H]+
-Y
-S
-H
-R
*
-G
*
Counts
Mass (m/z)

Figure 2-2

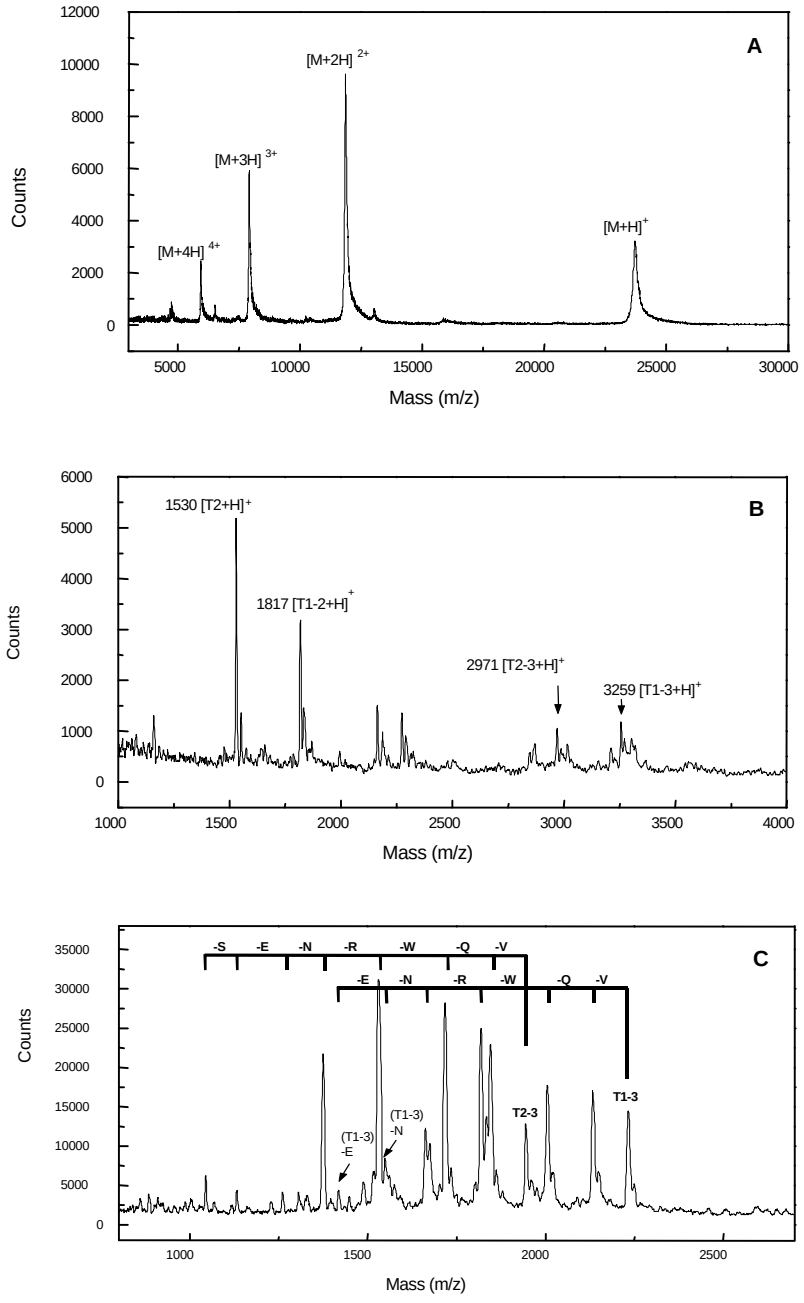
A
[M+2H] 2+
[M+3H] 3+
[M+4H] 4+
[M+H]+
Counts
Mass (m/z)
B
1530 [T2+H]+
1817 [T1-2+H]+
2971 [T2-3+H]+
3259 [T1-3+H]+
Counts
Mass (m/z)
C
-S -E -N -R -W -Q -V
-E -N -R -W -Q -V
T1-3
T2-3
(T1-3) -N
(T1-3) -E
Counts
Mass (m/z)

Figure 2-3

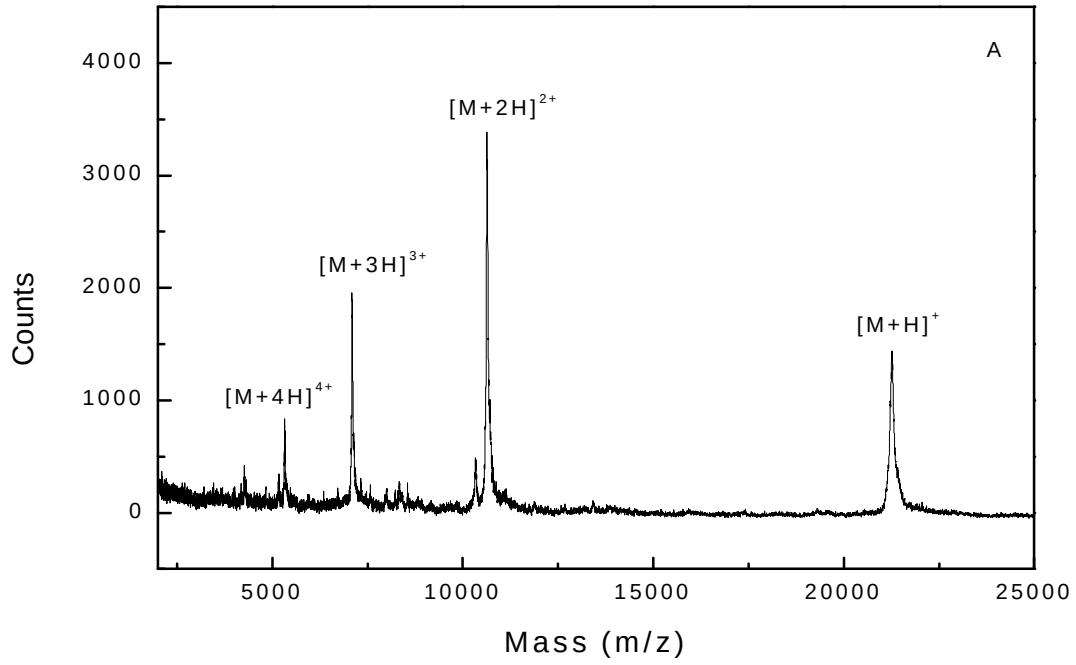
A
Counts
4000
3000
2000
1000
0
[M+2H]2+
[M+3H]3+
[M+4H]4+
[M+H]+
5000
10000
15000
20000
25000
Mass (m/z)

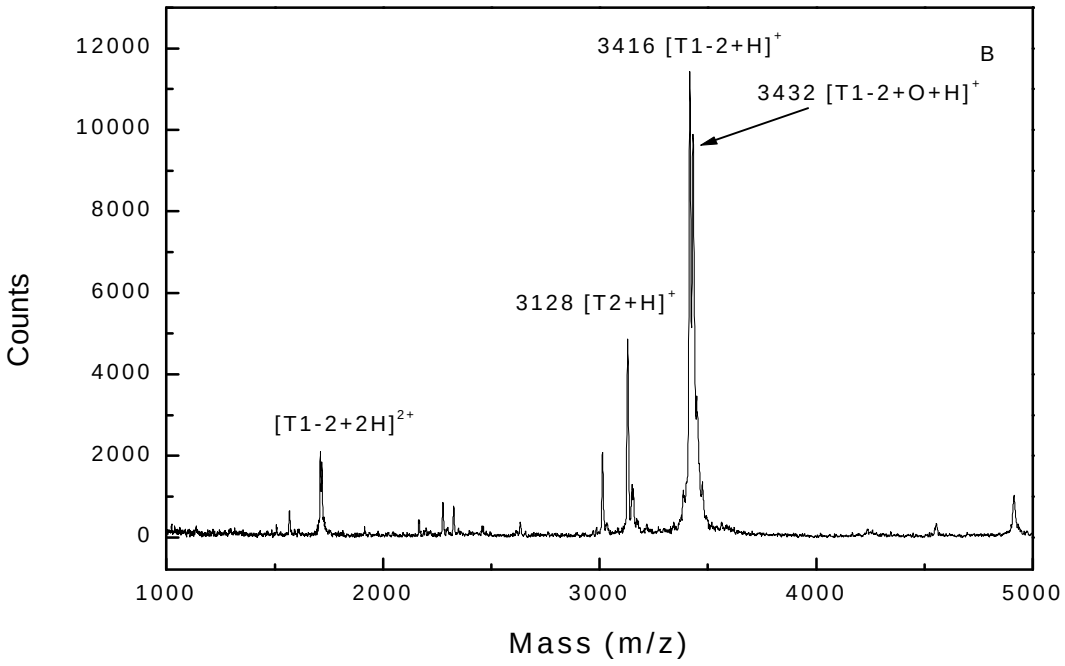
B
Counts
12000
10000
8000
6000
4000
2000
0
3416 [T1-2+H]+
3432 [T1-2+O+H]+
3128 [T2+H]+
[T1-2+2H]2+
1000
2000
3000
4000
5000
Mass (m/z)

Figure 2-4

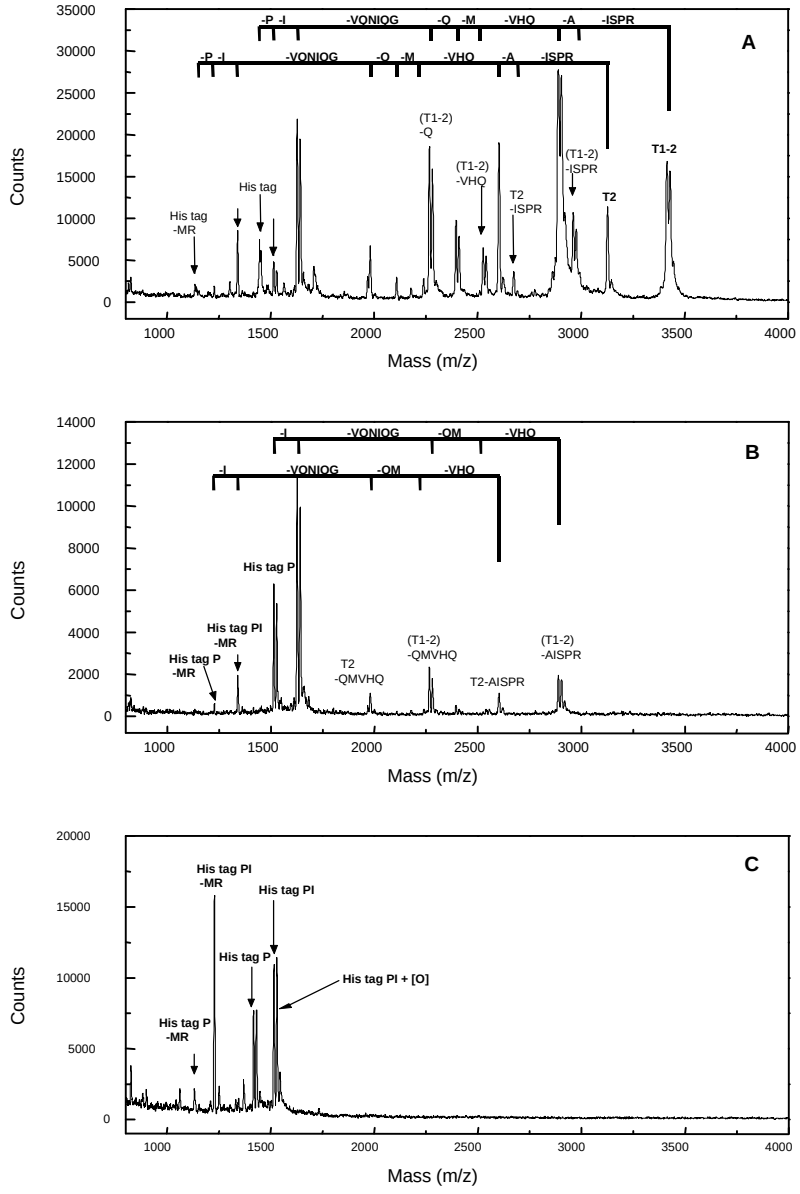
A
-P -I
-VQNIOG
-O -M
-VHQ
-A
-ISPR
His tag -MR
His tag
(T1-2) -Q
(T1-2) -VHQ
T2 -ISPR
(T1-2) -ISPR
T1-2
T2
Counts
Mass (m/z)
B
-I
-VQNIOG
-QM
-VHQ
His tag P
His tag PI -MR
His tag P -MR
T2 -QMVHQ
(T1-2) -QMVHQ
T2-AISPR
(T1-2) -AISPR
Counts
Mass (m/z)
C
His tag PI -MR
His tag PI
His tag P
His tag PI + [O]
His tag P -MR
Counts
Mass (m/z)

Figure 2-5

Chapter 3

Selective Detection and Sequencing of Phosphopeptides Affinity-Bound to Immobilized Metal Ion Beads by Matrix-Assisted Laser Desorption/Ionization Mass Spectrometry

Wei Zhou, B. Alex Merrick, Morteza G. Khaledi, Kenneth B. Tomer

J. Am. Soc. Mass Spectrom. in press

ABSTRACT

Consecutive enzymatic reactions of analytes which are affinity-bound to immobilized metal ion beads with subsequent direct analysis of the products by matrix-assisted laser desorption/ionization mass spectrometry (MALDI/MS) have been used for detecting phosphorylation sites. The usefulness of this method was demonstrated by analyzing two commercially-available phosphoproteins, β-casein and α-casein. Agarose loaded with either Fe^{3+} or Ga^{3+} was used to isolate phosphopeptides from the protein digest. Results from using the two metal ions were complementary. Less overall suppression effect was achieved when Ga^{3+}-loaded agarose was used to isolate phosphopeptides. The selectivity for monophosphorylated peptides, however, was better with Fe^{3+}-loaded agarose. This technique is easy to use and has the ability to analyze extremely complicated phosphopeptide mixtures. Moreover, it eliminates the need for prior

HPLC separation or radiolabeling, thus greatly simplifying the sample preparation.

INTRODUCTION

The reversible phosphorylation/dephosphorylation of protein, mainly on serine, threonine, and tyrosine residues, is probably the most common and important regulatory modification of proteins. Phosphorylation is involved in the regulation of gene expression and protein synthesis which controls cell growth, division or differentiation [1-4]. In order to better understand the molecular basis of these regulatory mechanisms, it is necessary to identify these phosphorylation sites.

Identification of protein phosphorylation sites usually entails a combination of techniques even when the sequence of a protein is known. Conventional strategies usually involve isolation of radiolabeled [^{32}P] target protein [5-8], phosphoamino acid analysis to determine the modified amino acid, tryptic mapping using TLC or HPLC separation schemes, and automated Edman degradation to determine the amino acid sequence of candidate peptides with the appearance of ^{32}P at a specific cycle [9]. *In vitro* kinase reactions using peptide substrates homologous to various regions of the target protein, site-directed mutagenesis, isoelectric focusing and use of anti-ser/thr/tyr antibodies are complementary methods which can be integrated into the preceding strategy for site-specific localization of phosphorylation in a target protein [10-13].

However, conventional approaches using ^{32}P may not be sufficiently sensitive since many phosphoproteins in cell signaling are in low abundance, the amount of biological sample is often limited, and the process of radiolabel incorporation into protein under cellular conditions is generally inefficient. These factors underscore the need for continued development of methods for enrichment and increasingly sensitive detection of phosphopeptides to find the precise site of phosphorylation.

Mass spectrometry has proven to be very useful in mapping posttranslational modifications of proteins, such as phosphorylation and glycosylation [14,15]. The analysis is rapid and does not require radiolabeling. Both matrix-assisted laser desorption/ionization mass spectrometry (MALDI/MS) and electrospray ionization mass spectrometry (ESI/MS) have been used to determine the phosphorylation sites on proteins [16-19, 33-34]. In the MS analysis of protein digests, however, components are not always detected due either to suppression effects or to low ionization efficiency [16]. This is particularly problematic when phosphopeptides are present, because phosphorylated peptides usually exhibit low response to MS in positive ion mode due to the negative charge of a phosphate group. Negative charge interference in detection becomes even worse when multiple phosphate groups exist in the peptide.

To reduce suppression effects and enhance the detectability of these components, the digests can be subjected to HPLC separation. The HPLC eluent can be either directly analyzed using ESI/MS/MS to locate the phosphorylation sites or HPLC fractions can be collected and subjected individually to MALDI/MS analysis. After phosphatase treatment, phosphopeptide identification by MALDI can be facilitated by the 80 Da difference in the MALDI spectrum between the observed mass of the peptide and that calculated on the basis of the nonphosphorylated sequence [16]. MALDI-based peptide sequencing can also be achieved by post source decay (PSD), which produces predicted fragmentation along the peptide backbone [18]. The HPLC separation, however, is laborious, and incomplete separation can sometimes make data analysis difficult. Moreover, the loss of sample during the HPLC separation makes the analysis of cellular phosphoproteins present at very low concentrations more difficult.

The use of immobilized metal ion affinity chromatography (IMAC) to isolate phosphopeptides from mixture has been shown to be useful in both MALDI/MS and ESI/MS structure studies of phosphoproteins. Immobilized metal ions, such as Fe^{3+}, Al^{3+} bind with high specificity to phosphoproteins and peptides [23-25]. Recently, Tempst demonstrated that Ga^{3+} has a better selectivity for the phosphopeptides [20]. By selective isolation of phosphopeptides using metal ion affinity media before MS analysis, suppression effects or low net average charge due to the presence of the doubly negatively charged phosphate group combined

with the positively charged amino groups can be greatly reduced. This technique has been used successfully with both on-line and off-line coupling to MS analysis [26-30, 35]. However, elution of phosphopeptides from the metal ion column before MS analysis could result in loss of sample. We have previously shown that it is not necessary to elute affinity bound analytes, including phosphopeptides, from affinity media prior to MS analysis. For example, we observed that affinity-bound phosphoprotein and peptide, such as human apotransferrin and phosphokemptide, could be analyzed directly from Fe^{3+}-loaded sepharose using MALDI/MS [21]. We also found that consecutive enzymatic reactions could be carried out on affinity-bound analytes, including those immobilized on Ni^{2+} ion media. Subsequent direct analysis of the products by MALDI/MS could further accurately define the amino acid sequence of the bound peptides [22].

In this study, a method that minimizes suppression effects and enables direct analysis of phosphopeptides from the protein digest without any HPLC separation is demonstrated. Agarose loaded with either Fe^{3+} or Ga^{3+} is used to isolate phosphopeptides from the protein digest (Figure 3-1). The affinity-bound phosphopeptides are treated with phosphatase, and the number of phosphorylation sites are determined from 80 Da (or multiples of 80 Da) mass shifts. Carboxypeptidase Y treatment of the affinity-bound phosphopeptides then is used to cleave the amino acids from the C-terminus, with subsequent direct analysis of the enzymatic products by MALDI/MS to locate the phosphorylation

sites on the bound phosphopeptides. We have applied this method to the analysis of two commercially available proteins, β-casein and α-casein. Results from using either Fe^{3+} or Ga^{3+} metal ions are complementary. Ga^{3+}-loaded agarose shows less overall suppression effect and the ability to isolate phosphopeptides with multiple phosphate groups. However, the selectivity for monophosphorylated peptides is better using Fe^{3+}-loaded agarose. High sensitivity, absence of the need for radiolabeling or HPLC separation, ease of use, and the ability to analyze extremely complicated phosphopeptide mixtures make this method attractive.

MATERIALS AND METHODS

Chemicals and Reagents. Ni-NTA (nickel-bound nitrilotriacetic, a quadradentate metal-chelator) agarose was purchased from QIAGEN Inc. (Chatsworth, CA, USA). Hi-trap chelating IDA (iminodiacetic, a tridentate metal-chelator) sepharose was obtained from Pharmacia Biotech (Piscataway, NJ). The β-casein, α-casein and carboxypeptidase Y were obtained from Sigma (St. Louis, MO, USA). Calf intestinal alkaline phosphatase and buffer sets were obtained from Gibco BRL Products (Grand Island, NY, USA). Immobilized trypsin was from PerSeptive Biosystems (Framingham, MA, USA). Ferric chloride was from Allied Chemical (Morristown, NJ, USA). The α-cyano-4-hydroxycinnamic acid, gallium (III) chloride, and other reagents were purchased from Aldrich Chemical Co. (Milwaukee, WI, USA). Compact reaction columns and filters were made by Amersham Pharmacia Biotech (Piscataway, NJ).

Methods

Tryptic Digest. Phosphoproteins were digested by immobilized trypsin to avoid trypsin autodigestion products. A 10 μL aliquot of immobilized trypsin slurry was washed with 50 μL of 50:50 acetonitrile:0.1 M ammonium bicarbonate (3x), followed by 50 μL of 5:95 acetonitrile:0.1 M ammonium bicarbonate (3x) to activate the enzyme. A 40 μL (1μg/μL) aliquot of protein and 50 μl 100 mM ammonium bicarbonate digestion buffer (pH=7.8) were added to the treated immobilized trypsin. The mixture was incubated at 37 °C for four hours on a rotator.

IMAC Column. IMAC columns were prepared by adding 30 μL 50% slurry of Ni-NTA resin into a compact reaction column. The column was washed with 30 μL 100 mM EDTA (3x) to remove any bound Ni^{2+} metal ions. The column was then washed sequentially with 30 μL water (3x), 30 μL 0.1 M acetic acid (3x), and 30 μL 60 mM $GaCl_3$ or 100 mM $FeCl_3$ (3x) to load the column with metal ions. The column was then washed with 30 μL water (3x) followed by 30 μL 0.1 M acetic acid (3x) to remove any unbound metal ions. Binding of phosphopeptides to the metal chelator was achieved by loading the protein digest (2 μg protein digest dissolved in 50 μL 0.1 M acetic acid) onto the IMAC column and incubated at 37 °C for 30 min on a rotator. The column was washed with 50 μL water (3x) and 50 μL 0.1 M acetic acid (3x) to remove less tightly bound analytes. A 0.5 μL

aliquot of the resin was placed directly onto the MALDI target followed by a 0.5 μL aliquot of the matrix solution. The sample was then allowed to dry at room temperature before loading into the mass spectrometer. In some experiments, a 0.5 μL aliquot of the resin, a 0.5 μL aliquot of the matrix solution and a 0.5 μL aliquot of 25 mM ammonium citrate were placed onto MALDI target and allowed to dry at room temperature. Ammonium citrate has been reported to be able to enhance the detection of phosphopeptides in MALDI/MS analysis [32].

On-gel Carboxypeptidase Y Digest. 40 μL of digestion buffer (50 mM sodium citrate, pH=6.0) was added to the phosphopeptides bound to Ga-NTA beads. Carboxypeptidase Y solution was then added (enzyme to peptide ratio is 1:1 by weight). The mixture was incubated at 37 °C on a rotator. The digestion course was monitored by removing a small aliquot of the reaction mixture at specific time. The mixture was centrifuged and the supernatant was discarded. The resin was then washed three times with 50 μL of 0.1 M acetic acid followed by MALDI/MS analysis.

On-gel Dephosphorylation. A small amount (5 μL) of phosphopeptide affinity-bound to immobilized metal ion agarose was mixed with 1 unit of calf intestine alkaline phosphatase, 1 μL digestion buffer and 2 μL water. The mixture was incubated at 37 °C on a rotator. The dephosphorylation course was monitored by removing a 0.5 μL aliquot of the reaction mixture (both beads and

supernatant) at specific times and analyzing the resulting products by MALDI/MS.

MALDI/MS. Mass spectra were acquired on a Voyager-RP (PerSeptive Biosystem, Framingham, MA, USA) equipped with a nitrogen laser (λ=337nm). The accelerating voltage used was 30 kV. All spectra were recorded in the positive linear mode except spectra from the carboxypeptidase digest experiments which were recorded in the negative ion mode. A saturated solution of recrystallized α-cyano-4-hydroxycinnamic acid in ethanol:water:formic acid (45:45:10), prepared fresh daily, was used as the MALDI matrix. Samples were prepared by mixing equal volumes of analyte and matrix solution on the target and letting them dry. When ammonium citrate additive was used, an equal volume of ammonium salt solution was also mixed with the analyte and matrix solutions. Mass calibration was performed by using angiotensin I [$(M+H)^+$=1297.51] and insulin (bovine) [$(M+H)^+$=5734.59] as external standards.

RESULTS AND DISCUSSION

Selective Detection of Phosphorylation Sites in β-Casein: Bovine β-casein was chosen as a model compound because it is a commercially available phosphoprotein and has five well-characterized phosphorylation sites at serine residues [36,37]. Tryptic digests of this protein were loaded onto Ga^{3+}-NTA beads. After extensive washing to remove any unbound digest, the Ga^{3+}-NTA beads were analyzed directly by MALDI/MS. Two major peaks, m/z 2062 and

3124, were observed in the MALDI spectrum, shown in Figure 3-2A. A number of smaller signals corresponding to sodium adducts of the major peaks and a peak of m/z 3044 were also observed. The still affinity-bound peptides were then treated by phosphatase. The dephosphorylation course was monitored by taking a small aliquot (0.5 μL) of the reaction mixture at specific time points for direct MALDI/MS analysis. The reaction was complete within one hour. Figure 3-2B shows that the peak at m/z 2062 shifted –80 Da to m/z 1982 indicating there was only one phosphorylation site on this peptide. Based on the known protein sequence, T6, FQSEEQQQTEDELQDK, with a calculated $[M+H]^+$ at 1982, fits the data. Since there was only one serine in this peptide, the monophosphorylated peptide can be unambiguously assigned as T6 (1P), FQpSEEQQQTEDELQDK. The peak at m/z 3124 shifted -320 Da to m/z 2804 indicating there were four phosphorylation sites on this peptide, while the m/z 3044 peak was no longer seen, indicating that it, too, shifted to m/z 2804 and had three phosphorylation sites. Based on the known protein sequence, T1-2, RELEENVPGEIVESLSSSEESITR, with a calculated $[M+H]^+$ of 2804 fits these data. Because there were five serines, but only four phosphorylated residues on this peptide, the still affinity-bound phosphopeptides were treated with carboxypeptidase Y with subsequent direct analysis of the reaction products by MALDI/MS to locate the phosphorylation sites. Figure 3-3 shows the time course study of the carboxypeptidase Y reaction of T1-2 (4P). A MALDI mass spectrum of the resulting mixtures yielded the molecular weight information corresponding to each fragment affinity-bound to the Ga^{3+}-NTA beads. The mass difference

between consecutive peaks can be directly related to the mass of one or more amino acid residues from the C-terminus of T1-2 (4P). After overnight treatment with carboxypeptidase Y, the still affinity-bound phosphopeptides were treated with phosphatase, Figure 3D shows that there were -320 Da shifts for both carboxypeptidase Y digest products. The molecular weights of these two peptides matched the molecular weights of -RELEENVPGEIVESLSSSEES and -RELEENVPGEIVESLSSSEE. The results demonstrate that the carboxypeptidase Y could cleave through the first serine of T1-2 from the C-terminal. However, the enzyme could not cleave further indicating that glutamic acid may interact with the gallium ions [24]. The interaction is apparent sufficiently strong that it prevented the enzymatic reaction from going further. Both resulting fragments still had four phosphorylation sites, indicating that the first serine from the C-terminus was not phosphorylated. The tetraphosphorylated T1-2 peptide is, therefore, assigned as RELEENVPGEIVEpSLpSpSpSEESITR. Peaks could still be observed with a mass 80 Da lower than the tetraphosphorylated peptides, indicating that the non-phosphorylated serine in the triphosphorylated peptide was located within the SLSSS sequence. From the MALDI/MS spectra, it also can be seen that these two peptides, especially T1-2, had a strong tendency to form multiple sodium adducts. This may have been due to the multiple phosphate groups and negatively charged amino acids on this peptide.

We also probed the Ga^{3+}-NTA bound phosphopeptides with aminopeptidase, but no cleavage was observed. This may be due either to the affinity media binding the metal ion required for the activity of enzyme or the steric hindrance of the cleavage sites by affinity media. The same results were also observed when aminopeptidase was used to cleave the Ni-NTA bound recombinant proteins [22].

Carboxypeptidase Y can rapidly hydrolyze most amino acids from the C-terminus. The release of G and D, however, is considerably retarded. The digest rate for phosphopeptide T6 is extremely slow due to the presence of D as the second residue from the C-terminus.

Selective Detection of Phosphopeptides in α-Casein: The same strategy was applied to the other commercially available phosphoprotein studied here, α-casein, another milk-derived protein possessing multiple phosphorylation sites. Carr [17] reported the presence of different variants in the commercially available α-casein by MS. He found that this protein contains at least two variants that have low sequence homology. Twelve out of eighteen predicted phosphorylation sites were observed using precursor scans. The method they used could not detect and sequence all the phosphopeptides present in the protein digest, especially those phosphopeptides with multiple phosphorylation sites. They proposed that this was due either to suppression effects or to the fact

the peptides observed in the negative ion mode may not always produce analytically-useful signals in the positive ion mode required for sequencing.

In the present study, agarose loaded with Ga^{3+} was used to isolate phosphopeptides from the protein tryptic digest. Direct analysis by MALDI/MS of the phosphopeptides affinity-bound to the Ga^{3+}-loaded agarose showed that two ions corresponding to phosphopeptides that had been observed in the β-casein tryptic digest analysis in addition to the expected phosphopeptides from these two α-casein variants (shown in Figure 3-4A). There were also a few unidentified peaks that may be either from unknown variants of the protein or nonphosphorylated peptides that co-purified. The still affinity-bound phosphopeptides were treated with phosphatase. As shown in Figure 3-4B and Table 3-1, the m/z of most of the resulting peaks matched the predicted tryptic peptides. These results show that using Ga^{3+} loaded agarose allows the detection of phosphopeptides with multiple phosphate groups. Due to the complexity of the sample, carboxypeptidase Y digest was not performed on the analytes to further locate the phosphorylation sites. Sequence information of mixtures of bound phosphopeptides may also be achieved using PSD [18]. As the purpose of the present experiment was to test the usefulness of the Ga^{3+} to isolate phosphopeptides from protein tryptic digests, no attempt was made to further locate the phosphorylation sites on the phosphopeptides by PSD.

Selectivity Evaluation of Metal Ions: Tryptic digests of β-casein and α-casein were also analyzed using Fe^{3+}-loaded agarose. It is interesting to note that Fe^{3+} and Ga^{3+} exhibited different selectivities for phosphopeptides. Shown in Figure 3-5A, direct analysis of phosphopeptides from the β-casein tryptic digest affinity-bound to Fe^{3+}-loaded agarose showed only the monophosphorylated peptides T6(1P) and T4-6(1P). However, T1-2 (m/z 2804) and T1-2 (1P) (m/z 2884) appeared after the treatment of the affinity-bound phosphopeptides with phosphatase, shown in Figure 3-5B. This implies that Fe^{3+}-loaded agarose may also bind to multiphosphorylated peptides, but the binding is sufficiently strong that the multiphosphorylated peptides are not easily dissociated from the agarose by the laser, making detection very difficult. Direct analysis of phosphopeptides from an α-casein tryptic digest affinity-bound to Fe^{3+}-loaded agarose only showed the monophosphorylated peptides T14-15(1P) and T15(1P) from the S1 variant of α-casein. After phosphatase treatment of the digest affinity-bound to Fe^{3+}-loaded agarose, the m/z of the resulting peaks matched the predicted tryptic digests (Figure 3-6).

In summary, eight tryptic phosphopeptides containing a total of 21 phosphorylated residues from the three phosphoproteins could be identified by using both Fe^{3+} and Ga^{3+}-loaded agarose beads as shown in table 1. Only one expected tryptic phosphopeptide, containing two phosphorylated residues, was not observed. This may be due to suppression effects or to a very low yield of this peptide from the digest.

It was noticed that Fe^{3+}-loaded IDA agarose showed less specificity for the phosphorylated peptides than Fe^{3+}-loaded NTA agarose (data not shown). Unlike NTA agarose, some unphosphorylated peptides were also co-isolated using IDA agarose. This may be due to the NTA agarose having a higher affinity to Fe^{3+}, thus avoiding the nonspecific adsorption of non-phosphorylated peptides onto the matrix. This result was also consistent with the published data where MALDI/MS was performed on the phosphopeptides eluted from Fe^{3+}-loaded agarose [30,31].

CONCLUSIONS

We have shown that the rapid identification of phosphorylation sites can be achieved by direct analysis of enzymatic digestion products affinity bound to metal ions by MALDI/MS. The number of phosphorylation sites can be easily obtained based on the molecular weight shift before and after treatment with phosphatase. The use of carboxypeptidase Y enables the determination of the exact location of the phosphorylation sites. This method eliminates HPLC separation, and thus greatly simplifies the sample preparation.

This method was successfully tested on two commercially available phosphoproteins. Both metal ion-loaded agaroses show selectivity for phosphopeptides. While Ga^{3+}-loaded agarose has better overall selectivity for phosphopeptides, Fe^{3+}-loaded agarose shows higher selectivity for the monophosphorylated peptide. It is our recommendation that the phosphoproteins

should be analyzed with both metal ions to have the greatest chance for the characterization of all the phosphorylation sites.

ACKNOWLEDGMENT

Support for the purchase of the MALDI/TOF instrument by the NIH, Office of AIDS Research is gratefully acknowledged.

REFERENCES:

1. Krebs, E. G. The Growth of Research on Protein Phosphorylation. *Trends Biol. Sci.,* **1994,** *19*, 439-439.
2. Hunter, T. Protein Kinases and Phosphatases: the Yin and Yang of Protein Phosphorylation and Signaling. *Cell*, **1995,** *80*, 225-236.
3. Posada, J., Cooper, J. A. Molecular Signal Integration. Interplay between Serine, Threonine, and Tyrosine Phosphorylation. *Mol. Biol. Cell*, **1992,** *3*, 583-592.
4. Kemp, B. E. Ed. *Peptides and Protein Phosphorylation*, CRC: Boca Raton, FL, 1990.
5. Yan, J. X., Packer, N. H., Gooley, A. A., Williams, K. L. Protein Phosphorylation: Technology for the Identification of Phosphoamino Acids. *J. Chromatogr.*, **1998**, *808*, 23-41.
6. Boyle, W. J., Geer, Van der P., Hunter, T. Phosphopeptide Mapping and Phosphoamino Acid Analysis by Two-Dimensional Separation on Thin-Layer Cellulose Plates. *Methods Enzymol*., **1991,** *201*, 110-149.
7. Aebersold, R., Watts, J. D., Morrison, H. D., Bures, E. Determination of the Site of Tyrosine Phosphorylation at the Low Picomole Level by Automated Solid-Phase Sequence Analysis. *Anal. Biochem.*, **1991,** *199*, 51-60.
8. Wettenhall, R. E. H., Aebersold, R., Hood, L. E. Solid-Phase Sequencing of ^{32}P-labeled Phosphopeptides at Picomole and Subpicomole Levels. *Methods Enzymol*., **1991,** *201*, 186-200.

9. Guy, G. R., Philiip, R., Tan, Y. H. Analysis of Cellular Phosphoproteins by Two-Dimensional Gel Electrophoresis: Applications for Cell Signaling in Normal and Cancer Cells. *Electrophoresis,* **1994**, *15*, 417-444.
10. Zhao, J. Y., Kuang, J., Adlakha, R. C., Rao, P. N. Threonine Phosphorylation is Associated with Mitosis in Hela Cells. F*EBS Lett*., **1989,** *249*, 389-395.
11. Abu-lawi, K. I., Sultzer, B. M. Induction of Serine and Threonine Protein Phosphorylation by Endotoxin-Associated Protein in Murine Resident Peritoneal Macrophages. *Infect. Immun*., **1995,** *63*, 498-502.
12. Hardie, D. G., ed. Protein Phosphorylation. A Practical Approach, c. **1993,** Oxford University Press, Inc., NY.
13. Arad-Dann, H., Beller, U., Haimovitch, R., Gavrieli, Y., Ben-Sasson, S. A. Immunohistochemistry of Phosphotyrosine Residues: Identification of Distinct Intracellular Patterns in Epithelial and Steroidogenic Tissues. *J. Histochem. Cytochem*., **1993,** *41*, 513-519.
14. Annan, R. S., Carr. S. A. The Essential Role of Mass Spectrometry in Characterizing Protein Structure: Mapping Posttranslational Modifications. *J. Protein Chem.,* **1997**, *16,* 391-402.
15. Qin, J., Chait, T. Identification and Characterization of Posttranslational Modifications of Proteins by MALDI Ion Trap Mass Spectrometry. *Anal. Chem.,* **1997,** *69*, 4002-4009.
16. Liao, P. C., Leykam, J., Andrews, P. C., Cage, D. A., Allison, J. An Approach to Locate Phosphorylation Sites in a Phosphoprotein: Mass Mapping by

Combining Specific Enzymatic Degradation with Matrix-Assisted Laser Desorption/Ionization Mass Spectrometry. *Anal. Biochem.*, **1994**, *219*, 9-20.

17. Carr, S. A., Huddleston, M. J., Annan, R. S. Selective Detection and Sequencing of Phosphopeptides at the Femtomole Level by Mass Spectrometry. *Anal. Biochem.*, **1996,** *239*, 180-192.
18. Annan, R. S., Carr, S. A. Phosphopeptide Analysis by Matrix-Assisted Laser Desorption Time-of-Flight Mass Spectrometry. *Anal. Chem.,* **1996,** *68*, 3413-3421.
19. Immler, D., Gremm, D., Kirsch, D., Spengler, B., Presek, P., Meyer, H. E. Identification of Phosphorylated Proteins from Thrombin-activated Human Platelets Isolated by Two-Dimensional Gel Electrophoresis by Electrospray Ionization-Tandem Mass Spectrometry (ESI-MS/MS) and Liquid Chromatography-Electrospray Ionization-Mass Spectrometry (LC-ESI-MS). *Electrophoresis*, **1998,** *19*, 1015-1023.
20. Posewitz, M., Tempst, P. Immobilized Gallium (III) Affinity Chromatography of Phosphopeptides. *Anal. Chem.,* **1999,** *71,* 2883-2892.
21. Papac, D. I., Hoyes, J., Tomer, K. B. Direct Analysis of Affinity-Bound Analytes by MALDI/TOF MS. *Anal. Chem.,* **1994,** *66*, 2609-2613.
22. Qian, X. H., Zhou, W., Khaledi, M. G., Tomer, K. B. Direct Analysis of the Products of Sequential Cleavages of Peptides and Proteins Affinity-Bound to Immobilized Metal Ion Beads by Matrix-Assisted Laser Desorption/Ionization Mass Spectrometry. *Anal. Biochem.,* **1999,** 274, 174-180.

23. Anderrsson, L., Porath, J. Isolation of Phosphoproteins by Immobilized Metal (Fe^{3+}) Affinity Chromatography. *Anal. Biochem.,* **1986,** *154*, 250-254.

24. Muszynska, G., Dobrowolska, G., Medin, A., Ekamn, P., Porath, J. O. Model Studies on Iron (III) Ion Affinity Chromatography II. Interaction of Immobilized Iron (III) Ions with Phosphorylated Amino Acids, Peptides and Proteins. *J. Chromatogr*., **1992,** *604*, 19-28.

25. Olcott, M. C., Bradley, M. L., Haley, B. E. Photoaffinity Labeling of Creatine Kinase with 2-Azido-and 8-Azidoadenosine Triphosphate: Identification of Two Peptides from the ATP-Binding Domain. *Biochem.*, **1994,** *33*, 11935-11941.

26. Nuwaysir, L. M., Stults, J. T. Electrospray Ionization Mass Spectrometry of Phosphopeptides Isolated by On-Line Immobilized Metal-Ion Affinity Chromatography. *J. Am. Soc. Mass Spectrom*., **1993,** *4*, 662-669.

27. Michel, H., Hunt, D. F., Shabanowitz, J., Bennett, J. Tandem Mass Spectrometry Reveals that Three Photosystem II Proteins of Spinach Chloroplasts Contain N-Acetyl-O-Phosphothreonine at Their NH_2 Termini. *J. Biol. Chem.,* **1988,** *263*, 1123-1130.

28. Hanger, D. P., Betts, J. C., Loviny, T. L. F., Blackstock, W. P., Anderton, B. H. New Phosphorylation Sites Identified in Hyperphosphorylated Tau (Paired Helical Filament-Tau) from Alzheimer's Disease Brain Using Nanoelectrospray Mass Spectrometry. *J. Neurochem.,* **1998,** *71 (6)*, 2465-2476.

29. Cleverley, K. E., Betts, J. C., Blackstock, W. P., Gallo, J-M., Anderton, B. H. Identification of Novel in Vitro PKA Phosphorylation Sites on the Low and Middle Molecular Mass Neurofilament Subunits by Mass Spectrometry. *Biochem.,* **1998,** *37*, 3917-3930.

30. Neville, D. C. A., Rozanas, C. R., Price, E. M., Gruis, D. B., Verkman, A. S., Townsend, R. R. Evidence for Phosphorylation of Serine 753 in CFTR using a Novel Metal-Ion Affinity Resin and Matrix-Assisted Laser Desorption Mass Spectrometry. *Protein Science*, **1997,** *6*, 2436-2445.

31. Hochuli, E., Dobeli, H., Schacher, A. New Metal Chelate Adsorbent Selective for Proteins and Peptides Containing Neighbouring Histidine Residues. *J. Chromatogr*., **1987,** *411*, 177-184.

32. Asara, J. M., Allison, J. Enhanced Detection of Phosphopeptides in Matrix-Assisted Laser Desorption/Ionization Mass Spectrometry Using Ammonium Salts. *J. Am. Soc. Mass Spectrom.,* **1999**, *10*, 35-44.

33. Neubauer, G., Mann, M. Mapping of Phosphorylation Sites of Gel-Isolated Proteins by Nanoelectrospray Tandem Mass Spectrometry: Potentials and Limitations. *Anal. Chem.*, **1999**, *71*, 235-242.

34. Zhang, X. L., Herring, C. J., Romano, P. R., Szczepanowska, J., Brzeska, H., Hinnebusch, A. G., Qin, J. Identification of Phosphorylation Sites in Proteins Separated by Polyacrylamide Gel Electrophoresis. *Anal. Chem.,* **1998,** *70*, 2050-2059.

35. Li, S., Dass, C. Iron(III)-Immobilized Metal Ion Affinity Chromatography and Mass Spectrometry for the Purification and Characterization of Synthetic Phosphopeptides. *Anal. Biochem*., **1999**, *270*, 9-14.
36. Dumas, B. R., Brignon G., Grosclaude, F., Mercier, J-C. Structure Primaire de la Casein β Bovine. *Eur. J. Biochem*., **1972**, *25*, 505-514.
37. Dumas, B. R., Brignon G., Grosclaude, F., Mercier, J-C. Structure Primaire de la Casein β Bovine. *Eur. J. Biochem*., **1971**, *20*, 264-268.

Figure 3-1: Scheme of the identifying phosphorylation sites by IMAC/MALDI/TOF/MS

Figure 3-2: MALDI/TOF mass spectra of (A) Ga^{3+}-NTA bound phosphopeptides from β-casein tryptic digest, (B) the same peptides after the phosphatase treatment (both beads and supernatant). T6 (1P): FQpSEEQQQTEDELQDK, T1-2 (4P): RELEENVPGEIVEpSLpSpSpSEESITR.

Figure 3-3: MALDI/TOF mass spectra of (A-C) Ga^{3+}-NTA bound phosphopeptides from β-casein tryptic digest after carboxypeptidase Y digest for (A) 25 min, (B) 4 hr, (C) overnight, (D) peptides after the phosphatase treatment of the Ga^{3+}-NTA bound phosphopeptides from β-casein tryptic digest after carboxypeptidase Y digest overnight (both beads and supernatant). T1-2 (4P): RELEENVPGEIVEpSLpSpSpSEESITR. Spectra A-C were recorded in the negative mode.

Figure 3-4: MALDI/TOF mass spectra of (A) Ga^{3+}-NTA bound phosphopeptides from the α-casein tryptic digest, (B) the same peptides after the phosphatase treatment (both beads and supernatant). 25 mM ammonium citrate was in the matrix.

Figure 3-5: MALDI/TOF mass spectra of (A) Fe^{3+}-NTA bound phosphopeptides from the β-casein tryptic digest, (B) the same peptides after the phosphatase

treatment (both beads and supernatant). T6 (1P): FQpSEEQQQTEDELQDK, T4-6 (1P): KIEKFQpSEEQQQTEDELQDK, T1-2 (4P): RELEENVPGEIVEpSLpSpSp SEESITR. *: unidentified peak.

Figure 3-6: MALDI/TOF mass spectra of (A) Fe^{3+}-NTA bound phosphopeptides from the α-casein tryptic digest, (B) the same peptides after the phosphatase treatment (both beads and supernatant). T15 (1P): VPQLEIVPNPSAEER, T14-15 (1P): YKVPQLEIVPNPSAEER. 25 mM ammonium citrate was in the matrix.

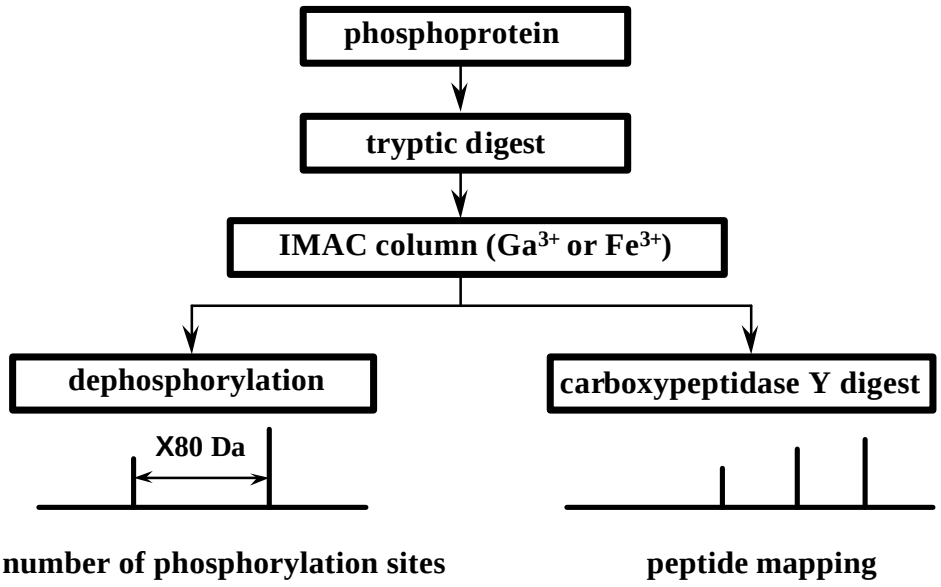
phosphoprotein
tryptic digest
IMAC column (Ga^{3+} or Fe^{3+})
dephosphorylation
carboxypeptidase Y digest
X80 Da
number of phosphorylation sites
peptide mapping

Figure 3-1

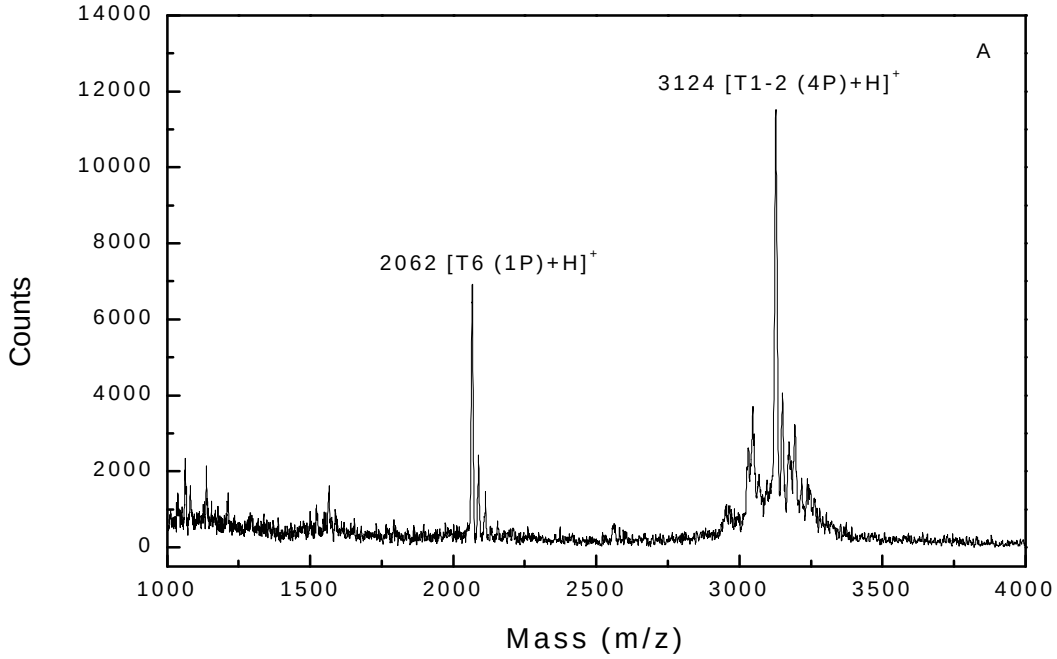
A
3124 [T1-2 (4P)+H]+
2062 [T6 (1P)+H]+
Counts
Mass (m/z)
14000
12000
10000
8000
6000
4000
2000
0
1000
1500
2000
2500
3000
3500
4000

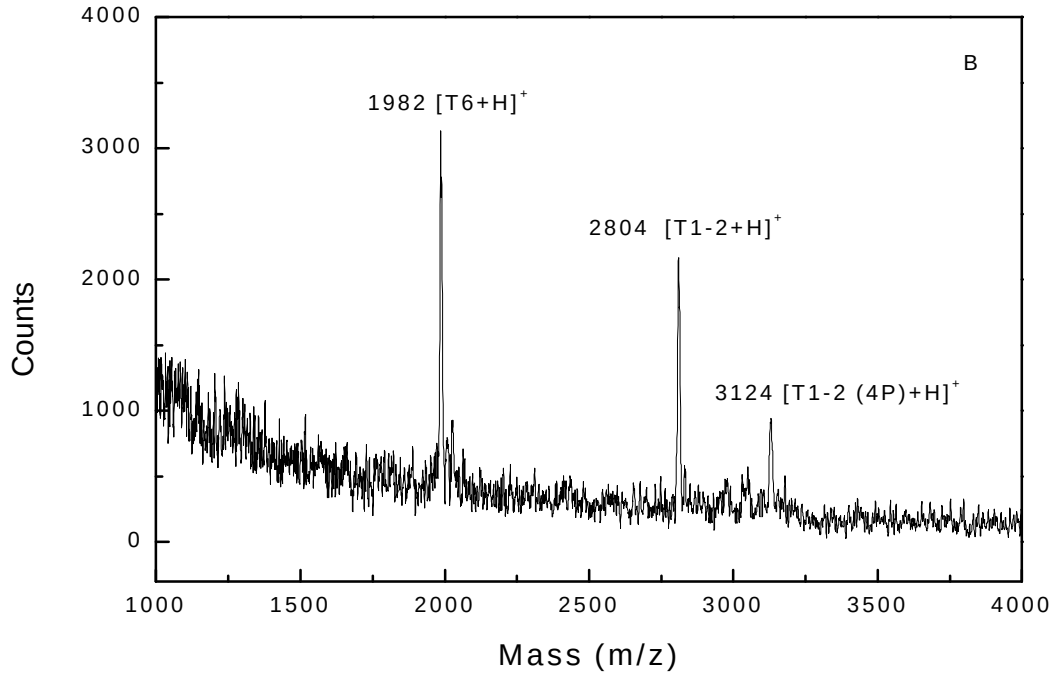
B
1982 [T6+H]+
2804 [T1-2+H]+
3124 [T1-2 (4P)+H]+
Counts
Mass (m/z)
4000
3000
2000
1000
0
1000
1500
2000
2500
3000
3500
4000

Figure 3-2

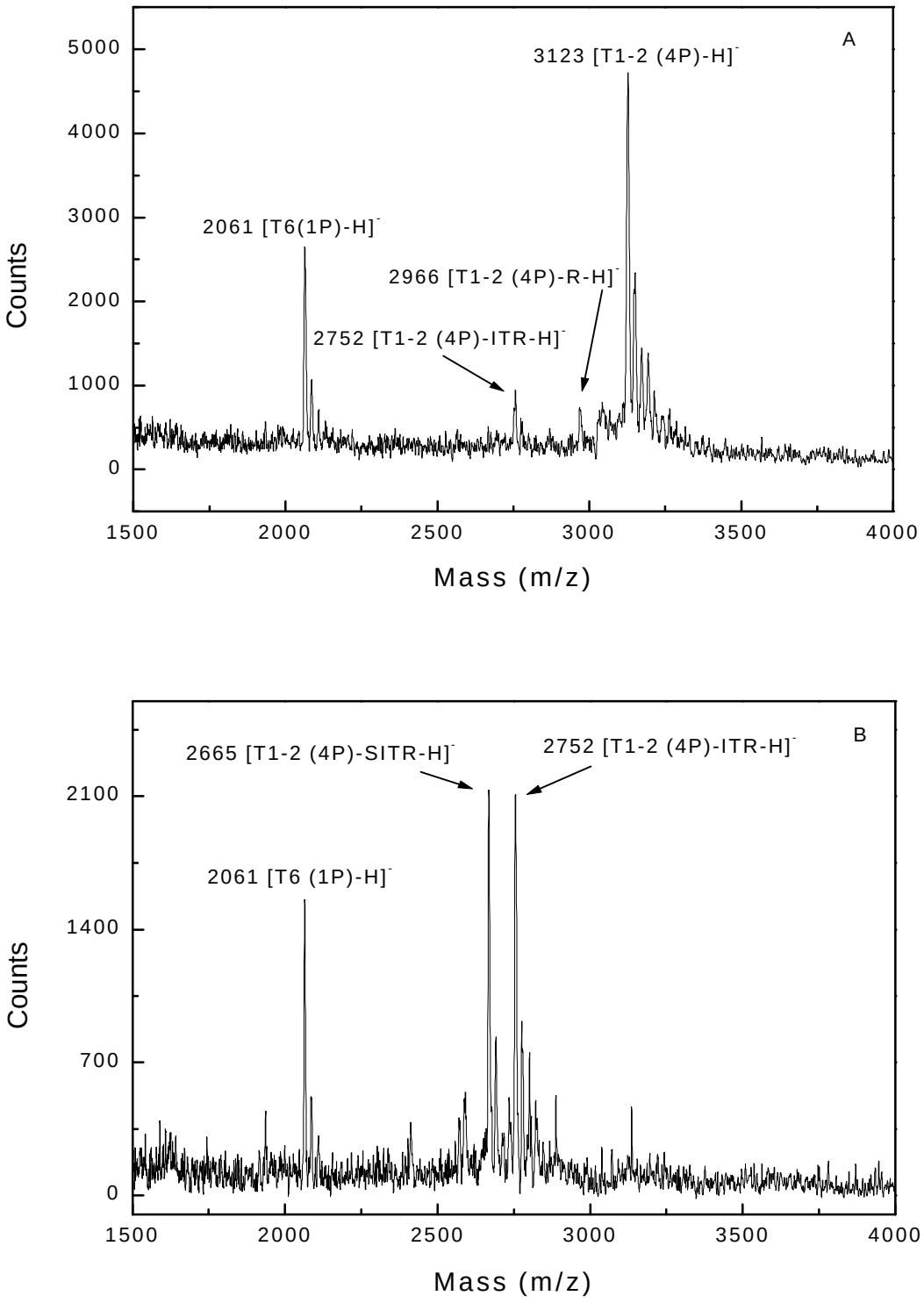
A
3123 [T1-2 (4P)-H]-
2061 [T6(1P)-H]-
2966 [T1-2 (4P)-R-H]-
2752 [T1-2 (4P)-ITR-H]-
Counts
Mass (m/z)
B
2665 [T1-2 (4P)-SITR-H]-
2752 [T1-2 (4P)-ITR-H]-
2061 [T6 (1P)-H]-
Counts
Mass (m/z)

Figure 3-3

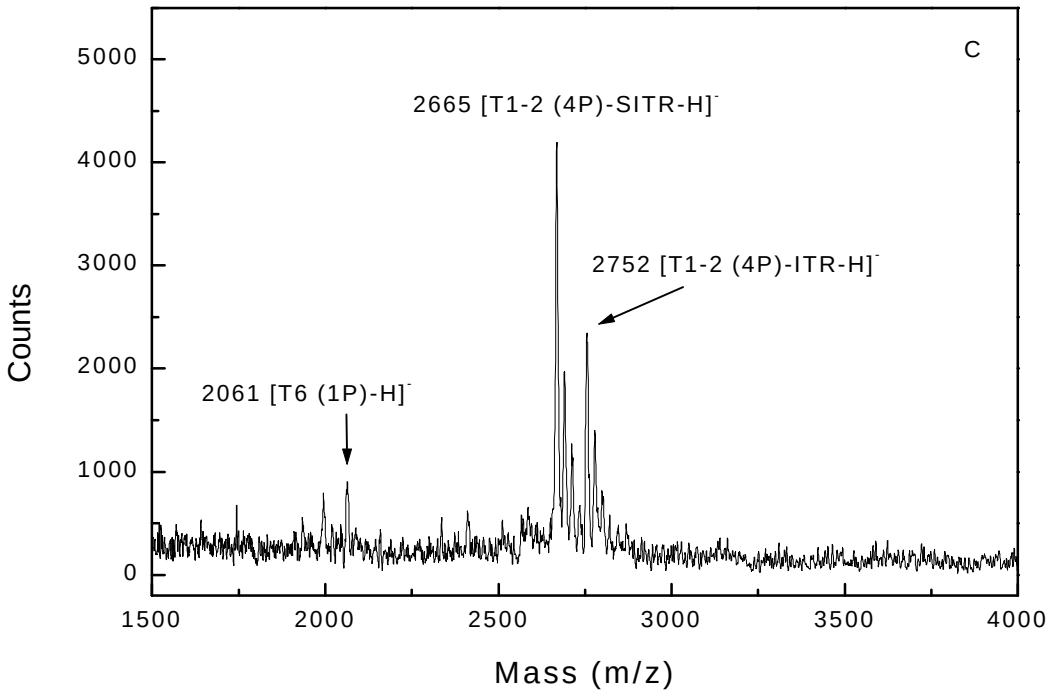
C
2665 [T1-2 (4P)-SITR-H]-
2752 [T1-2 (4P)-ITR-H]-
2061 [T6 (1P)-H]-
Counts
Mass (m/z)
5000
4000
3000
2000
1000
0
1500
2000
2500
3000
3500
4000

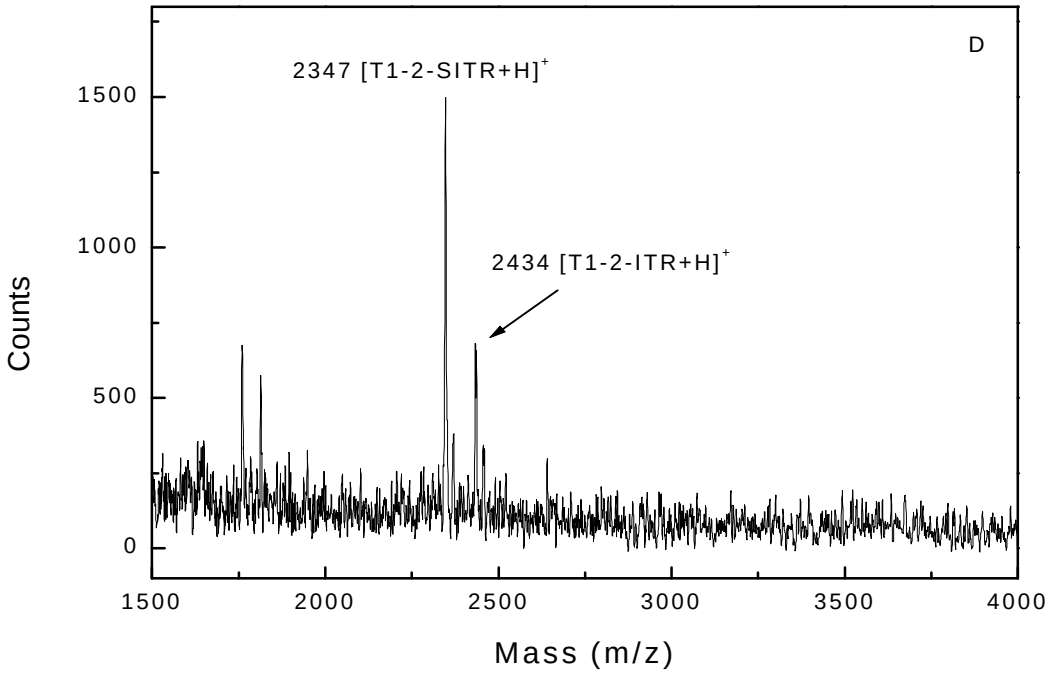
D
2347 [T1-2-SITR+H]+
2434 [T1-2-ITR+H]+
Counts
Mass (m/z)
1500
1000
500
0
1500
2000
2500
3000
3500
4000

Figure 3-3

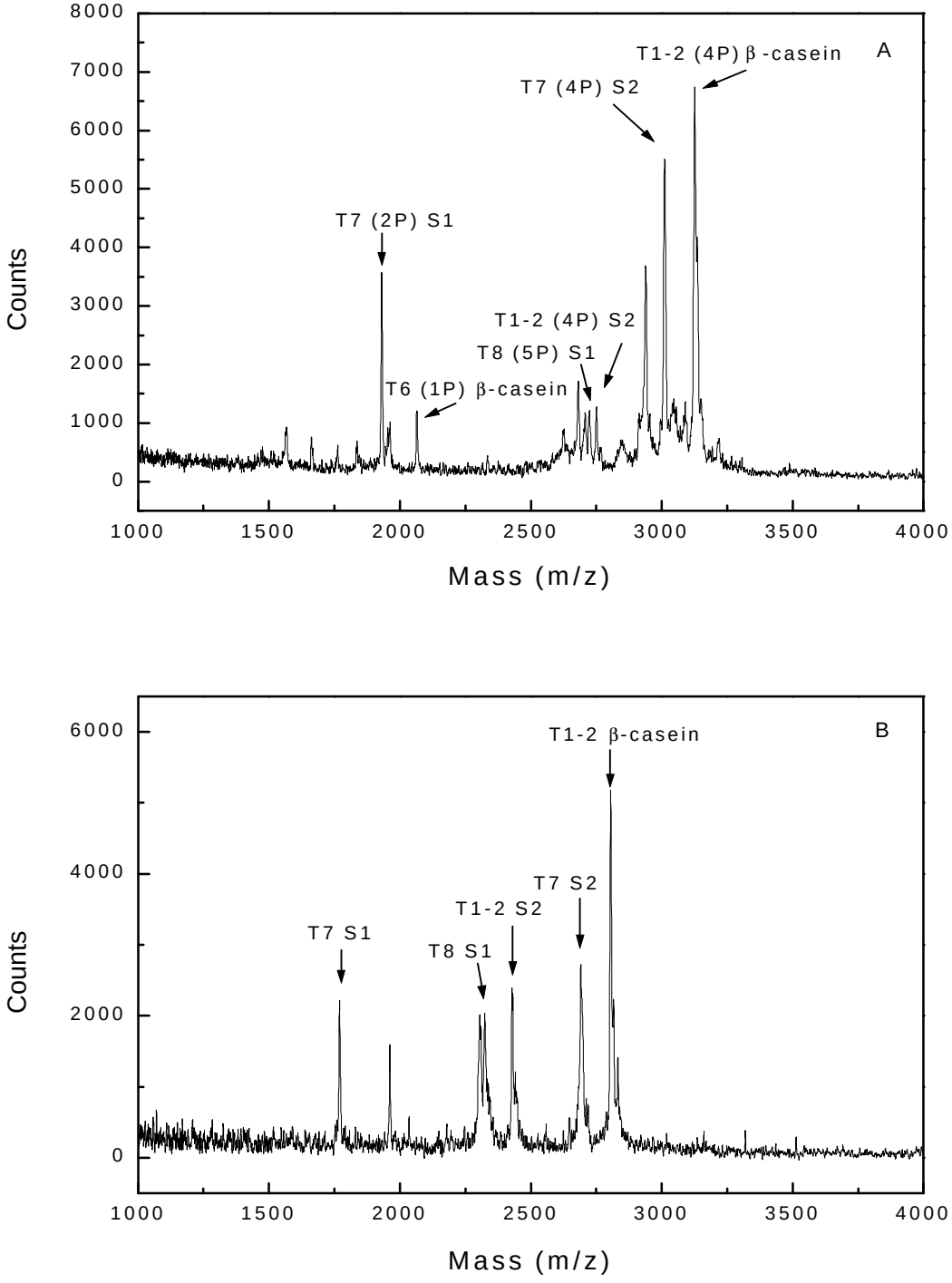
A
T1-2 (4P) β-casein
T7 (4P) S2
T7 (2P) S1
T1-2 (4P) S2
T8 (5P) S1
T6 (1P) β-casein
Counts
Mass (m/z)
B
T1-2 β-casein
T7 S2
T1-2 S2
T7 S1
T8 S1
Counts
Mass (m/z)

Figure 3-4

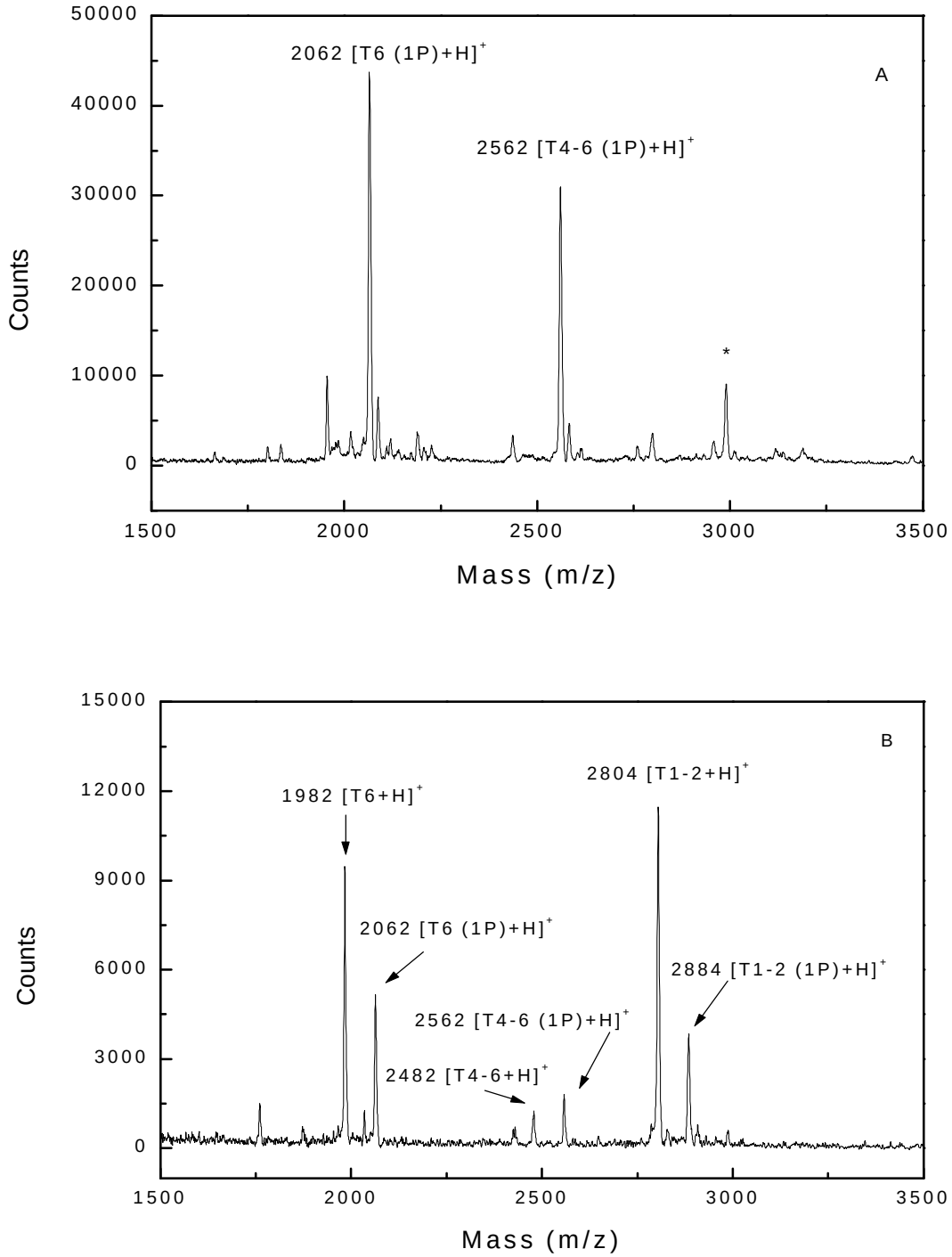
A
2062 [T6 (1P)+H]+
2562 [T4-6 (1P)+H]+
*
Counts
Mass (m/z)
B
1982 [T6+H]+
2804 [T1-2+H]+
2062 [T6 (1P)+H]+
2884 [T1-2 (1P)+H]+
2562 [T4-6 (1P)+H]+
2482 [T4-6+H]+
Counts
Mass (m/z)

Figure 3-5

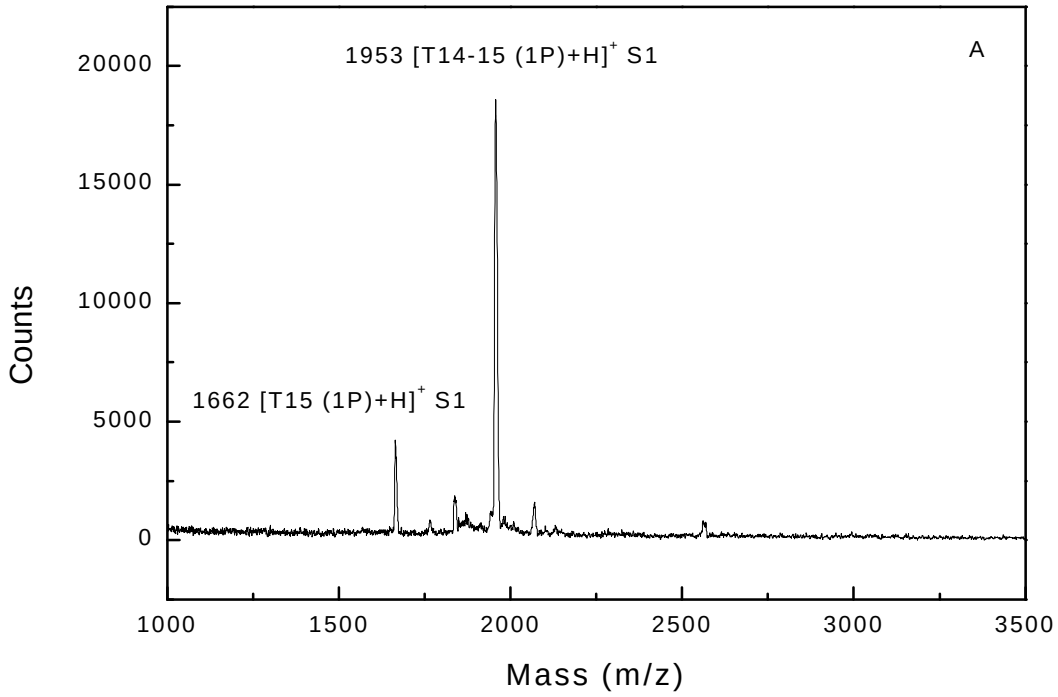
1953 [T14-15 (1P)+H]+ S1
A
1662 [T15 (1P)+H]+ S1
Counts
Mass (m/z)

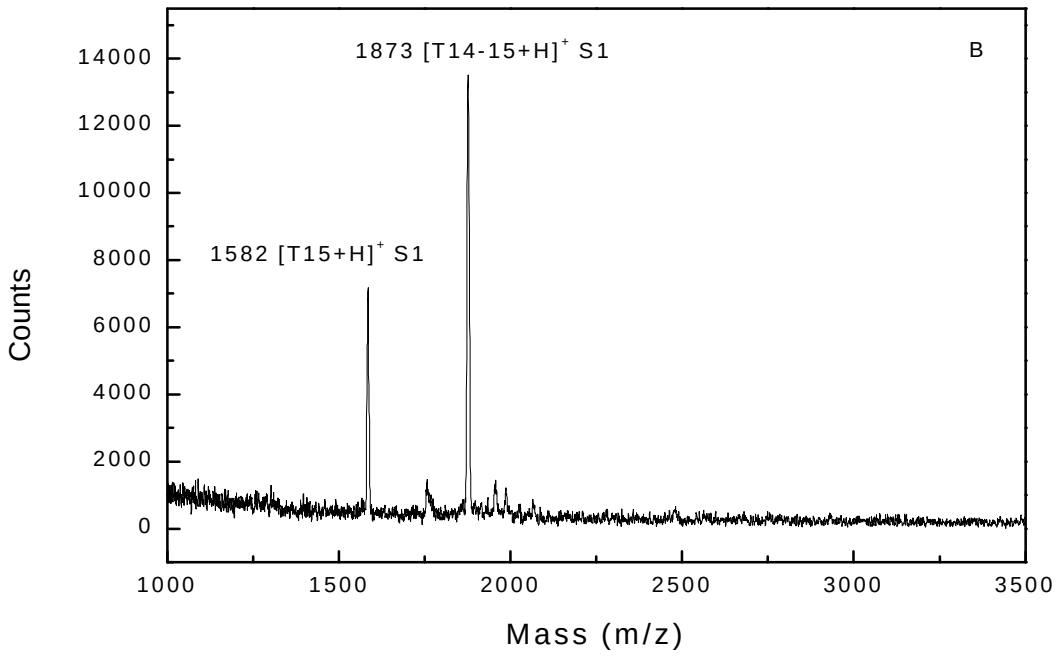
1873 [T14-15+H]+ S1
B
1582 [T15+H]+ S1
Counts
Mass (m/z)

Figure 3-6

Table 3-1. Expected Phosphopeptides in the Tryptic Digest of α-Casein and β-Casein

tryptic fragment	peptide sequence	source	# of phosphorylation sites	calculated $[M+H]^+$	observed $[M+H]^+$	observed $[M+H]^+$ after dephosphorylation
T15 (aa106-119)	VPQLEIVPN$_P$SAEER	S1 variant	1	1662	1662	1582
T14-15 (aa104-119)	YKVPQLEIVPN$_P$SAEER	S1 variant	1	1953	1954	1874
T7 (aa43-58)	DIG$_p$SE$_p$STEDQAMEDIK	S1 variant	2	1929	1930	1770
T8 (aa59-79)	QMEAE$_p$SI$_p$S$_p$S$_p$SEEIVPN$_p$SVEQK	S1 variant	5	2722	2723	2324
T1-2 (aa1-21)	KNTMEHV$_P$S$_P$S$_P$SEES IIP$_P$SQETYK	S2 variant	4	2749	2750	2430
T7 (aa46-70)	NANEEEYSIG$_P$S$_P$S$_P$S EE$_P$SAEVATEEVK	S2 variant	4	3010	3011	2691
T14 (aa126-136)	EQL$_P$ST$_p$SEENSK	S2 variant	2	1412	*	*
T1-2 (aa1-25)	RELEELNVPGEIVE$_P$SL $_P$S$_P$S$_P$S EESITR	β-casein	4	3124	3125	2805
T4-6 (aa29-48)	KIEKFQ$_P$SEEQQQTEDEL QDK	β-casein	1	2561	2558	2478
T6 (aa33-48)	FQ$_P$SEEQQQTEDELQDK	β-casein	1	2062	2064	1984

*: not observed with this method.

Chapter 4

Application of Immobilized Metal Ion Affinity Chromatography Combined with Matrix Assisted Laser Desorption/Ionization Mass Spectrometry to the Detection of Phosphorylation Sites on Protein p53 and p21

Wei Zhou, B. Alex Merrick, Christopher Borchers, Kenneth B. Tomer,

Morteza G. Khaledi

ABSTRACT

Phosphorylation is believed to be an important regulatory mechanism of the proteins p53 and p21 which play important role in apotosis. In this study, we have developed a method that combined immobilized metal ion affinity chromatography with matrix assisted laser desorption/ionization mass spectrometry to detect the phosphorylation sites on recombinant p53 and the putative phosphorylation site on p21 during peptide mapping. We were able to detect one phosphorylation site at N-terminus of p53 that has not been previously reported. This method also allows isolation and detection of low molecular weight synthetic phosphopeptides in kinase reactions. Fast identification of putative phosphorylation sites on p21 employing low molecular weight peptides was achieved.

INTRODUCTION

Since the discovery of p53 as one of the most important proliferation control proteins, there have been numerous studies of the phosphorylation sites and the of effect of phosphorylation on the function of the protein p53 [1-7]. Studies have shown that phosphorylated regions on p53 are mainly concentrated on the N and the C termini [1-3] (Figure 4-1). The N-terminus region appears to be the most extensively phosphorylated part of the protein and a target of many kinases. Possible phosphorylation sites within the amino terminus are at serines 6, 9, 15, 20, 33 and 37 and threonine 18 [8]. Mutating some of these potential phosphorylation sites affects the transactivation activity of p53 [1-3]. Serines 315, 371, 376, 378, and 392 are possible phosphorylation sites within the carboxy terminus of p53. Phosphorylation at the C-terminus region of p53 changes the conformation of the protein [1-3]. Different conformational states of p53 can be correlated with its functions as an inhibitor or as a stimulator of proliferation. Phosphorylation at the C-terminus of the protein also regulates its DNA binding ability. Studies have shown that unphosphorylated p53 has low affinity to DNA. However, DNA binding is greatly increased when the protein had been phosphorylated *in vitro* [1-3]. Studies conducted so far have indicated that phosphorylation on p53 has a significant effect on the biochemical and functional properties of p53, such as DNA binding, conformation and stability, transactivation, transformation inhibition and growth suppression [1-3].

Protein p21 is a cyclin-kinase inhibitor important in mediating p53-dependent cell-cycle arrest [23-25]. The increase in the amount of p53 results in transcriptional activation of the p21 gene due to the increase in the sequence-specific DNA-binding activity of activated p53 [26]. As a result, the level of p21 is increased. Studies have also shown many other pathways that increase p21 expression that are total independent of p53, such as high levels of toxic oxygen species, vitamin D, etc. [27, 28]. High level of p21 in response to both p53-dependent and p53 independent signals are believed to mediate cell-cycle arrest and differentiation through inhibition of cyclin-dependent kinases (Cdks), a group of kinases that control cell cycle progression [23, 29-31]. Despite the important biological function of the protein p21, phosphorylation sites and their effects on the function of the protein p21 have not yet been thoroughly studied.

Studies of phosphorylation sites and their relationships to biological activities of proteins have been mainly limited to using site-directed mutagenesis at putative or identified phosphorylation sites [5], or using phosphospecific antibodies [9]. Amino acid substitutions, however, at single or several suspected phosphorylation sites within p53 have often yielded conflicting and confusing results, probably because of the interdependent nature of the multiple phosphorylations upon p53 activity [10]. Using antibodies directed against serine 15, 37 or 392 can detect increased phosphorylation after DNA damage in cells exposed to ionizing or UV irradiation [11]. This method, however, requires that each potential phosphorylation site be examined individually with different

antibodies. Besides of the high cost, generation of phosphospecific antibodies requires prior knowledge of the phosphorylation sites, which limits its application in the detection of unknown phosphorylation sites. For example, though a few papers have indicated the existence of phosphorylation on p21 [12], the exact location and the consequence of p21 phosphorylation have not been reported. It is, therefore, difficult to generate all the possible phosphospecific antibodies needed to determine the phosphorylation sites on p21.

Mass spectrometry (MS) has been shown to be a sensitive, rapid and unambiguous technique for study of phosphorylation sites on proteins [18-22]. In addition, MS does not require prior knowledge of the unknown phosphorylation sites, thus, making this method more attractive for the study of undefined proteins. Recent studies have demonstrated the usefulness of MS in the study of phosphorylation sites on p53. The presence of phosphate groups at both serine 375 and 389 have been verified by LC/MS analysis of the tryptic digest of p53 expressing in baculovirus infected insect cells [9]. Other studies have used nanospray ion trap MS to study the increased phosphorylation of serines 33 and 37 in p53 as a result of ultraviolet or ionizing radiation [4]. Detecting phosphorylation sites on p53 by MS, however, has its difficulties. First, the level of p53 present in cells frequently falls below the sensitivity of MS. Second, p53 is phosphorylated at multiples sites, some of the which are clustered. Due to the interference of the negative charge on the phosphate group for positive ion MS detection, it can often be difficult to detect a phosphopeptide with multiple

phosphorylation sites. There have, therefore, been relatively few studies of the phosphorylation sites on p53 and their effect on biochemical functions by MS.

Immobilized metal ion affinity chromatography (IMAC) combined with MS has been shown to be very useful in detecting phosphopeptides with multiple phosphorylation sties [16,22]. In this study, a baculovirus expression system was used to generate sufficient amounts of p53 in its normal phosphorylation site for MS analysis. Treatment of the cells with okadaic acid, a phosphatase inhibitor, during the final stage of expression creates a hyper-phosphorylated form of p53 that alters transcriptional activation of p53 *in vitro* and in animal studies [13,14]. IMAC combined with MALDI/MS was used to study the phosphorylation status of both forms of p53 and to determine the specific changes in phosphorylation induced by okadaic acid treatment. The high sensitivity of this method enabled us to detect one phosphorylation site at the N-terminus of p53 that has not been previously reported.

10- to 15-mer peptides which cover almost the whole sequence of p21 were synthesized and used to determine the putative phosphorylation sites on p21 *in vitro*. The synthetic peptide was first reacted with Cdk2, a cell cycle regulating cyclin dependent kinase 2, to phosphorylate serine in the sequence. The resulting reaction mixture was then analyzed by IMAC/MALDI/MS to detect the formation of a phosphopeptide. The method enables isolation and detection of low mass synthetic phosphopeptide in a kinase reaction. Rapid identification of

the phosphorylation site during the peptide mapping is, therefore, achieved. The results obtained indicate the possible phosphorylation sites on p21.

MATERIALS AND METHODS

Chemicals and Reagents. Ni-NTA agarose was purchased from QIAGEN Inc. (Chatsworth, CA, USA). Immobilized trypsin was from PerSeptive Biosystems (Framingham, MA, USA). Ferric chloride was from Allied Chemical (Morristown, NJ, USA). The α-cyano-4-hydroxycinnamic acid, gallium (III) chloride, and other reagents were purchased from Aldrich Chemical Co. (Milwaukee, WI, USA). Compact reaction columns and filters were made by Amersham Pharmacia Biotech (Piscataway, NJ).

Methods

Expression of p53. Recombinant p53 was immunoaffinity purified from a baculovirus system using a sf9 insect cell [11]. Hyper phosphorylated p53 was isolated from sf9 cells treated with 25 μM okadaic acid during the final 12 hr of expression.

HPLC Purification and Separation. Both recombinant forms of p53 were purified by HPLC (HP 1100) using a Vydac C-4 column. The gradient is from 9-54% acetonitrile in 0.1% TFA over 45 min at a flow rate of 1 mL/min. Tryptic digest of both forms of p53 were separated on a Vydac C-18 column.

Tryptic Digest. HPLC purified both forms of p53 were lyophilized and redissolved in 20 μL 50% acetonitrile. A 2 μg trypsin in 80 μL 50 mM ammonium bicarbonate digestion buffer (pH=7.8) was added and the resulting mixture was incubated at 37 °C for four hours on a rotator.

Kinase Assay. Serine phosphopeptides were generated enzymatically by an *in vitro* kinase reaction. All the synthetic peptides were synthesized commercially (Sigma-Genosys Biotechnologies, Inc., The Woodlands, TX) at 95% purity. The carboxy-terminus was amidated. Cdk2-cyclin kinase complexes were used as the enzyme source and were isolated by immunoprecipitation from HT1080 human fibrosarcoma cells [15]. Briefly, cells were lysed with an immunoprecipitation buffer (50 mM Tris pH 8, 130 mM NaCl, 20 mM NaF, 1 mM EDTA, 1% NP-40 with protease and phosphatase inhibitors). Whole cell lysates were created by progressive shearing with 19 and 23 gauge needles to fragment DNA. Cell debris was pelleted by centrifugation at 12,000 x g for 20 min at 4°C. The protein concentration of the lysate was determined, and 200 μg of protein was incubated with anti-cdk2 (M-2 antibody; Santa Cruz Biotech., Santa Cruz, CA). Immune complexes were collected by rotation with protein-G agarose beads reacted with anti-rabbit IgG. The beads were washed four times with immunoprecipitation buffer and twice with kinase buffer (50 mM HEPES pH 7.6, 10 mM $MgCl_2$ and 1 mM dithiothreitol). Each immunoprecipitate received 15 μL of kinase buffer also containing 1 mM NaF, 10 mM β-glycerylphosphate, 200 μM ATP and 0.5 mM of synthetic peptide as a substrate. Reactions were conducted

at 30°C for 30 min. Supernatants from five kinase reactions were pooled and frozen on dry ice until MS analysis.

IMAC Column. IMAC columns were prepared by adding 30 μL of a 50% slurry of Ni-NTA resin into a compact reaction column. The column was washed with 30 μL 100 mM EDTA (3x) to remove any bound Ni^{2+} metal ions. The column was then washed sequentially with 30 μL water (3x), 30 μL 0.1 M acetic acid (3x), and 30 μL 60 mM $GaCl_3$ or 100 mM $FeCl_3$ (3x) to load the column with metal ions. The column was then washed with 30 μL water (3x) followed by 30 μL 0.1 M acetic acid (3x) to remove any unbound metal ions. Binding of phosphopeptides to the metal chelator was achieved by loading the protein digest or a kinase reaction mixture onto the IMAC column and incubating at 37 °C for 30 min on a rotator. The column was washed with 50 μL water (3x) and 50 μL 0.1 M acetic acid (3x) to remove non-phosphorylated peptides. A 0.5 μL aliquot of the resin was placed directly onto the MALDI target followed by a 0.5 μL aliquot of the matrix solution. The sample was then allowed to dry at room temperature before loading into the mass spectrometer. In the analysis of p53, a 0.5 μL aliquot of the resin, a 0.5 μL aliquot of the matrix solution and a 0.5 μL aliquot of 25 mM ammonium citrate were placed onto MALDI target and allowed to dry at room temperature. Ammonium citrate has been reported to be able to enhance the detection of phosphopeptides in MALDI/MS analysis [23].

MALDI/MS. Mass spectra were acquired on a Voyager-RP (PerSeptive Biosystem, Framingham, MA, USA) equipped with a nitrogen laser (λ=337nm). The accelerating voltage used was 30 kV. All spectra were recorded in the positive ion linear mode. A saturated solution of recrystallized α-cyano-4-hydroxycinnamic acid in ethanol:water:formic acid (45:45:10), prepared fresh daily, was used as the MALDI matrix. Samples were prepared by mixing equal volumes of analyte and matrix solution on the target and letting them dry. Ammonium citrate additive was used in the p53 analysis. An equal volume of ammonium salt solution was mixed with the analyte and matrix solutions. Mass calibration was performed by using angiotensin I [$(M+H)^+$=1297.51] and insulin (bovine) [$(M+H)^+$=5734.59] as external standards.

RESULTS AND DISCUSSION

Application of IMAC/MALDI/MS to the Analysis of p53: To elucidate the role of phosphorylation of p53, the baculovirus expression system was employed to express recombinant p53 for MS analysis in this study. This system allows one to mimic different phosphorylation states of recombinant proteins by employing the phosphatase inhibitor, okadaic acid, during the final stage of expression. Under normal conditions, the protein is partially phosphorylated at its potential phosphorylation sites, with perhaps, only a fraction of the molecules being phosphorylated. This is called the normal phosphorylation form. Upon

treatment of the cells with okadaic acid, p53 is activated by transformation to a highly phosphorylated state in which it is phosphorylated at additional sites and in a major fraction of the molecules. It is termed the hyper-phosphorylated form. Studies have shown that when the DNA damage overwhelms its repair system, p53 is transformed from its normal phosphorylation state to its hyper-phosphorylation state, which alters transcriptional activation of p53 and triggers cell death [14]. Studying the phosphorylation status of different forms of p53 and determining specific changes in phosphorylation induced by okadaic acid treatment, therefore, are important in understanding functional changes of the protein.

Both forms of the expressed p53 were purified by HPLC. MALDI/MS analysis of normal and hyper-phosphorylated p53 after HPLC purification shows that the M_r of normal phosphorylated p53 was approximately 43893 and M_r of hyper phosphorylated p53 was approximately 44058 (data not shown). Because the characteristic molecular weight of one phosphate group is 80 Da, the 165 Da mass difference between normal and hyper phopshorylated p53 indicates that there are at least two and possibly more phosphate groups on hyper-phosphorylated p53 compared to normal p53. As discussed before, proteins with multiple phosphorylation sites may exhibit low MS response, though this is a much more significant effect in small peptides than in large proteins. Information obtained from the direct analysis of p53 by MALDI, therefore, only indicates the minimum number of additional phosphate groups on hyper phosphorylated p53.

The different forms of p53 were treated with trypsin. Figure 4-2 shows the MALDI/MS spectra of tryptic peptides from normal and hyper phosphorylated p53. Some tryptic peptides from p53 could be identified based on the known protein sequence. In addition, the MALDI/MS spectrum (Figure 4-2A) of tryptic peptides from normal phosphorylated p53 showed an ion corresponding to the tryptic fragment T2 (^{25}LLPENNVLSPLPSQAMDDLMLSPDDIEQWFTEDPGPDEA PR^{65}) and the ion corresponding to T2 with one phosphorylation site, although T2 contains as many as four potential phosphorylation sites. The MALDI/MS spectrum (Figure 4-2B) of tryptic peptides from hyper phosphorylated p53 does not show an ion due to the tryptic fragment T2, which may be due to a combination of suppression effects and the low MS response of phosphopeptides with multiple phosphate groups. In order to overcome the suppression effects, HPLC was performed prior to MS analysis. The LC/MS analysis shows the degree of phosphorylation of hyper-phosphorylated p53 was higher than that of the normal phosphorylated form (Figure 4-3). Only one phosphorylation site, however, can be detected on T2 even with HPLC separation. Again, no ions arising from more highly phosphorylated T2 species were observed which may due to the low MS response of phosphopeptides with multiple phosphate groups.

Metal ions, such as Fe^{3+}, Al^{3+} or Ga^{3+} exhibit high specificity for phosphopeptides. Among the different metal ions, Ga^{3+} shows higher specificity for phosphopeptides with multiple phosphate groups. It also shows less

interference from peptides containing negatively charged amino acid, such as E or D [16,22]. Tryptic digests from different forms of p53 were loaded onto a Ga^{3+} metal ion column. The column was washed with buffer to remove non-phosphopeptides. By isolating phosphopeptides from the tryptic digest prior to MS analysis, suppression effects are greatly minimized. Affinity-bound phosphopeptides were then analyzed directly by MALDI/MS, which reduced sample loss. Figure 4-4 shows the MALDI/MS spectra of phosphopeptides from normal and hyper-phosphorylated p53 after tryptic digest and Ga^{3+} beads isolation. Three peaks with a mass difference of 80 Da were detected after isolation with Ga^{3+} resin. Based on the known protein sequence, these three ions corresponded to the tryptic peptide T2 with one, two or three phosphate groups. Although it has been reported that serines 33 and 37 are phosphorylated on T2 [4]. there has been no report regarding possible phosphorylation on serine 46 or threonine 55 of tryptic peptide T2. IMAC combined with MALDI/MS data clearly showed that there are three phosphorylated sites on T2. The degree of phosphorylation also increased dramatically after the okadaic acid treatment. As indicated in Figure 4B, the relative abundance of the ion corresponding to T2 with three phosphate groups increased significantly. Due to the limited amount of the peptide isolated, carboxypeptidase Y digest was unsuccessful at locating the exact phosphorylation sites.

Application of IMAC/MALDI/MS to the Analysis of p21: The experimental approaches to the determination of putative phosphorylation sites

on proteins often employ synthetic peptides. Peptides with 10 to 15 amino acids corresponding to a part of the protein sequence were synthesized, and these synthetic peptides were allowed to react with a kinase. The resulting reaction mixtures were then analyzed by various methods to determine the formation of phosphorylated peptides. Though the actual phosphorylation sites may change *in vivo*, results obtained by these methods provide useful information relevant to the elucidation of potential phosphorylation sites on proteins.

Although some synthetic peptides with large molecular weights can be radiolabeled using ^{32}P-ATP with the ^{32}P-labeled peptides being separated by polyacrylamide gel electrophoresis and detected by autoradiography with high sensitivity, the practical lower limit for effective separation of the labeled peptide from unreacted ^{32}P-ATP is about 2,000 Da. Studies employing 10- to 15-mer peptides to determine putative phosphorylation sites can suffer from poor detectability due to poor separation by electrophoresis [17]. Direct MALDI/MS analysis of reaction mixture may be unable to detect the presence of a phosphopeptide if the stoichiometry of the kinase reaction is low. HPLC also may have difficulty in separating phosphopeptides from the parent peptide. In the present study, immobilized metal ion affinity chromatography combined with MALDI/MS was used to isolate and detect phosphopeptides from kinase reactions. IMAC can rapidly concentrate and separate the phosphopeptides from enzyme reactants and provide definitive evidence of phosphorylation based on

MS analysis. An early example of the direct analysis of metal ion affinity-bound peptides demonstrated femtomole level sensitivity [16].

Shown in Figure 4-5 is the MALDI mass spectrum of a synthetic peptide (RDFYHpSKRRLI, m/z 1570) containing serine 153 of p21 that was tested before and after using Fe^{3+}-loaded agaroses for phosphopeptide isolation. The substrate showed low affinity and low phosphopeptide production under a variety of kinase conditions. Using ^{32}P, the phosphoppeptide product was barely visible upon tricine gel electrophoretic separation using autoradiographic detection (data not shown). Direct analysis of the kinase reaction mixture by MALDI/MS failed to detect the formation of a phosphopeptide due to the low stoichiometry of the kinase reaction (Figure 4-5A). Instead, multiple sodium adducts were observed indicating that negatively charged amino acids on this peptide have a tendency to coordinate with sodium ions in solution. After intensive washing of the sample affinity-bound to Fe^{3+}-loaded agarose, we were able to observe the phosphorylated peptide. The relative abundance of the signal due to the phosphorylated peptide increased dramatically after another intensive wash cycle on Fe^{3+}-loaded agarose (Figure 4-5B). It was difficult, however, to wash off the parent peptide completely due to its relatively high concentration.

In order to evaluate the selectivity difference between the two metal ions, Ga^{3+} and Fe^{3+}, analysis of this peptide was also tested using isolation with Ga^{3+}-loaded agarose as shown in Figure 4-6. Ga^{3+}-loaded agarose showed affinity for

the mono-phosphopeptide as well. The phophorylated peptide peak, however, was markedly reduced after a second wash cycle on Ga^{3+}-loaded agarose, suggesting that Ga^{3+} has a weaker affinity for the mono-phosphorylated peptides than does Fe^{3+}-loaded agarose. Apparently, although both Fe^{3+} and Ga^{3+} have high specificity for phosphopeptides, the Fe^{3+} ion shows higher affinity for mono-phosphorylated peptide. More highly phosphorylated peptides showed decreased sensitivity using Fe^{3+} in this analytical approach, possibly, due to high binding affinity leading to insufficient dissociation for analysis upon addition of the MALDI matrix. On the other hand, the Ga^{3+} ion binds more weakly to multi-phosphorylated peptide than does Fe^{3+}, enabling the efficient dissociation and detection of the phosphopeptides.

Shown in Figure 4-7 is the MALDI/MS spectra of the kinase reaction product of a synthetic peptide (RRPGTSPALLQ m/z 1195) containing serine 98 of p21 that was tested before and after isolation using Fe^{3+}-loaded agarose. No signs of phosphorylation occurred in this peptide, indicating that serine 98 is not phosphorylated by Cdk2. Several other synthetic peptides containing different possible phosphorylation sites were also examined. Results are summarized in Table 4-1. Peptides containing serines 146, 155 and 163 of p21 were phosphorylated by kinase Cdk2, while peptides containing serines 98 and 130 were not phosphorylated by Cdk2. Given the fact that p21 is the primary downstream protein of p53, phosphorylation should be an important means of regulating its activity as a Cdk-cyclin inhibitor, its protein-protein interactions or its

degradation. The information we obtained in this study will facilitate future investigations of p21 phosphorylation and its biological effects by other methods, such as mutagenesis or phosphospecific antibodies.

CONCLUSIONS

IMAC combined with MALDI/MS has been used to study the phosphorylation sites on the cancer suppressor protein p53. We were able to detect one phosphorylation site that has not previously been reported. This method also enabled us to detect the difference in the degree of phosphorylation before and after okadaic acid treatment of p53, thus, providing useful information for understanding functional changes of the treated protein. We also successfully applied this method to the study of putative phosphorylation sites in p21. Several potential phosphorylation sites in p21 were detected. The ability to detect phosphopeptides from the low stoichiometry reaction mixture should enable the application of this method in detecting phosphorylation sites of proteins in living cell, where only small fraction of protein will be modified. In addition, high sensitivity, short analysis time and low cost make this method very attractive for the determination of phosphorylation sites.

ACKNOWLEDGMENT

Support for the purchase of the MALDI/MS instrument by the NIH, Office of AIDS Research is gratefully acknowledged.

REFERENCES

1. Milczarek, G. J., Martinez, J., Bowden, G. T. p53 Phosphorylation: Biochemical and Functional Consequences. *Life Sci.,* **1997,** *60,* 1-11.
2. Prives, C., Hall, P. A. The p53 Pathway. *J. Pathol.,* **1999,** *187*, 112-126.
3. Steegenga, W. T., Van Der Eb, A., Jochemsen, A. G. How Phosphoryaltin Regulates the Activity of p53. *J. Mol. Biol.,* **1996,** *263,* 103-113.
4. Sakaguchi, K., Herrera, J. E., Saito, S., Miki, T., Bustin, M., Vassilev, A., Anderson, C. W., Appella, E. DNA Damage Activates p53 Through a Phosphorylation-Acetylation Cascade. *Genes & Dev*., **1998,** *12*, 2831-2841.
5. Hecker, D., Page, G., Lohrum, M., Weiland, S., Scheidtmann, K. H. Complex Regulation of the DNA-Binding Activity of p53 by Phosphorylation: Different Effects of Individual Phosphorylation Sites on the Interaction with Different Binding Motifs. *Oncogene,* **1996,** *12,* 953-961.
6. Martinez, J. D., Craven, M. T., Joseloff, E., Milczarek, G., Bowen, G. T. Regulation of DNA Binding and Transactivation in p53 by Nuclear Localization and Phosphorylatio. *Oncogene,* **1997,** *14,* 2511-2520.
7. Chernov, M. V., Ramana, C. V., Adler, V. V., Stark, G. R. Stabilization and Activation of p53 are Regulated Independently by Different Phosphorylation Events. *Proc. Natl. Acad. Sci., USA,* **1998,** *95,* 2284-2289.
8. Craig, A. L., Burch, L., Vojtesek, B., Mikutowska, J., Thompson, A., Hupp, T. R. Novel Phosphorylation Sites of Human Tumour Suppressor Protein p53 at Ser ^{20} and Thr ^{18} that Disrupt the Binding of mdm2 (Mouse Double Minute 2) Protein are Modified in Human Cancers. *Biochem. J.,* **1999**, *342*, 133-141.

9. Otvos L., Hoffman, R., Xiang, Z. Q., O, I., Deng, H., Ertl. H. C. J. A Monoclonal Antibody to a Multiphosphorylated, Conformational Epitope at the Carboxy-Terminus of p53. *Biochi. Biophy. Acta*, **1998,** *1404*, 457-474.
10. Ashcroft, M., Kubbutat, M. H., Vousden, K. H. Regulation of p53 Function and Stability by Phosphorylation. *Mol. Cell. Biol*., **1999,** 19, 1751-1758.
11. Patterson, R. M., He C., Selkirk, J. K., Merrick, B. A. Human p53 Expressed in Baculovirus-Infected Sf9 Cells Displays a Two-Dimension Isoform Pattern Identical to Wild-Type p53 from Human Cells. *Archiv. Biochem. Biophysi.,* **1996**, *330*, 71-79.
12. Esposito, F., Cuccovillo, F., Vanoni, M., Cimino, F., Anderson, C. W., Appella, E., Russo, T. Redox-Mediated Regulation of p21(waf1/cip1) Expression Involves a Post-Transcriptional Mechanism and Activation of the Mitogen-Activated Protein Kinase Pathway. *Eur. J. Biochem*., **1997,** *245,* 730-737.
13. Fuchs, B., Hecker, D., Scheidtmann, H. K. Phosphorylation Studies on Rat p53 Using the Baculovirus Expression System Manipulation of the Phosphorylation State with Okadaic Acid and Influence on DNA Binding. *Eur. J. Biochem*., **1995**, *228*, 625-639.
14. Yatsunami, J., Komori, A., Ohta, T., Suganuma, M., Fujiki, H. Hyperphosphorylation of Retinoblastoma Protein and p53 by Okadaic Acid, a Tumor Promoter. *Cancer Res*., **1993,** *53*, 239-241.
15. Hitomi, M., Shu, J., Strom, D., Hiebert, S. W., Harter, M. L., Stacey. D. W. Prostaglandin A_2 Blocks the Activation of G_1 Phase Cyclin-Dependent Kinase

without Altering Mitogen-Activated Protein Kinase Stimulation. *J. Biol. Chem.,* **1996,** *271*, 9376-9383.

16. Zhou, W., Merrick, B. A., Khaledi, M., Tomer, K. B. Selective Detection and Sequencing of Phosphopeptides Affinity-Bound to Immobilized Metal Ion Beads by Matrix-Assisted Laser Desorption/Ionization Mass Spectrometry. *J. Am. Soc. Mass. Spectrom*. in press.
17. Hardie, D.G., Campbell, D.G., Caudwell, F. B., Haystead, T. A. J. in *Protein Phosphorylation* Ed. by D.G. Hardie; IRL Press at Oxford University Press, New York **1993**, p. 61.
18. Liao, P. C., Leykam, J., Andrews, P. C., Cage, D. A., Allison, J. An Approach to Locate Phosphorylation Sites in a Phosphoprotein: Mass Mapping by Combining Specific Enzymatic Degradation with Matrix-Assisted Laser Desorption/Ionization Mass Spectrometry. *Anal. Biochem.*, **1994**, *219*, 9-20.
19. Carr, S. A., Huddleston, M. J., Annan, R. S. Selective Detection and Sequencing of Phospeptides at the Femtomole Level by Mass Spectrometry. *Anal. Biochem.*, **1996,** *239*, 180-192.
20. Annan, R. S., Carr, S. A. Phosphopeptide Analysis by Matrix-Assisted Laser Desorption Time-of-Flight Mass Spectrometry. *Anal. Chem.,* **1996,** *68*, 3413-3421.
21. Immler, D., Gremm, D., Kirsch, D., Spengler, B., Presek, P., Meyer, H. E. Identification of Phosphorylated Proteins from Thrombin-activated Human Platelets Isolated by Two-Dimensional Gel Electrophoresis by Electrospray Ionization-Tandem Mass Spectrometry (ESI-MS/MS) and Liquid

Chromatography-Electrospray Ionization-Mass Spectrometry (LC-ESI-MS). *Electrophoresis*, **1998,** *19*, 1015-1023.

22. Posewitz, M., Tempst, P. Immobilized Gallium (III) Affinity Chromatography of Phosphopeptides. *Anal. Chem.,* **1999,** *71,* 2883-2892.
23. Asara, J. M., Allison, J. Enhanced Detection of Phosphopeptides in Matrix-Assisted Laser Desorption/Ionization Mass Spectrometry Using Ammonium Salts. *J. Am. Soc. Mass Spectrom.,* **1999**, *10*, 35-44.
24. Cox, L. S. Multiple Pathways Control Cell Growth and Transformation: Overlapping and Independent Activities of p53 and p21 $^{Cip1/WAF1/Sdi1}$. *J. Pathol.,* **1997,** *183*, 134-140.
25. Nakayama, K.; Nakayama, K. Cip/Kip Cyclin-Dependent Kinase Inhibitors: Brakes of the Cell Cycle Engine During Development. *BioAssay.,* **1998,** *20*, 1020-1029.
26. El-Deiry, W., Tokino, T., Velculescu, V., Levy, D., Parsons, R., Trent, J., Lin, D., Mercer, W., Kinzler, K., Vogelstein, B. WAF1, a Potential Mediator of p53 Tumor Suppression. *Cell*, **1993,** *75*, 817-825.
27. Qiu, X., Forman, H. J., Schonthal, A. H., Cadenas, E. Induction of p21 Mediated by Reactive Oxygen Species Formed during the Metabolism of Aziridinylbenzoquinones by HCT116 Cells. *J. Biol. Chem*., **1996,** *271*, 31915-31921.
28. James, S. Y., Mackay, A. G., Colston, K. W. Effects of 1, 25-Dihydroxyvitamin D3 and its Analogues on Induction of Apoptosis in Breast Cancer Cells. *J. Steroid. BioChem. Mol. Biol*., **1996,** *58,* 395-401.

29. Gartel, A. L., Tyner, A. L. Transcriptional Regulation of the p21 Gene. *Experi. Cell. Res*., **1999**, *246*, 280-289.

30. Cox, L. S., Lane, D. P. Tumour Suppressors, Kinases and Clamps: How p53 Regulates the Cell Cycle in Response to DNA Damage. *BioEssays.,* **1995,** *17*, 501-508.

31. Sherr C. J., Roberts, J. M. Inhibitors of Mammalian G1 Cyclin-Dependent Kinases. *Genes & Dev*., **1995,** *9,* 1149-1163.

Figure 4-1: Amino acid sequences for phosphoproteins (A) p53 and (B) p21.

Figure 4-2: MALDI/TOF mass spectra of a tryptic digest of (A) normal and (B) hyper phosphorylated p53.

Figure 4-3: LC/MS spectra of tryptic peptide T2 from (A) normal and (B) hyper phosphorylated p53.

Figure 4-4: MALDI/TOF mass spectra of Ga^{3+}-NTA bound tryptic peptide T2 from (A) normal and (B) hyper phosphorylated p53.

Figure 4-5: MALDI/TOF mass spectra of the peptide: RDFYHpSKRRLI (A) before and (B) after the isolation with Fe^{3+}-NTA beads.

Figure 4-6: MALDI/TOF mass spectra of the Ga^{3+}-NTA bound peptide: RDFYHpSKRRLI (A) before and (B) after intensively washing Ga^{3+}-NTA beads with 30 μl water (3x) followed by 30 μl 0.1 M acetic acid (3x). *: unidentified peak.

Figure 4-7: MALDI/TOF mass spectra of the peptide: RRPGTSPALLQ (A) before and (B) after the isolation with Fe^{3+}-NTA beads.

Table 4-1: Summary of the synthetic peptides examined by Fe^{3+}-NTA beads combined with MALDI/TOF/MS.

sequences of synthetic peptides	$[M+H]^+$	#of phosphorylation site
RRPGT^{98}SPALLQ	1196	0
EQAEG^{130}SPGGPGDSQGRK	1658	0
RKRRQT^{146}SMTDF	1426	1
RDFYH^{153}SKRRLI	1491	1
KRRLIF^{163}SKRKP	1429	1

(A) MEEPQ SDPSV EPPLS QETFS DLWKL LPENN VL^{33}SPL P^{37}SQAM DDLML ^{46}SPDDI EQWF^{55}T EDPGP DEAPR MPEAA PRVAP APAAP TPAAP APAPS WPLSS SVPSQ KTYQG SYGFR LGFLH SGTAK SVTCT YSPAL NKMFC QLAKT CPVQL WVDST PPPGT RVRAM AIYKQ SQHMT EVVRR CPHHE RCSDS DGLAP PQHLI RVEGN LRVEY LDDRN TFRHS VVVPY EPPEV GSDCT TIHYN YMCNS SCMGG MNRRP ILTII TLEDS SGNLL GRNSFEVRVC ACPGR DRRTE EENLR KKGEP HHELP PGSTK RALPN NTSSS PQPKK KPLDG EYFTL QIRGR ERFEM FRELN EALEL KDAQA GKEPG GSRAH SSHLK SKKGQ STSRH KKLMF KTEGP DSD

(B) MSEPA GDVRQ NPCGS KACRR LGGPV DSEQL SRDCD ALMAG CIQEA RERWN FDFVT ETPLE GDFAW ERVRG LGLPK LYLPT GPRRG RDELG GGRRP GT^{98}SPA LLQGT AEEDH VDLSL SCTLV PRSGE QAEG^{130}S PGGPG DSQGR KRRQT ^{146}SpMTDF YH^{153}SpKR RLIF^{160}Sp KRKP

Figure 4-1

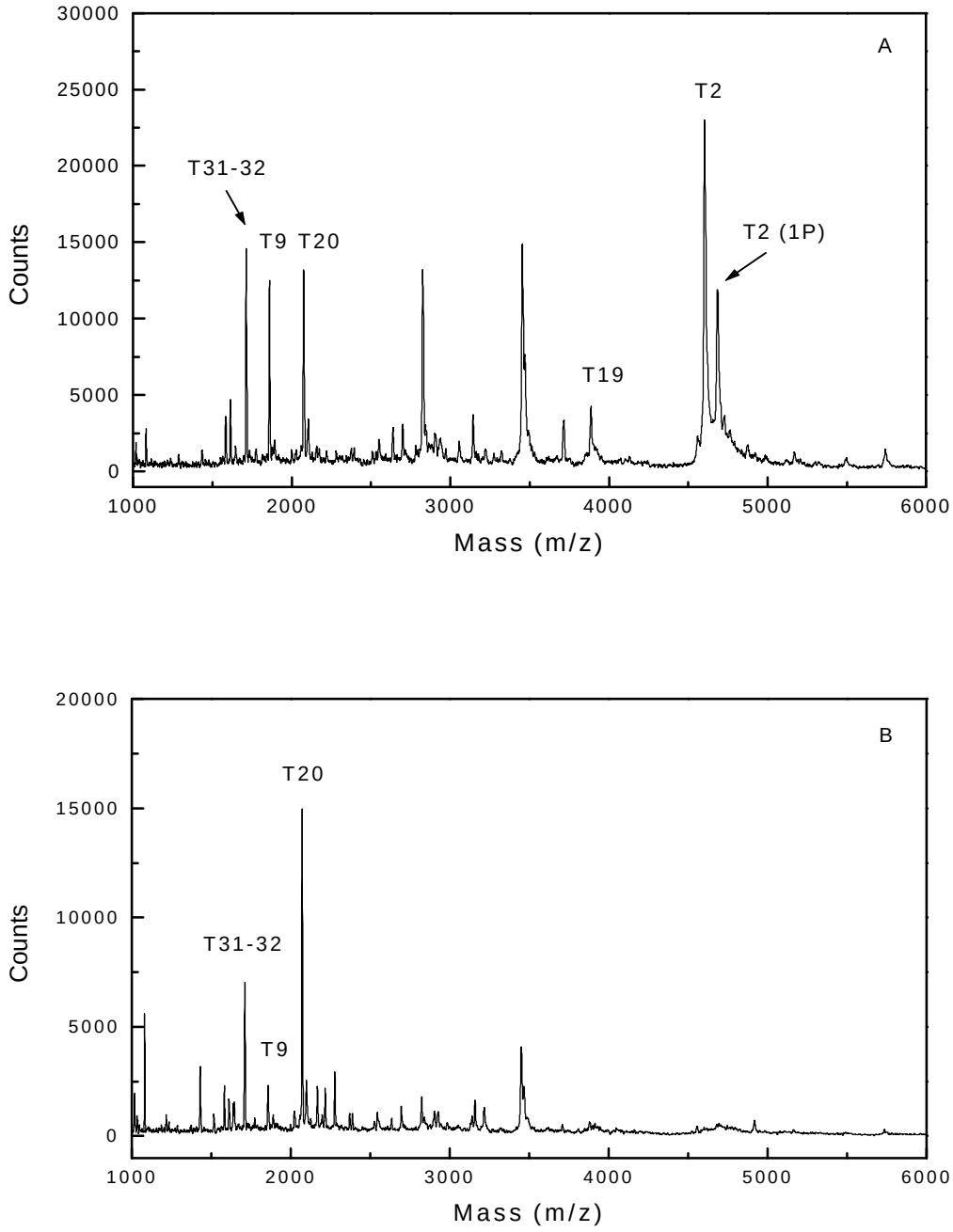
A
T2
T31-32
T9 T20
T2 (1P)
T19
Counts
Mass (m/z)
B
T20
T31-32
T9
Counts
Mass (m/z)

Figure 4-2

T2: ^{25}LLPENNVLSPLPSQAMDDLMLSPNNIEQWFTENPGPNEAPR^{65}

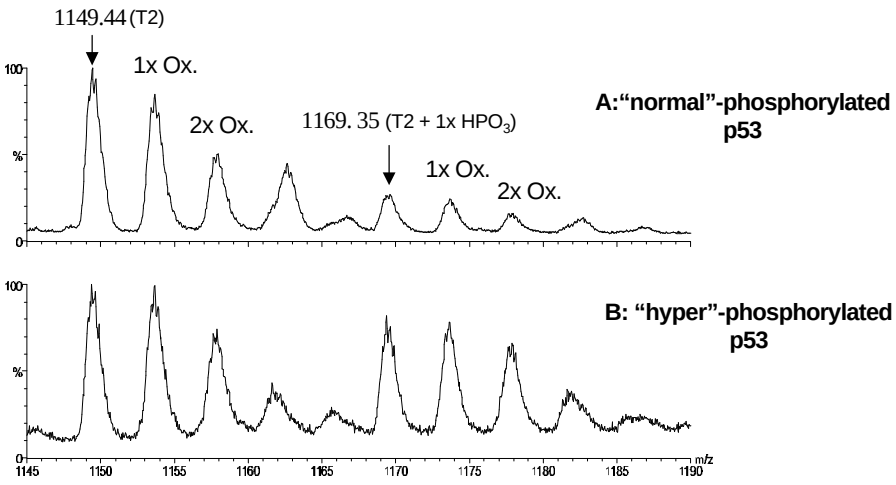

Figure 4-3

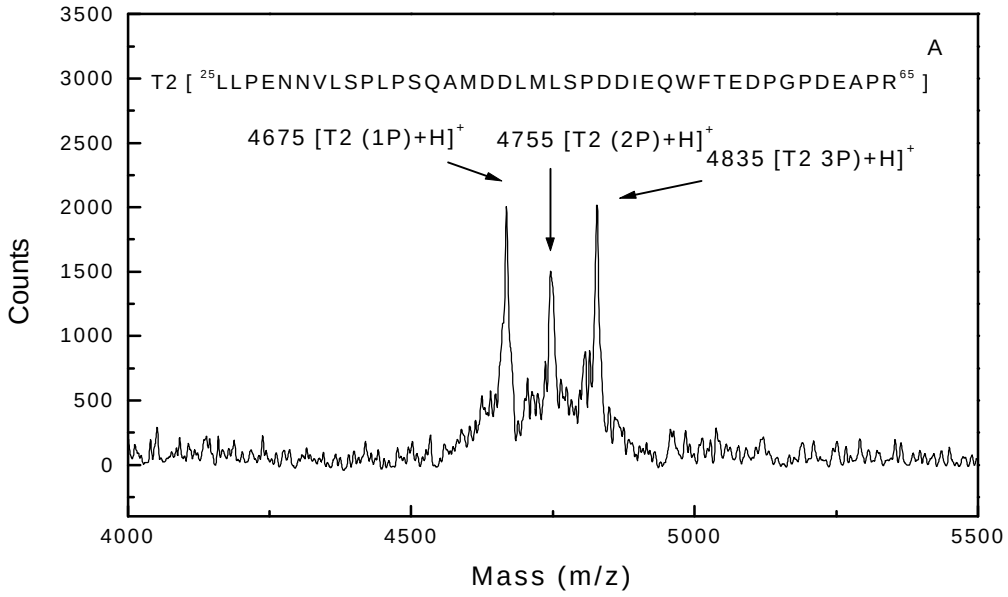
A
T2 [25LLPENNVLSPLPSQAMDDLMLSPDDIEQWFTEDPGPDEAPR65]
4675 [T2 (1P)+H]+
4755 [T2 (2P)+H]+
4835 [T2 3P)+H]+
Counts
Mass (m/z)
3500
3000
2500
2000
1500
1000
500
0
4000
4500
5000
5500

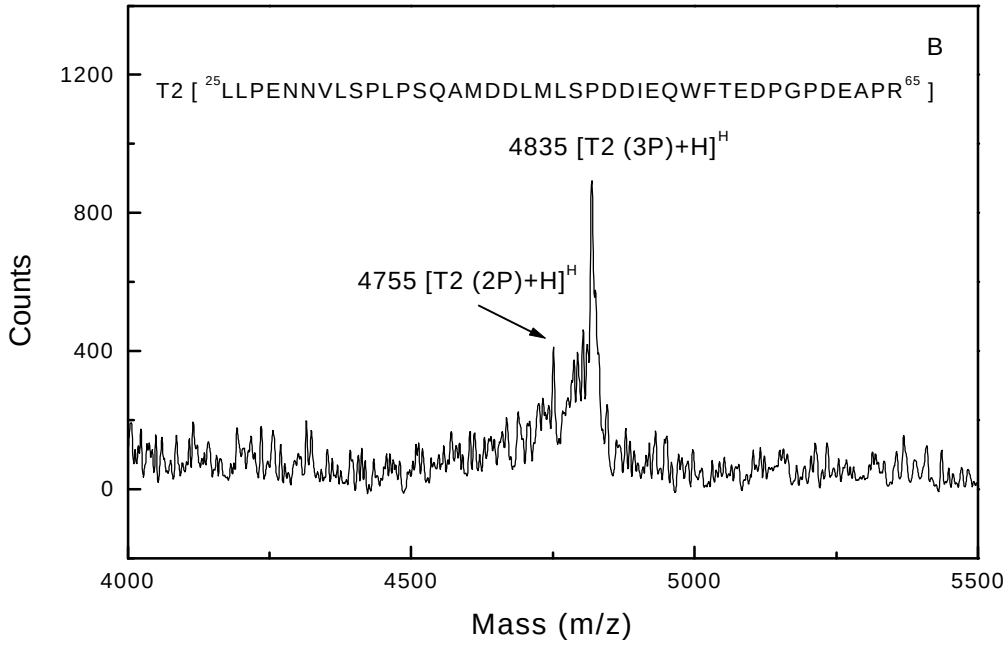
B
T2 [25LLPENNVLSPLPSQAMDDLMLSPDDIEQWFTEDPGPDEAPR65]
4835 [T2 (3P)+H]H
4755 [T2 (2P)+H]H
Counts
Mass (m/z)
1200
800
400
0
4000
4500
5000
5500

Figure 4-4

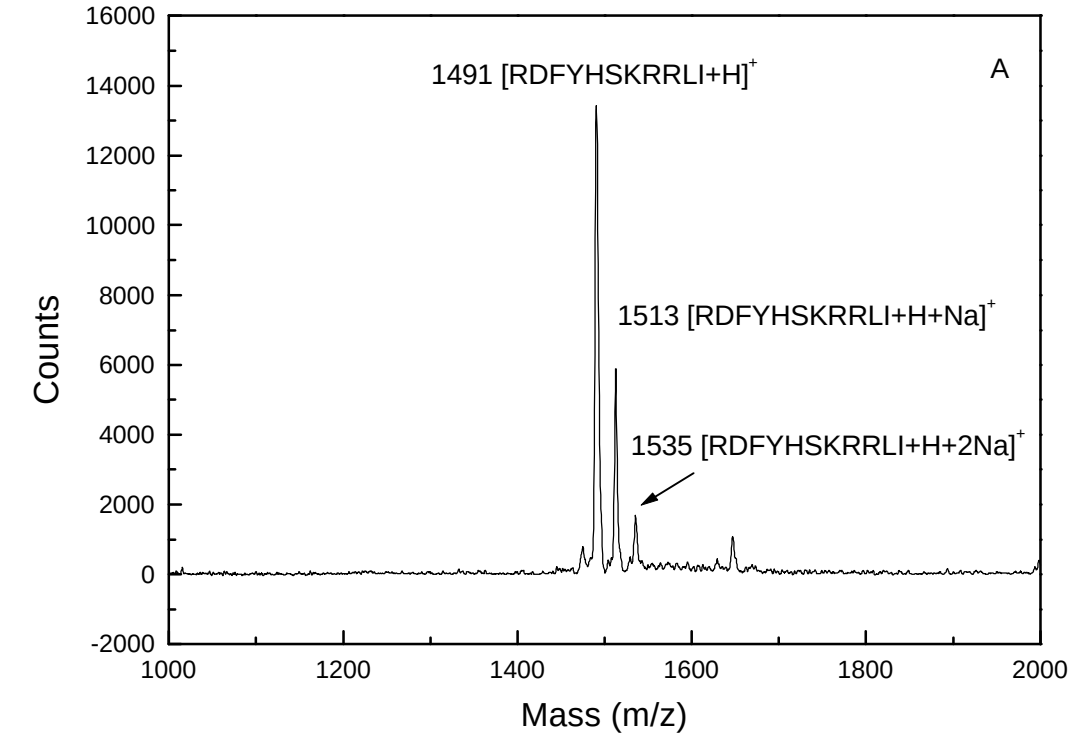
A
1491 [RDFYHSKRRLI+H]+
1513 [RDFYHSKRRLI+H+Na]+
1535 [RDFYHSKRRLI+H+2Na]+
Counts
Mass (m/z)
16000
14000
12000
10000
8000
6000
4000
2000
0
-2000
1000
1200
1400
1600
1800
2000

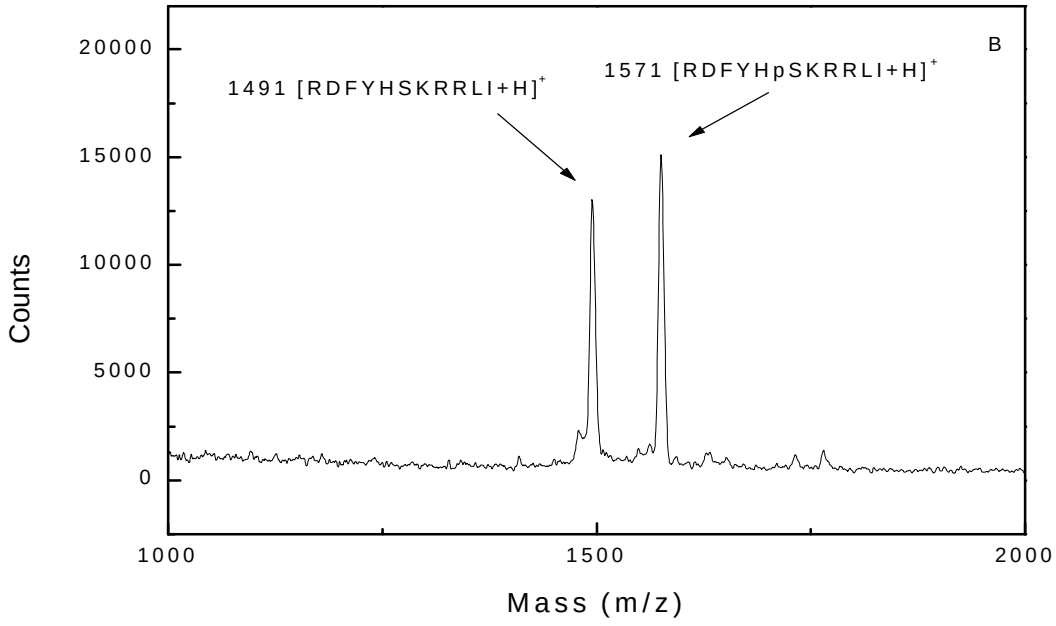
B
1491 [RDFYHSKRRLI+H]+
1571 [RDFYHpSKRRLI+H]+
Counts
Mass (m/z)
20000
15000
10000
5000
0
1000
1500
2000

Figure 4-5

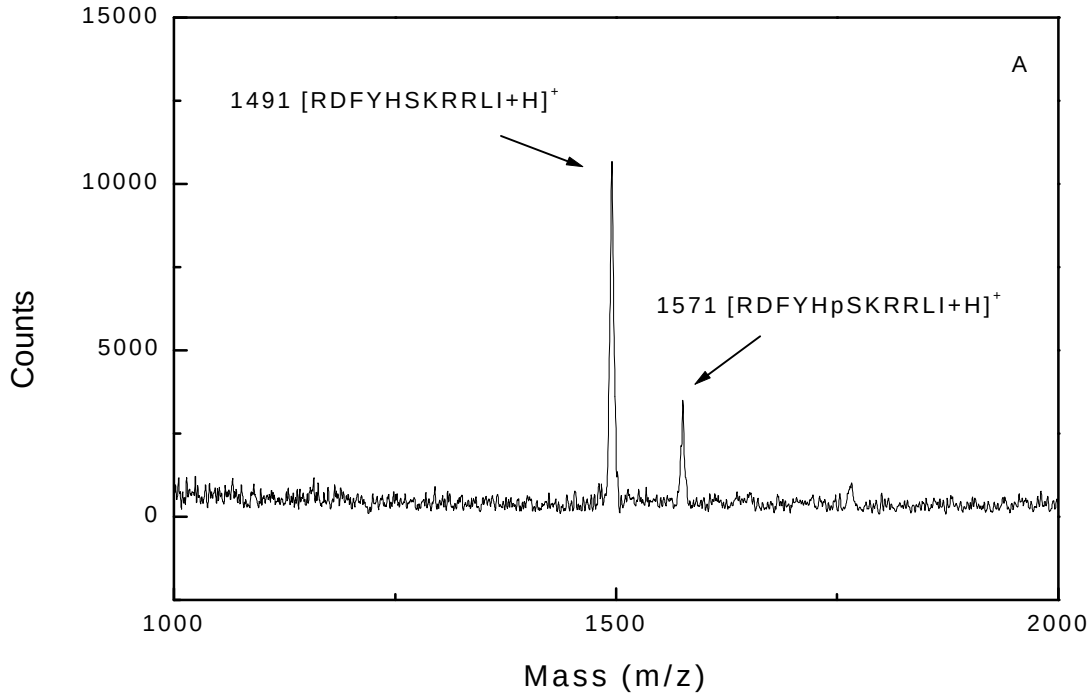
15000
10000
5000
0
Counts
A
1491 [RDFYHSKRRLI+H]+
1571 [RDFYHpSKRRLI+H]+
1000
1500
2000
Mass (m/z)

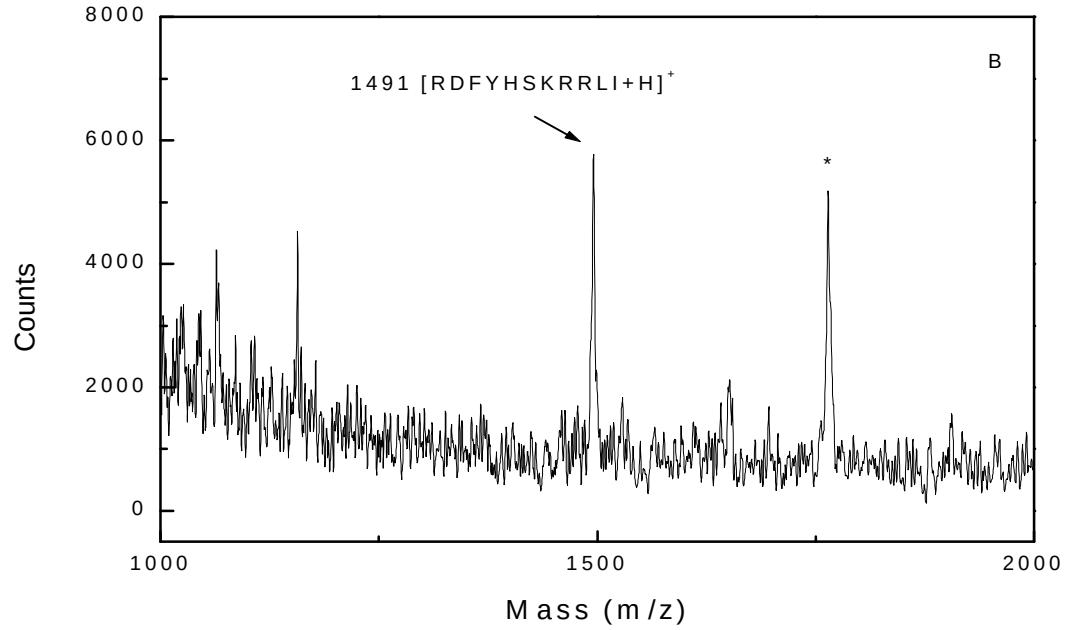
8000
6000
4000
2000
0
Counts
B
1491 [RDFYHSKRRLI+H]+
*
1000
1500
2000
Mass (m/z)

Figure 4-6

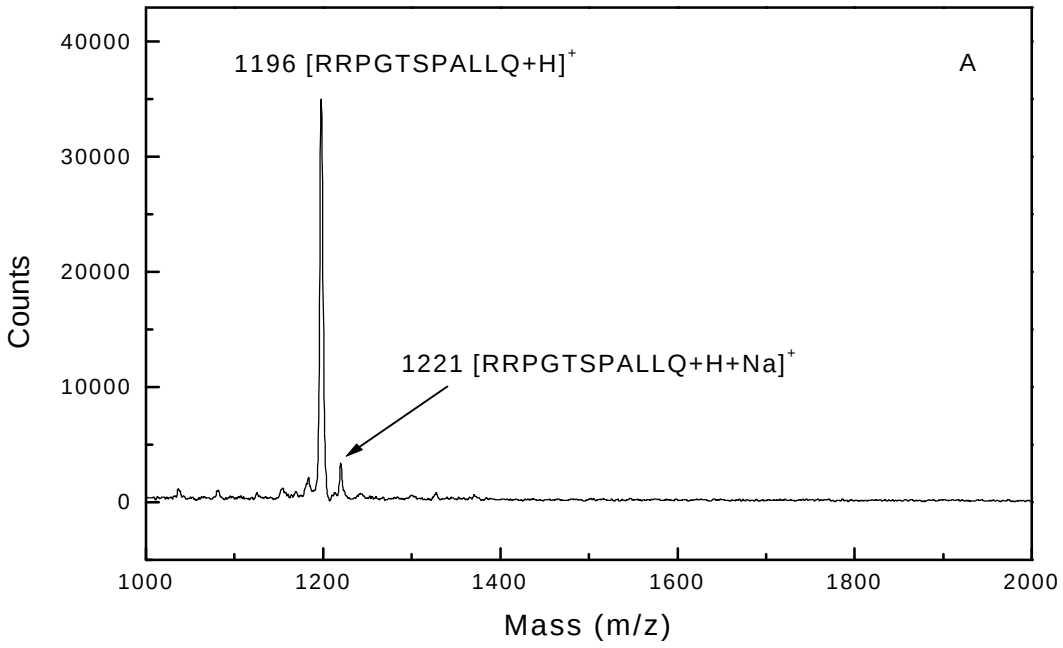
40000
30000
20000
10000
0
Counts
1196 [RRPGTSPALLQ+H]+
A
1221 [RRPGTSPALLQ+H+Na]+
1000
1200
1400
1600
1800
2000
Mass (m/z)

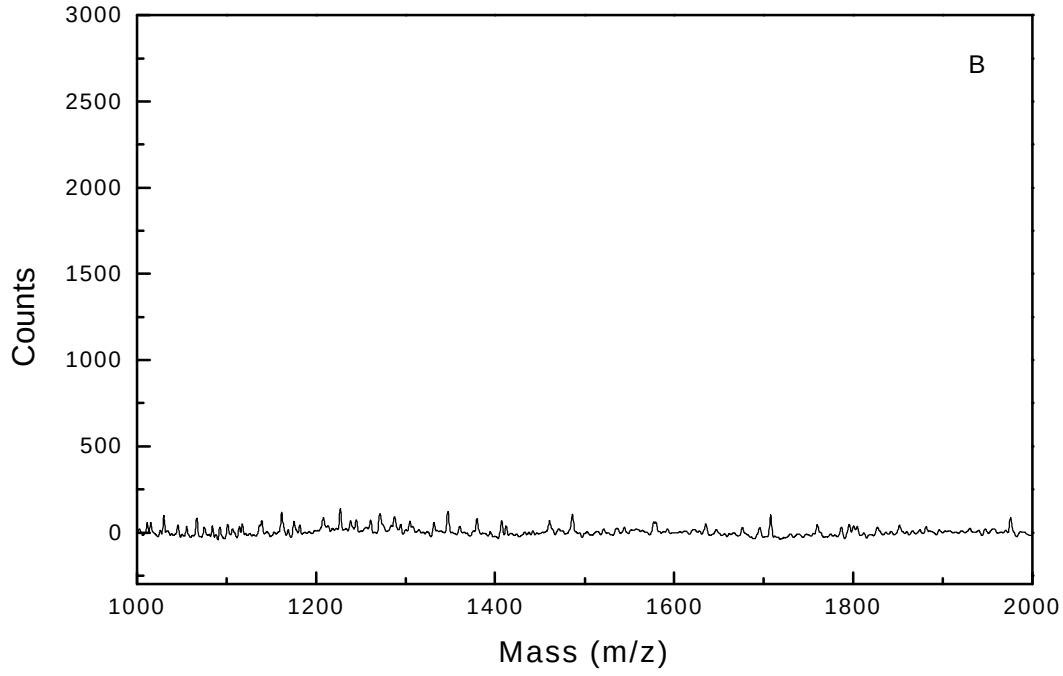
3000
2500
2000
1500
1000
500
0
Counts
B
1000
1200
1400
1600
1800
2000
Mass (m/z)

Figure 4-7

Chapter 5

Evaluation of the Binding between Potential Anti-HIV Drugs and Viral Envelope Glycoprotein gp120 by Capillary Electrophoresis with Laser-Induced Fluorescence Detection

Wei Zhou, Kenneth B. Tomer, Morteza G. Khaledi

ABSTRACT

The fusion of the human immunodeficiency virus (HIV) with the target cell was assisted by the interaction between the viral envelope glycoprotein HIV-1 gp120 and a chemokine receptor. Studies have shown that the efficiency of the binding depends on the presence of the V3 loop of the gp120 which is known to interact with polyanions, such as phosphorothioate oligodeoxynucleotides (Sd, potential anti-HIV drugs). In this study, capillary electrophoresis with laser induced fluorescence detection (CE-LIF) was used to systematically evaluate binding between Sd and HIV-1 gp120. A 25-mer fluorescently-tagged phosphorothioate oligodeoxynucleotide (GEM) was employed as a probe to study this interaction. The dissociation constant (K_d) between GEM and gp120 was determined to be 0.98 nM by Scatchard analysis. The competition constants (K_c) of a set of Sd that compete with GEM for binding to gp120 were also determined. The results showed that the interaction had a strong dependence on the sulfur phosphorothioate backbone. Chain length and the sequence of Sd also affect binding to gp120. The ability to study the protein-drug binding in the

solution with minimal sample consumption, makes CE-LIF very attractive for biological studies.

INTRODUCTION

The entrance of human immunodeficiency virus (HIV) into the target cell is initiated by binding of the viral envelope glycoprotein gp120 with CD4, a surface glycoprotein of the target cell [1-2]. This interaction induces a number of conformational changes in gp120 which enable it to interact with a chemokine coreceptor. The coreceptor can be either CCR5 or CXCR4, depending on the strain of the virus [3-6]. These interactions lead to the fusion of the viral envelope with the membrane of the target cell. Drugs designed to block any of these interaction sites, therefore, may inhibit or prevent infection.

Recently, the X-ray crystal structure of a partially deglycosylated gp120 core complexed with a two-domain fragment of human CD4 and a neutralizing human antibody that blocks chemokine-receptor binding was reported [7-8]. The crystal structure reveals the CD4 binding sites on gp120. Although the precise nature of the chemokine coreceptor binding site on gp120 remains to be determined, the V3 loop of gp120 is believed to be an important determinant [9-11]. Studies have shown that a V3-deleted version of gp120 does not bind the chemokine coreceptor CCR5. In addition, antibodies to the V3 loop interfere with binding between gp120 and CCR5 [12-14]. Targeting drugs to the V3 loop, therefore, is one of the major goals of anti-HIV drug design.

Although variable in its primary sequence, the V3 loop of gp120 of all pathogenic strains of HIV-1 is positively charged and is known to interact with polyanions, such as dextran sulfate and phosphorothioate oligodeoxynucleotides (Sd) [15-18]. A Sd is a phosphodiester oligodeoxynucleotide (Od) in which a single oxygen on each phosphorus atom is replaced by a sulfur atom (Figure 5-1). This substitution not only maintains the original charge and aqueous solubility properties of normal oligodeoxynucleotides but also provides resistance to nuclease degradation. Studies have shown that Sd inhibit HIV infection by binding to the V3 loop of gp120 [19,22], and also interfere with the binding of gp120 to CD4 [19]. From a therapeutic point of view, what is important is that Sd are not toxic. Therefore, a systematic evaluation of the binding between Sd and gp120 is of great clinical interest.

Sd have been studied for their potential to inhibit HIV infection by several traditional biological binding assays [20-25]. A number of studies have shown that Sd inhibit HIV infection via an interaction that strongly depends on the sulfur phosphorothioate backbone and the length of the oligodeoxynucleotide [19,22]. It has also been reported that the interaction is augmented by the presence of four consecutive guanine residues in the oligodeoxynucleotide sequence [21]. The binding experiments performed so far, however, require either radiolabeling or covalent immobilization of the protein. Besides being time consuming, radiolabeling can fail to give accurate results due to the nonspecific background

on the X-ray film, usually an error of 15% is assumed in radiolabeling measurement [22]. Immobilization of proteins may cause changes in the biological activity of the protein, which also may yield misleading results. Moreover, none of the studies performed so far has accurately determined the dissociation constants between Sd and gp120, though it has been reported that the dissociation constant between biotinylated Sd ($T_2G_4T_2$) and gp120 is less than 1 μM [21]. In order to further understand the nature of the interaction, it is essential to determine the dissociation constants by an accurate and rapid method.

The popularity of affinity capillary electrophoresis (ACE) as a separation technique and as a probe for molecular interaction has expanded tremendously in the past few years. The high efficiency, ease of automation, short analysis time, and low sample consumption have made this method very attractive for studying biomolecular interactions, such as protein-drug, antibody-antigen, and protein-sugar [26-32]. Moreover, this solution-based method allows one to study the binding of proteins in their native conformations, and, consequently, the binding constants derived from ACE reflect the native interactions between molecules.

In this study, the binding between HIV-1 gp120 and Sd was evaluated by affinity capillary electrophoresis with laser-induced fluorescence detection (ACE-LIF). ACE-LIF is well suited to study oligonucleotide-protein interactions for a

number of reasons [33-35]. First, nucleic acids and proteins can be well separated by CE due to their very different electrophoretic mobilities. Second, well defined peaks of the complexes are readily obtained because the binding between oligodeoxynucleotides and proteins is usually so strong that the complexes often dissociate slowly relative to the ACE separation time scale. Third, determination of the dissociation constants of strongly bound complexes requires measuring the ligand at trace levels. Thus, a highly sensitive detection technique, such as laser induced fluorescence detection, is required in order to obtain accurate measurements. Here, we report the ACE-LIF determination of the dissociation constant (K_d) between HIV-1 gp120 and a 25-mer fluorescently-tagged phosphorothioate oligodeoxynucleotide (GEM, FITC-CTC TCG CAC CCA TCT CTC TCC TTC T) using Scatchard analysis. Using GEM as a probe, competition constants (K_c) of a series of unlabeled Sd that compete with GEM for binding to gp120 were also determined by competitive assay. The effects of the sulfur phosphorothioate backbone structure, chain length, and the sequence of oligodeoxynucleotides on their binding to HIV-1 gp120 are also discussed.

MATERIALS AND METHODS

Chemicals: Fluorescein isothiocyanate (FITC) isomer I 98% (HPLC), proline (SigmaUltra > 99%) were purchased from Sigma Chemical Co. (St. Louis, MO). A 25-mer phosphorothioate oligodeoxynucleotide with a fluorescent tag was kindly donated by Hybridon, Inc., (Cambridge, MA). The sequence is FITC-CTC TCG CAC CCA TCT CTC TCC TTC T (GEM). Human immunodeficiency

virus 1 (HIV-1, SF2) envelope protein gp120 was obtained from Austral Biologicals (San Ramon, CA). Ultra-pure Tris was purchased from Schwarz/Mann Biotech (Cleveland, OH). All of the oligonucleotides were synthesized by Genosys Biotechnologies, Inc. (The Woodlands, TX). All solutions were prepared with deionized water purified by a Model RO 40 ultra-pure water system (Hydro Corp., Research Triangle Park, NC).

Sample Preparation

Preparation of FITC-proline (internal standard): A stock solution of 100 μM FITC-proline was prepared according to the method used by Tao [33]. A 0.1 mL aliquot of 1 mM FITC solution (dissolved in acetone) was mixed with 0.9 mL of 1 mM proline (dissolved in 20 mM sodium bicarbonate buffer, pH=9.0). The solution was mixed thoroughly, left in the dark at room temperature for five hours, and then diluted to the desired concentration with running buffer prior to CE analysis.

Preparation of Samples for the Measurement of the Dissociation Constant (K_d) of GEM and HIV-1 gp120: HIV-1 gp120 stock solution (8 μM) was used as received and diluted to the desired concentrations with running buffer. A stock solution (100 μM) of GEM was prepared by dissolving the required amount of solid GEM into the running buffer. Various GEM solutions were prepared by serial dilution of the stock solution with running buffer. All sample solutions were prepared by adding 10 μL of HIV-1 gp120 solution, 10 μL

of the buffer solution and 10 μL of the FITC-proline solution at constant concentrations to 10 μL of the GEM solutions of different concentrations. The final volume of each sample was 40 μL. The final concentrations of FITC-proline and HIV-1 gp120 were 6.25 nM and 40 nM respectively. The concentrations of GEM varied from 25 nM to 43.75 nM. Each sample was then mixed thoroughly and incubated at room temperature for 30 min before CE analysis.

Preparation of Samples for Competitive Assay: Stock solutions of Sd (2 mM) were prepared by dissolving Sd as received into the certain volume of running buffer. The stock solutions of Sd $G_4(T_4G_4)_3$ and Sd ($G_4T_4G_4$) were 1 mM in concentration due to the limited amount of Sd $G_4(T_4G_4)_3$ and Sd ($G_4T_4G_4$) available. The oligodeoxynucleotide solutions were prepared by serial dilution of the stock solution with running buffer. All sample solutions were prepared by adding 10 μL of HIV-1 gp120 solution, 10 μL of GEM solution and 10 μL FITC-proline at constant concentrations to 10 μL of the oligodeoxynucleotide solutions at varying concentrations. Each sample was mixed thoroughly and incubated at room temperature for 30 min prior to CE analysis. The final concentrations of FITC-proline, GEM and HIV-1 gp120 were 6.25 nM, 37.5 nM and 40 nM respectively. The concentration of oligodeoxynucleotide varied from 5 nM to 500 μM.

Capillary Electrophoresis: All CE experiments were performed on a homemade CE system with laser induced fluorescence detection [37].

Separations were carried out using a 50 μm i.d. × 365 μm o.d. fused silica capillary. All capillaries were purchased from Polymicro Technologies (Tucson, AZ). The buffer was 10 mM Tris at pH 8.0. A negative 30 kV voltage was applied across a 78 cm long capillary with an effective length (to the detection) of 30 cm using a Spellmann high voltage power supply (Model SL60PN30, Plainview, NY). The injection end was grounded. Samples were introduced into the capillary by gravity. The injection end was lifted by 2 cm for 1 s. To avoid sample carryover, after each injection, the injection end was immersed into a vial filled with running buffer before being placed in the buffer reservoir. At the beginning of each day, the capillary was rinsed sequentially with 1 N sodium hydroxide, methanol and water for 10 min each before being rinsed with running buffer for 30 min. The laser was an Ar ion laser emitting light at 515 nm. The laser beam was focused by a pair of elliptical mirrors (Model 670RTC, 670RCB, 13E20AL.2, Newport, Irvine, CA). The light went through a chopper (Model 651-1, EG&G Instruments, Trenton, NJ) which was used in combination with a lock-in amplifier (Model 5101, EG&G Instruments, Trenton, NJ) to filter noise from the signal. The modulated light then entered the 40× fluorite microscope (Model Nikon Labophot-2, Southern Micro, Atlanta, GA) that focused the excitation beam onto the capillary detection window as well as collecting the resulting emission that had traversed a series of filters (long pass filter, Model Chroma 400DCLP, narrow band-pass filter, Model Chroma D515/40, Southern Micro, Atlanta, GA). The signal output from the photomultiplifer (Model R928, Hamamatsu Photonics, Bridgewater, NJ) passed through a current to voltage preamplifier (Option #35, PSA 01, Products

for Research, Danvers, MA) and entered the lock-in-amplifier. Finally, data were acquired by computer using a program written in LabView (National Instruments, Austin, TX). Data reported here are the means of triplicate analyses.

Determination of GEM Concentration: Samples were prepared by adding 10 μL of GEM solutions at different concentrations to 10 μL FITC-proline solution, which serves as an internal standard, at constant concentration. Final concentration of FITC-proline is 6.25 nM. The concentration of GEM varied from 6.25 nM to 25 nM. Each sample was mixed thoroughly prior to CE analysis. A plot of the ratio of peak areas of GEM/FITC-proline versus the concentration of GEM was used as a calibration curve. The calibration curve was linear up to 18.75 nM with R^2 of 0.98. In the binding assay, the concentrations of free GEM were determined from CE-LIF by calculating the ratios of peak area of GEM/FITC-proline and comparing them to the calibration plot which was obtained on the same day. Bound GEM was calculated as the difference between total GEM and free GEM in the solution.

RESULTS AND DISCUSSION

Determination of the Dissociation Constant between HIV-1 gp120 and GEM

The appropriate incubation time required for the reaction to reach equilibrium was determined by incubating gp120 with GEM (molar ratio: 1:1) at room temperature for 8 hours. The reaction mixture was tested by CE at certain time intervals during the incubation period (data not shown). No significant

change was observed in the area of peak due to complex formation between 30 minutes and 8 hours, indicating that equilibrium had been reached in solution within 30 minutes. All samples were, therefore, incubated for at least 30 minutes before CE analysis.

The human immunodeficiency viral envelope protein gp120 is a heavily glycosylated protein with a M_r of approximately 100,000. There are 26 consensus glycosylation sites on the gp120 [38] and sugar residues account for nearly 50% of the mass of the protein. These glycans shield the virus from antibodies that could destroy the virus before it enters human cells. Although the pI of gp120 is 9.83, the apparent pI of gp120 is much lower due to the shielding of the positive charges of the amino acids by the glycans. Another property of this glycoprotein is its microheterogeneity [39, 40]. Even at the same glycosylation site, the structure of the glycan varies. This microheterogeneity of the glycoprotein results in broad peaks in the CE separation.

Figure 5-2 shows the electropherograms used in the Scatchard analysis for the measurement of K_d between GEM and HIV-1 gp120. All samples contained 6.25 nM FITC-proline, which served as an internal standard, and 40 nM HIV-1 gp120 while the concentration of GEM was varied. HIV-1 gp120 migrated more slowly than the electroosmotic flow suggesting that the protein carried a negative charge under the separation conditions (data not shown). The peak corresponding to the gp120/GEM complex was broad due to the

microheterogeneity of gp120. The free GEM was well separated from the GEM/gp120 complex in the CE separation due to the large difference in their electrophoretic mobilities. All of the peak shapes were good with no evidence for dissociation of the complex during the separation. An accurate measurement of the concentrations of free and bound GEM, therefore, could be obtained. The binding constant could thus be determined.

In a Scatchard analysis, a plot of the ratio of bound to free GEM versus the concentration of bound GEM gives a straight line as described by Eqn.1 [33],

$$[P\text{-}D^*]/[D^*]=(1/K_d^*)\,(P_o-[P\text{-}D^*]) \qquad \text{Eqn.1}$$

Where [D*] is the concentration of free GEM, [P-D*] is the concentration of GEM/gp120 complex or bound GEM, P_o is the concentration of HIV-1 gp120. The slope of this equation equals the negative reciprocal of the dissociation constant and the x-axis intercept equals the protein concentration (Eqn. 1). Bound GEM was calculated as the difference between total GEM in the solution and free GEM obtained from the calibration plot as described in the experimental section. From the regression line (Figure 5-3), the dissociation constant (K_d) was determined to be 0.98 $\pm$ 0.46 nM (95% confidence interval). The X-axis intercept was 37 $\pm$ 14 nM (95% confidence interval) which includes the expected value of 40 nM. The linearity of the plot indicates that there is either only one binding site on HIV-1 gp120 for GEM, or, less likely, that there are multiple binding sites on HIV-1 gp120 with nearly identical binding constants to GEM.

Determination of Competition Constants (K_c) of Oligodeoxynucleotides Competing for GEM Binding to HIV-1 gp120

It is not cost effective to label all oligodeoxynucleotides. The measurement of the K_d between unlabeled phosphorothioate oligodeoxynucleotide and HIV-1 gp120, however, is difficult to achieve because the high affinity between HIV-1 gp120 and Sd requires the accurate measurement of the concentration of oligodeoxynucleotide at the low nanomolar level. A competitive assay was used as an alternative approach to study the binding of HIV-1 gp120 to unlabeled oligodeoxynucleotides [33]. In this method, unlabeled oligodeoxynucleotide were allowed to compete with GEM, the fluorescently labeled Sd, for the binding to HIV-1 gp120. The peak areas of the GEM/gp120 complex were measured, and the competition constants (K_c) of the oligodeoxynucleotides competing with GEM for binding to gp120 were determined according to the method of Cheng and Prusoff (Eqn. 2) [36],

$$K_c=IC_{50}/(1+[D^*]/K_d) \qquad \text{Eqn. 2}$$

where IC_{50} is the concentration of unlabeled oligodeoxynucleotide which causes a 50% decrease in the area of the GEM/gp120 complex peak. The peak areas of complexes were normalized using the internal standard FITC-proline to correct for fluctuations in injection volumes. The total concentration of the GEM ([D*]) was, in this experiment, 37.5 nM and the K_d was 0.98 nM as determined by Scatchard analysis.

Shown in Figure 5-4 are electropherograms representative of those used in the evaluation of binding between HIV-1 gp120 and Sd ($T_2G_4T_2$). All samples contained 6.25 nM FITC-proline, 40 nM HIV-1 gp120, 37.5 nM GEM, and the concentration of unlabeled Sd ($T_2G_4T_2$) was varied from 0 μM to 2.5 μM. The increase in the concentration of unlabeled Sd ($T_2G_4T_2$) in the sample increases the concentration of free GEM and decreases the concentration of the GEM/gp120 complex. At a concentration of 2.5 μM of Sd ($T_2G_4T_2$), the GEM/gp120 complex peak almost disappears. The peak areas of the GEM/gp120 complex as a function of the concentrations of unlabeled Sd ($T_2G_4T_2$) were measured as described above. The K_c value of Sd ($T_2G_4T_2$) competing with GEM for binding to HIV-1 gp120 was determined to be 18.06 μM, using Eqn. 2.

The interaction of HIV-1 gp120 with Od ($T_2G_4T_2$), a phosphodiester oligodeoxynucleotide with the same length and base sequence as Sd ($T_2G_4T_2$), was also examined (Figure 5-5). Even at a concentration of 500 μM, approximately 200 times higher than the concentration used for Sd ($T_2G_4T_2$), the GEM/gp120 complex peak is still observed. This is consistent with previous reports which showed that the polyanionic nature of oligodeoxynucleotide is not the only property that affects its binding to HIV-1 gp120 [19]. The phosphorothioate backbone may also be an important factor affecting its affinity for HIV-1 gp120. Notice that the peak corresponding to free GEM starts fronting when the concentration of Od ($T_2G_4T_2$) is higher than 250 μM. This may be due

to the high concentration of the sample causing conductivity differences between the sample and the background electrolyte solution, leading to electrophoretic dispersion. This electrophoretic dispersion also makes accurate measurement of the concentration of free GEM very difficult. The K_c value for Od ($T_2G_4T_2$), therefore, was not determined, but must be greater than 4000 μM.

Effects of the sequence and chain length on the binding of Sd to HIV-1 gp120 were also investigated. Interaction has been shown to be augmented by the presence of four consecutive guanines in Sd [21]. As shown in Figure 5-6, Sd ($T_2G_4T_2$) shows substantially higher affinity than does Sd $(GT)_4$, and binding of Sd $G_4(T_4G_4)_3$ is significantly higher than that of Sd C_{28}. Although the presence of the G_4 motif increases the binding strength between Sd and the V3 loop of gp120 compared to that of other Sd of the same size and base composition, Sd ($T_2G_4T_2$) has substantially lower affinity for HIV-1 gp120 than does Sd C_{28}. A possible reason for the increased binding of Sd with longer sequences may be an augmentation of bioavailability. In other words, the long sequence of Sd may have additional interaction that increases the binding of to HIV-1 gp120.

Table 5-1 summarizes K_c values obtained by this method. Our results indicate that the interaction has a strong dependence on the sulfur phosphorothioate backbone. Chain length and the sequence of the oligodeoxynucleotide also affect their ability to bind to gp120. The presence of four contiguous guanosine (G) residues improves the binding of Sd. Our results

obtained by ACE-LIF are consistent with published reports, however, the traditional binding assay which usually involves immobilization of protein failed to differentiate binding of Sd $G_4(T_4G_4)_3$ and of Sd C_{28} [22]. These ACE-LIF data clearly show that the presence of the G_4 motif also increases the binding ability of Sd with longer sequences.

CONCLUSIONS

With the assistance of laser-induced fluorescence detection, accurate determination of the dissociation constant of the very strong complex between GEM and HIV-1 gp120 was achieved. To our knowledge, this is the first report to evaluate the binding of gp120 to Sd by ACE-LIF. The dissociation constant (K_d) between GEM and gp120 was determined and the nature of the interaction between HIV-1 gp120 and unlabeled Sd was further studied by measuring the values of competition constant (K_c). The results demonstrate that ACE-LIF is a sensitive, rapid and convenient tool in obtaining reliable data on biological interactions. Given the important role of V3 loop in HIV pathogenicity, the results we obtained may provide useful information for drug design.

ACKNOWLEDGEMENTS

This project is financially supported by NIH, for which the authors are grateful. Hybridon, Inc. is acknowledged for the donation of the fluorescence tagged phosphorothioate oligodeoxynucleotide, GEM.

REFERENCES

1. McDougal, J. S., Kennedy, M. S., Sligh, J. M., Mawle, S. P., Nicholson, J. K. A. Binding of HTLV-III/LAV to $T4^+$ T Cells by a Complex of the 110K Viral Protein and the T4 Molecule. *Science*, **1985**, *231*, 382-385.
2. Dalgleish, A. G., Beverley, P. C. L., Clapham, P. R., Crawford, D. H., Greaves, M. R., Weiss, R. A. The CD4 (T4) Antigen is Essential Component of the receptor for the AIDS Retrovirus. *Nature*, **1984**, *312*, 763-767.
3. Deng, H. K., Liu, R., Ellmeiner, W., Choe, S., Unutmaz, D., Burkhart, M., Marzio, P. D., Marmon, S., Sutton, R. E., Landau, N. R., et al. Identification of Major Co-receptor for Primary Isolates of HIV-1. *Nature*, **1996**, *381*, 661-666.
4. Picard, L., Simmons, G., Power, C. A., Meyer, A., Weiss, R. A., Clapham, P. R. Multiple Extracellular Domains of CCR-5 Contribute to Human Immunodeficiency Virus Type 1 Entry and Fusion. *J. Virol.,* **1997**, *71 (7)*, 5003-5011.
5. Feng, Y., Broder, C. C., Kennedy, P. E., Berger, E. HIV-1 Entry Cofactor: Functional cDNA Cloning of a Seven-Transmembrane, G Protein-Coupled Receptor. *Science*, **1996**, *272*, 872-877.
6. Choe, H., Farzan, M., Sun, Y., Sullivan, N., Rollins, B., Ponath, P. D., Wu, L., Sodroski, C. J. et. al., The b-Chemokine Receptors CCR3 and CCR5 Facilitate Infection by Primary HIV-1 Isolates. *Cell*, **1996**, *85*, 1135-1148.
7. Wyatt, R., Sodroski, J. The HIV-1 Envelope Glycoproteins: Fusogens, Antigens, and Immunogens. *Science*, **1998**, *280*, 1884-1888.

8. Kwong, P. D. Structure of an HIV gp120 Envelope Glycoprotein in Complex with the CD4 Receptor and a Neutralizing Human Antibody. *Nature*, **1998**, *393*, 648-659.
9. Cocchi, F. A., DeVico, L., Garzino-Demo, A., Cara, A., Gallo, R. C., Lusso, P. The V3 Domain of the HIV-1 gp120 Envelope Glycoprotein is Critical for Chemokine-Mediated Blockade of Infection. *Nature Med*., **1996**, *2*, 1244-1247.
10. Hwang, S. S., Boyle, T. J., Lyerly, H. K., Cullen, B. R. Identification of the Envelope V3 Loop as the Primary Determinant of Cell Tropism in HIV-1. *Science*, **1991**, *253*, 71-74.
11. Rizzuto, C. R., Wyatt, R., Ramos, N. H., Sun, Y., Kwong, P. D., Hendrickson, W. A., Sodroski, J. A Conserved HIV gp120 Glycoprotein Structure Involved in Chemokine Receptor Binding. *Science*, **1998**, *280*, 1949-1953.
12. Trkola, A., Dragic, T., Arthos, J., Binley, J. M., Olson, W. C., Allaway, G. P., Cheng-Mayer, C., Robinson, J., Maddon, P. J., Moore, J. P. CD-4-Dependent, Antibody-Sensitive Interactions between HIV-1 and its Co-Receptor CCR-5. *Nature*, **1996**, *384*, 184-187.
13. lapham, C. K., Ouyang, J., Chandrasekhar, B., Nguyen, N. Y., Dimitrov, D. S., Golding, H. Evidence for Cell-Surface Association between Fusin and the CD4-gp120 Complex in Human Cell Lines. *Science*, **1996**, *274*, 602-605.
14. Bandres, J. C., Wang, Q. F., O'Leary, J., Baleaux, F., Amara, A., Hoxie, J. A., Zolla-Pazner, S., Gorny, M. K. Human Immunodeficiency Virus (HIV) Envelope Binds to CXCR4 Independently of CD4, and Binding can be

Enhanced by Interaction with Soluble CD4 or by HIV Envelope Deglycosylation. *J. Virol*., **1998**, *72*, 2500-2504.

15. Harrop, H. A., Coombe, D. R., Rider, C. C. Heparin Specifically Inhibits Binding of V3 Loop Antibodies to HIV-1 gp120, an Effect Potentiated by CD4 Binding. *AIDS*, **1994**, *8*, 183-192.
16. Lederman, S., Bergmann, J. E., Cleary, A. M., Yellin, M. J., Fusco, P. J., Lee, J. J., Chess, L. Sulfated Polyester Interactions with the CD4 Molecule and with the Third Variable Loop Domain (V3) of gp120 are Chemically Distinct. *AIDS Res. Hum. Retroviruses*, **1992**, *8*, 1599-1610.
17. Callahan, L. N., Phelan, M., Mallinson, M., Norcross, M. A. Dextran Sulfate Blocks Antibody Binding to the Principal Neutralizing Domain of Human Immunodeficiency Virus Type 1 without Interfering with gp120-CD4 Interactions. *J. Virol*., **1991**, *65*, 1543-1550.
18. Schols, D., Pauwels, R., Desmyter, J., Clerco, E. De Dextran Sulfate and other Polyanionic anti-HIV Compounds Specifically Interact with the Viral gp120 Glycoprotein Expressed by T-cells Persistently Infected with HIV. *Virology*, **1990a**, *175*, 556-561.
19. Stein, C. A., Cleary, A. M., Yakubov, L., Lederman, S. Phosphorothioate Oligodeoxynucleotides Bind to the Third Variable Loop Domain (V3) of Human Immunodeficiency Virus Type 1 gp120. *Antisense Research and Development,* **1993**, *3*, 19-31.
20. Wang, W., Chen, H. J., Warshofsky, M., Schwartz, A., Stein, C. A., Rabbani, I. E. Effect of S-dC28 on Vascular Smooth Muscle Cell Adhension and

Plasminogen Activator production. *Antisense & Nucleic Acid Drug Development,* **1997**, *7*, 101-107.

21. Wyatt, J. R., Vickers, T. A., Roberson, J. L., Buckheit, R. W. Jr., Klimkait, T., DeBates, E., Davis, P. W., Rayner, B., Imbach, J. L., Ecker, D. J. Combinatorially Selected Guanosine-Quarter Structure is a potent Inhibitor of Human Immunodeficiency Virus Envelope-Mediated Cell Fusion. *Proc. Natl. Acad. Sci. US,* **1994**, *91*, 1356-1360.
22. Lederman, S., Sullivan, G., Benimetskaya, L., Lowy, I., Land, K., Khaled, Z., Cleary, E. M., Yakubov, L., Stein, C. A. Polydeoxyguanine Motifs in a 12-mer Phosphorothioate Oligodeoxynucleotide Augment Binding to the V3 Loop of HIV-1 gp120 and Potency of HIV-1 Inhibition Independently of G-tetrad Formation. *Antisense & Nucleic Acid Drug Development,* **1996**, 6, 281-289.
23. Hotoda, H., Koizumi, M., Koga, R., Kaneko, M., Shimada, K. Biologically Active Oligodeoxyribonucleotides. 5.[1] 5'-End-Substituted d(TGGGAG) Possesses Anti-Human Immunodeficiency Virus Type 1 Activity by Forming a G-Quadruplex Structure. *J. Med. Chem*., **1998**, *41*, 3655-3663.
24. Tam, R. C., Wu-Pong, S., Pai, B., Lim, C., Chan, A., Thomas, D. F., Milovanovic, T., Bard, J., Middleton, P. J. Increased Potency of Aptameric G-Rich Oligonucleotides is Associated with Novel Functional Properties of Phosphorothioate Linkages. *Antisense & Nucleic Acid Drug Development,* **1999**, 9, 289-300.
25. Stein, C. A., Matsukura, M., Subasinghe, C., Broder, S., Cohen, J. S. Phosphorothioate Oligodeoxynucleotides are Potent Sequence Nonspecific

Inhibitors of De Novo Infection by HIV. *AIDS Res. Hum. Retroviruses*, **1989**, *5*, 639-646.

26. Heegard, N. H. H. Determination of Antigen-Antibody Affinity by Immuno-Capillary Electrophoresis. *J. Chromatogr. A,* **1994**, *680*, 405-412.
27. Liu, J., Volk, K. J., Lee, M. S., Kens, E. H., Rosenberg, I. E. Affinity Capillary Electrophoresis Applied to the Studies of Interaction of a Number of Heat Shock Protein Family with an Immunosuppressant. *J. Chromatogr. A*, **1994**, *680*, 395-403.
28. Rippel, G., Corstjens, H., Billiet, H. A. H., Frank, J. Affinity Capillary Electrophoresis. *Electrophoresis*, **1997**, *18*, 2175-2183.
29. Liu, J., Abid, S., Hail, M. E., Lee, M. S., Hangeland, J., Zein, N. Use of Affinity Capillary Electrophoresis for the Study of Protein and Drug Interaction. *Analyst*, **1998**, *123*, 1455-1459.
30. Rundlett, K. L., Armstrong, D. W. Method for the Estimation of Binding Constants by Capillary Electrophoresis. *Electrophoresis*, **1997**, *18*, 2194-2202.
31. Schmalzing, D., Nashabeh, W. Capillary Electrophoresis Based Immunoassays: a Critical Review. *Electrophoresis*, **1997**, *18*, 2184-2193.
32. Qian, X. H., Tomer, K. B. Affinity Capillary Electrophoresis Investigation of an Epitope on Human Immunodeficiency Virus Recognized by a Monoclonal Antibody. *Electrophoresis*, **1998**, *19*, 415-419.

33. Tao, L., Kennedy, R. T. Measurement of Antibody-Antigen Dissociation Constants using Fast Capillary Electrophoresis with Laser-Induced Fluorescence Detection. *Electrophoresis*, **1997**, *18*, 112-117.

34. Lausch, R., Reif, O. W., Riechel, P., Scheper, T. Analysis of Immunoglobulin G using a Capillary Electrophoresis Affinity Assay with Protein A and Laser-Induced Fluorescence Detection. *Electrophoresis*, **1995**, *16*, 636-641.

35. Xian, J., Harrington, M. G., Davidson. E. H. DNA-protein Binding Assays from a Single Sea Urchin Egg: a High Sensitivity Capillary Electrophoresis Method. *Proc. Natl. Acad. Sci. USA*, **1996**, *93 (1)*, 86-90.

36. Cheng, Y., Prusoff, W. H. Relationship between the Inhibition Constant (K_1) and the Concentration of Inhibitor which Causes 50 per cent Inhibition (I_{50}) of an Enzymatic Reaction. *Biochem. Pharmacol*., **1973**, *22*, 3099-3108.

37. Ward, V. L., Khaledi, M. G. Nonaqueous Capillary Electrophoresis with Laser Induced Fluorescence Detection. *J. Chromatogr. B Biomed. Sci. App.,* **1998,** *718,* 15-22.

38. Mizuochi, T., Spellman, M. W., larkin, M., Solomon, J., Basa, L. J., Feizi, T. Structural Characterization by Chromatographic Profiling of the Oligosaccharides of Human Immunodeficiency Virus (HIV) Recombinant Envelope Glycoprotein gp120 Produced in Chinese Hamster Ovary Cells. *Biomedical Chromatogr*., **1988**, *2*, 260-269.

39. Taverna, M., Baillet. A., Biou, D., Schluter, M., Werner, R., Ferrier, D. Analysis of Carbohydrate-Mediated Heterogeneity and Characterization of N-

Linked oligosaccharides of Glycoproteins by High Performance Capillary Electrophoresis. *Electrophoresis*, **1992**, *13*, 359-366.

40. Zhu, X., Borchers, C., Bienstock, R., Tomer, K. B. Mass spectrometric Characterization of the Glycosylation Pattern of HIV-gp120 Expressed in CHO Cells. Manuscript in preparation.

Figure 5-1. The structure of an oligodeoxynucleotide. B is adenine, guanine, cytosine, or thymine. X=O, phosphodiester oligodeoxynucleotide, X=S, phosphorothioate oligodeoxynucleotide.

Figure 5-2. Representative electropherograms used for the measurement of the dissociation constant between GEM and HIV-1 gp120 by ACE-LIF. All samples contained 37.5 nM FITC-proline, 40 nM HIV-1 gp120. Total concentrations of GEM were: (A) 25 nM, (B) 31.25 nM, (C) 37.5 nM, (D) 43.75 nM. Buffer: 10 mM Tris at pH 8.0. Applied voltage: 30 kV. Capillary: 78 cm (30 cm effective separation length) $\times$ 50 μm i.d..

Figure 5-3. Scatchard plot for the determination of the dissociation constant between GEM and HIV-1 gp120 by ACE-LIF. Electrophoresis conditions are as described in Figure 5-2.

Figure 5-4. Representative electropherograms used for the measurement of the competition constant between Sd ($T_2G_4T_2$) and HIV-1 gp120 by ACE-LIF. All samples contained 37.5 nM FITC-proline, 40 nM HIV-1 gp120, and 40 nM GEM. Total concentrations of Sd ($T_2G_4T_2$) were: (A) 0 μM, (B) 0.156 μM, (C) 0.313 μM, (D) 0.625 μM, (E) 1.25 μM, (F) 2.5 μM. Electrophoresis conditions are as described in Figure 5-2.

Figure 5-5. Representative electropherograms used for the measurement of the competition constant between Od ($T_2G_4T_2$) and HIV-1 gp120 by CE-LIF. All samples contained 37.5 nM FITC-proline, 40 nM HIV-1 gp120, and 40 nM GEM. Total concentrations of Od ($T_2G_4T_2$) were: (A) 0 μM, (B) 15.6 μM, (C) 31.3 μM, (D) 125 μM, (E) 250 μM, (F) 500 μM. Electrophoresis conditions are as described in Figure 5-2.

Figure 5-6. Effects of the structure of phosphorothioate oligodeoxynucleotide on GEM binding to HIV-1 gp120. Electrophoresis conditions are as described in Figure 5-2.

Table 5-1. Competition constants (K_c) of phosphorothioate oligodeoxynucleotides compete with GEM for binding to HIV-1 gp120.

Structure of Oligodeoxynucleotides	IC_{50} (μM)	HIV gp120 binding K_c (μM)
Sd $G_4(T_4G_4)_3$	0.029	1.14
Sd C_{28}	0.13	5.10
Sd $G_4T_4G_4$	0.32	12.56
Sd $T_2G_4T_2$	0.46	18.06
Sd $(GT)_4$	64.9	2548
Sd A_8	>100	>4000
Od $T_2G_4T_2$	>100	>4000

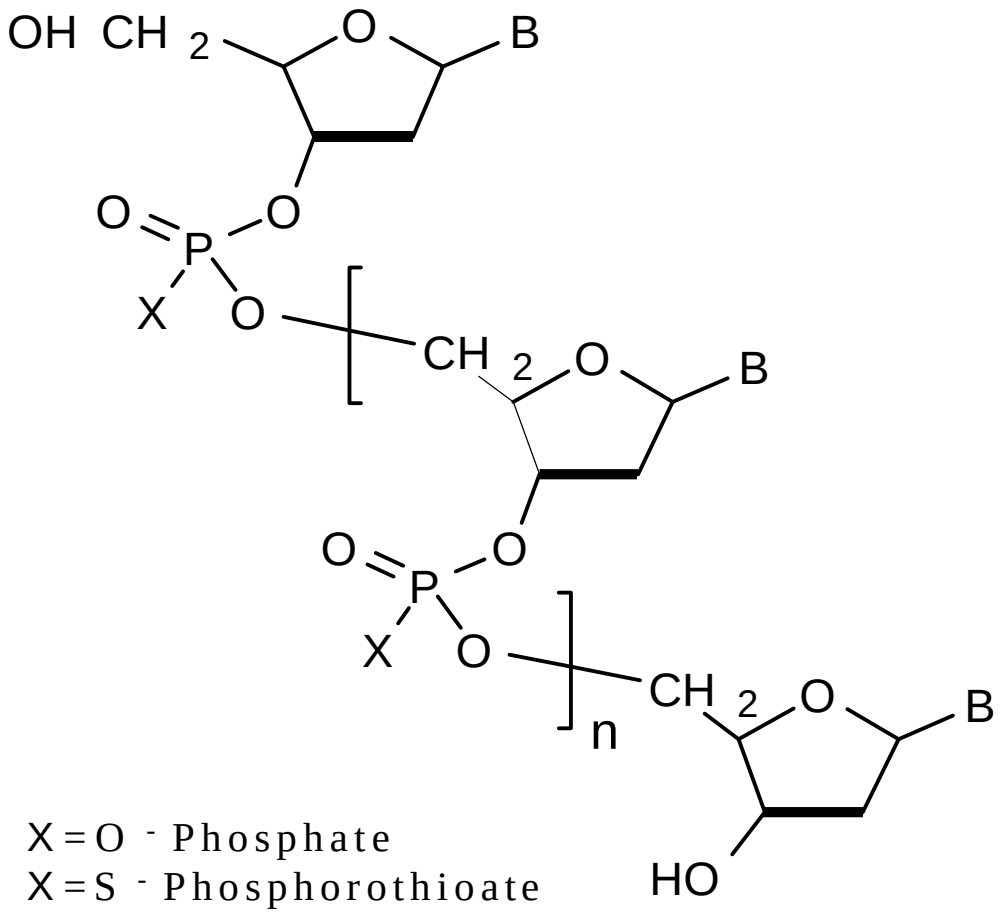
OH CH 2
O
B
O
O
P
X
O
CH 2
O
B
O
O
P
X
O
CH 2
O
B
n
HO
X = O - Phosphate
X = S - Phosphorothioate

Figure 5-1

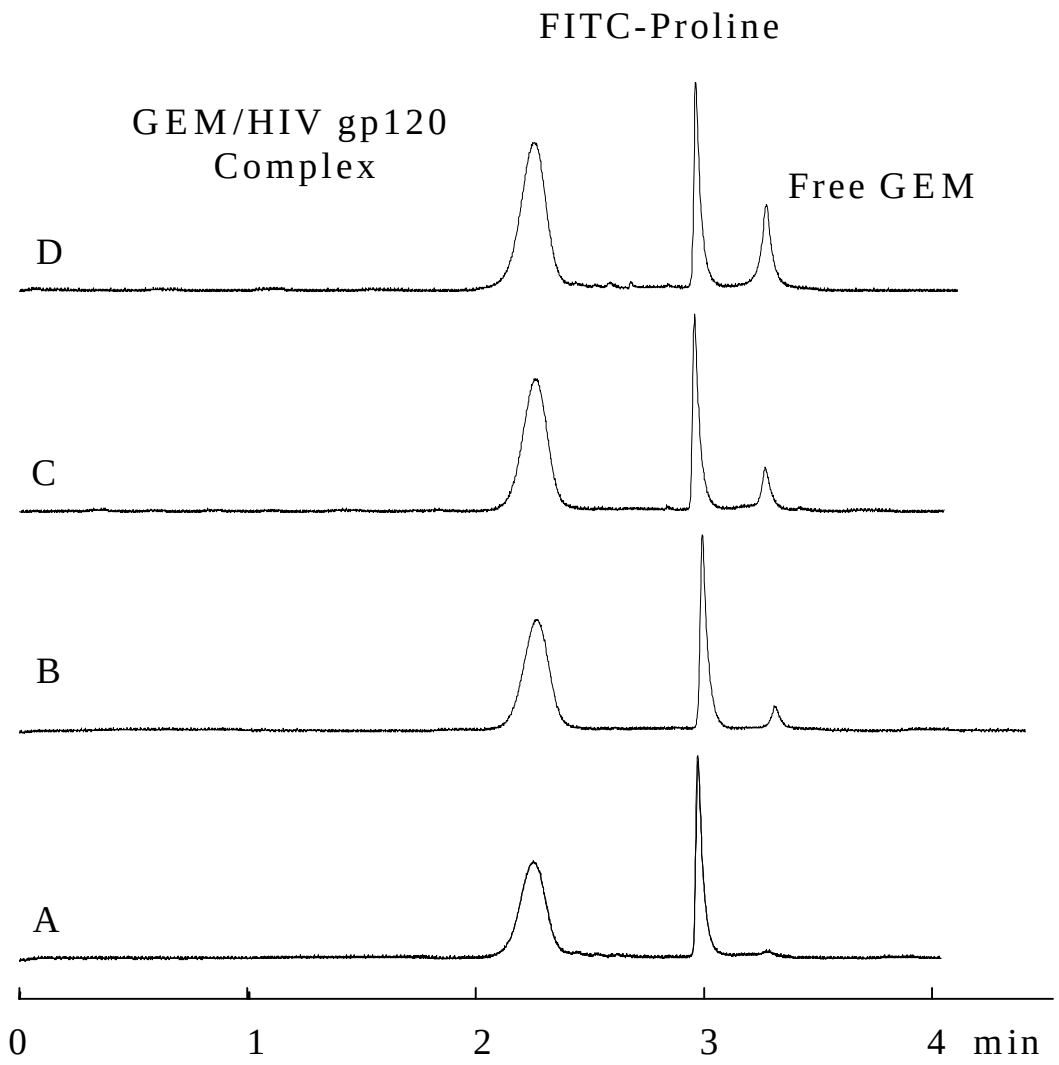

Figure 5-2

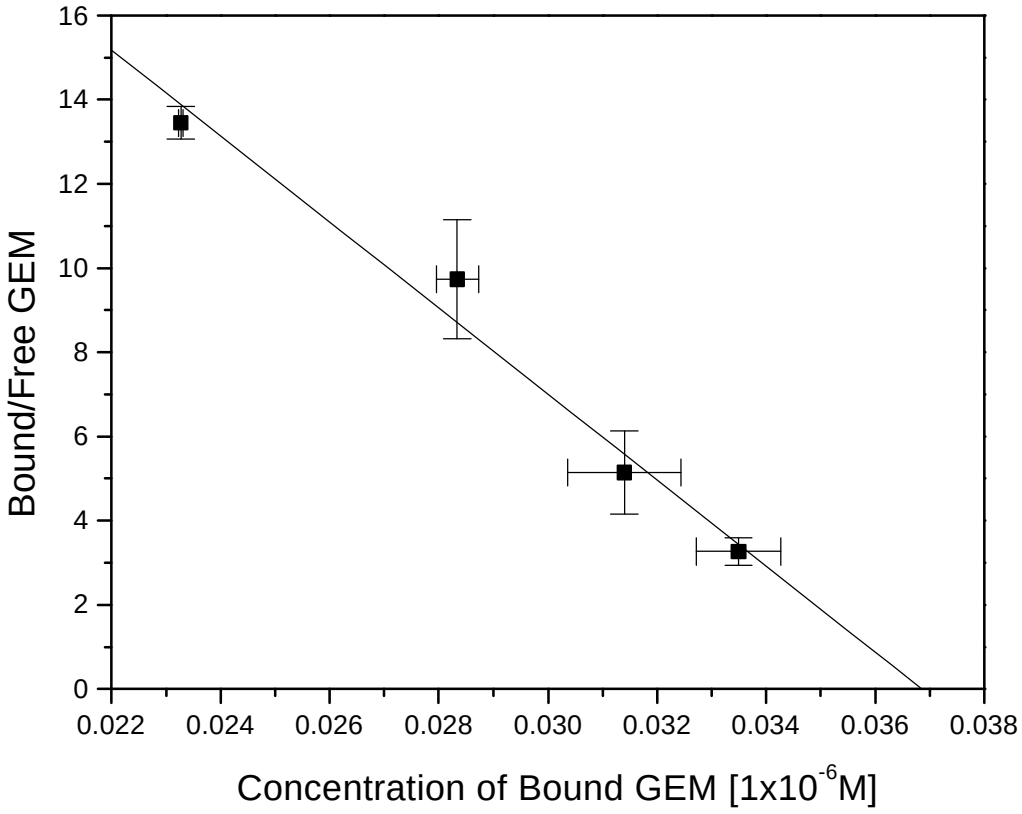
Bound/Free GEM
Concentration of Bound GEM [1x10-6M]
0
2
4
6
8
10
12
14
16
0.022
0.024
0.026
0.028
0.030
0.032
0.034
0.036
0.038

Figure 5-3

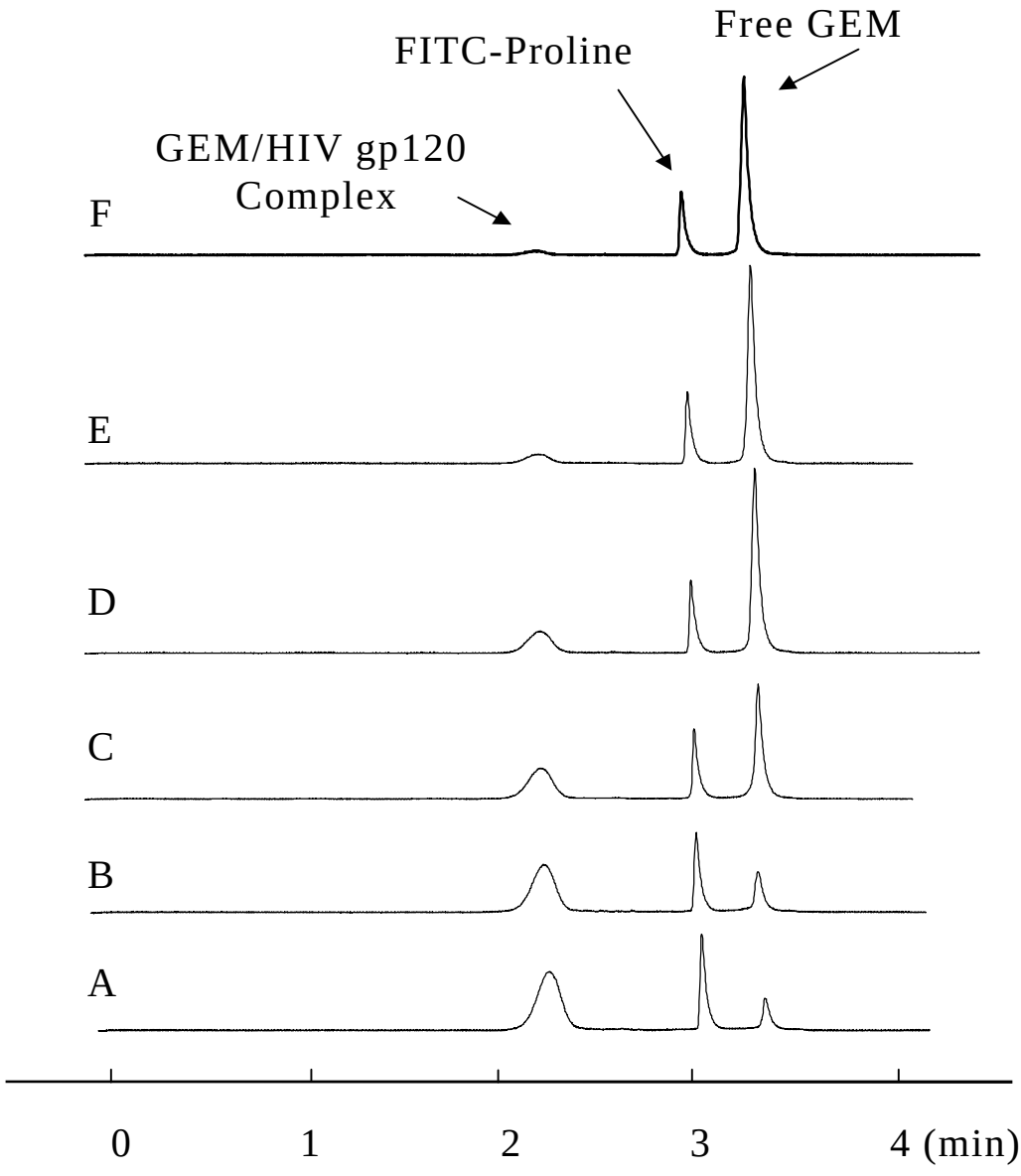
Free GEM
FITC-Proline
GEM/HIV gp120
Complex
F
E
D
C
B
A
0
1
2
3
4 (min)

Figure 5-4

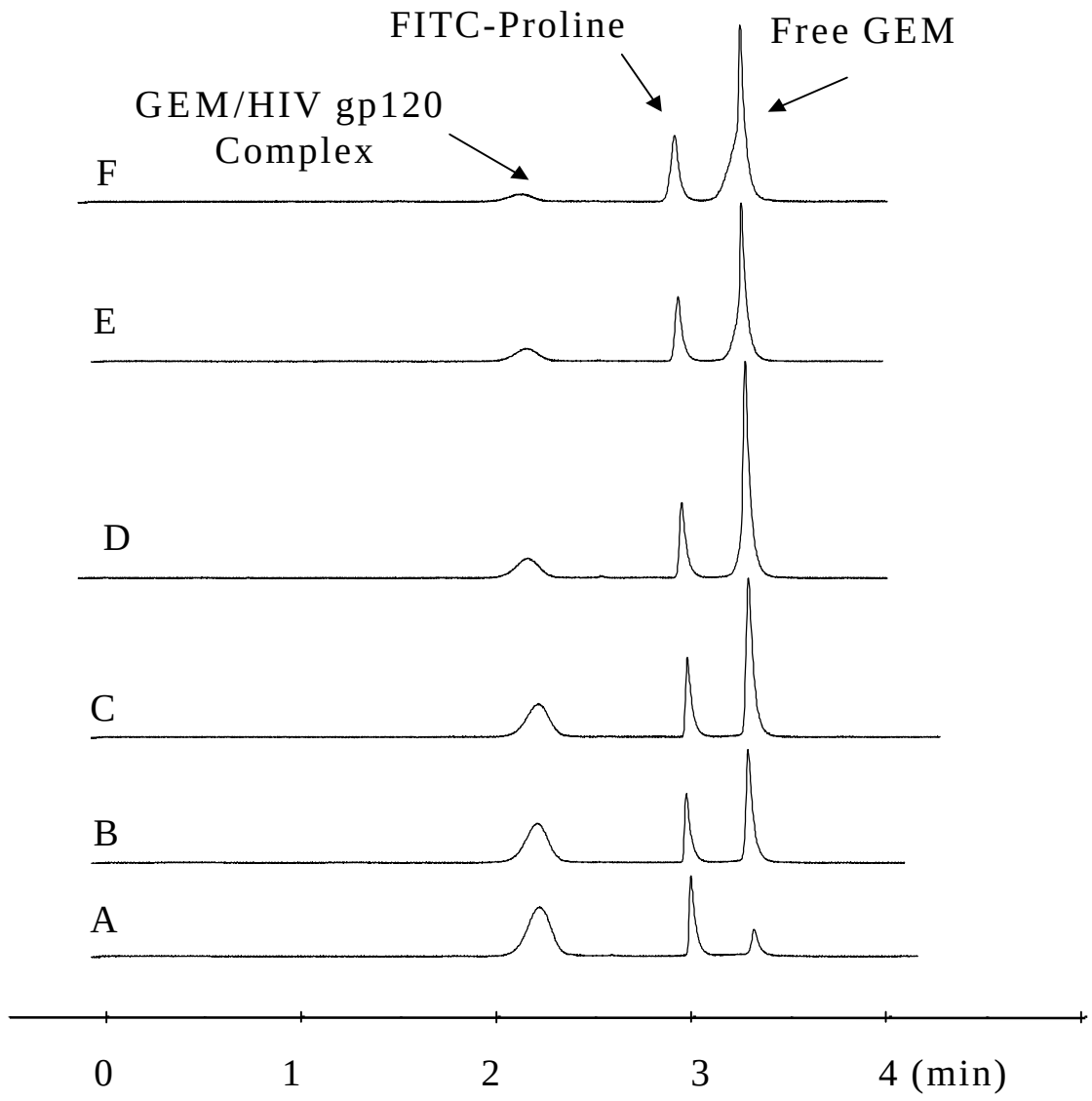
FITC-Proline
Free GEM
GEM/HIV gp120
Complex
F
E
D
C
B
A
0
1
2
3
4 (min)

Figure 5-5

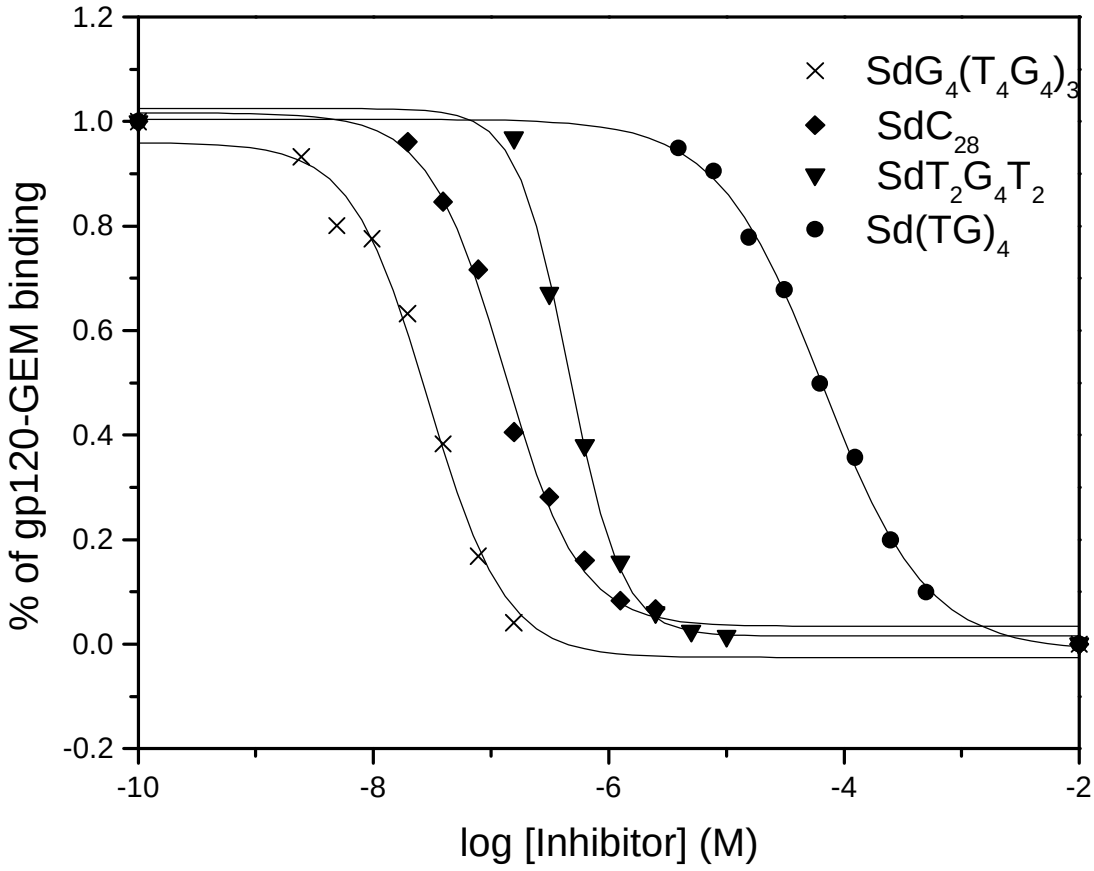
1.2
1.0
0.8
0.6
0.4
0.2
0.0
-0.2
% of gp120-GEM binding
-10
-8
-6
-4
-2
log [Inhibitor] (M)
SdG4(T4G4)3
SdC28
SdT2G4T2
Sd(TG)4

Figure 5-6

Chapter 6

Investigation of the Binding Site on Human Immunodeficiency Virus Recognized by a Monoclonal Antibody by Affinity Capillary Electrophoresis

Wei Zhou, Kenneth B. Tomer, Morteza G. Khaledi

ABSTRACT

Affinity capillary electrophoresis (ACE) was used to investigate the relative contribution of each amino acid on an epitope of human immunodeficiency virus (HIV-1) capsid protein p24 to its binding with an anti-p24 monoclonal antibody. Each amino acid within the epitope (^{83}VHPVHAGPIAP^{93}), previously determined by mass spectrometry, was successively replaced by alanine, and the effect of the substitutes on their affinity for the antibody was examined by ACE. The results showed that amino acids substitution within the sequence of ^{85}PVHAGPIAP^{93} have profound effects on binding to the antibody. Substitution of G89 with alanine almost abolished binding between the peptide and the antibody. Mutation of I91 $\rightarrow$ Ala, or H87 $\rightarrow$ Ala also significantly decreased the affinity of the antibody for the peptide. Results indicate that these three residues are crucial to recognition of the binding site by the antibody. Substitute V83 and H84 by alanine have little effect on the ability of the antibody to bind the peptide suggesting that the side chain of these two residues may not be important in the antigen and antibody interaction.

INTRODUCTION

The protein p24 is the major capsid protein of the human immunodeficiency virus (HIV-1). Antibodies against p24 are produced early after infection and their detection is widely used to diagnose for HIV-1 infection and as a screen for blood supplies [1-5]. As the infection progresses in humans, the level of the antibody to p24 decreases dramatically, except for patients from Central Africa [6-7]. The levels of anti-p24 antibodies, however, remain high in HIV infected nonhuman primates, where the infection does not progress to AIDs [8]. It has been suggested that antibodies to p24 may play an important role in the prevention of the progression of diseases, and an understanding of the contribution of specific amino acids of p24 associated with the immune response in human, therefore, may be useful in the development of a vaccine against infection.

Epitopes or antigenic determinants are the regions of proteins to which antibodies bind. Identification of epitope has been accomplished using a variety of experimental techniques, including X-ray crystallography [9], nuclear magnetic resonance (NMR) [10], site directed mutation [11], proteolytic footprinting combined with mass spectrometry (MS) [12,13] and rapid screening of the cross-reactivity of synthetic peptides from combinatorial libraries with anti-protein antibodies [14]. Knowledge of the structure, chemical and physical properties of the epitope enables the development of synthetic vaccines against infection. Synthetic peptides corresponding to the amino acid sequence of an epitope have

been used to induce virus-neutralizing antibodies [15,16]. It has been suggested that synthetic vaccines would be more stable and defined compared to the use of killed or live viruses because this eliminates the risk due to vaccine contamination [17,18]. If peptides are to be included in a vaccine, care must be taken to ensure that the selected peptide elicits the maximum response by the immune system. Peptides shorter than five residues tend to be conformationally unstable. Conversely, synthetic peptides longer than 20 amino acid in length become increasingly expensive and are also more difficult to synthesize. In general, 10-15 residues in length is practical [18].

Recently, MS combined with proteolytic footprinting has been used to identify the epitope on p24 recognized by a commercially available monoclonal antibody (13-102-100). A linear eleven amino acid sequence was identified as the most tightly affinity-bound fragment (^{84}HPVHAGPIAPG^{94}) [12]. Shortly after the publication, the results from an NMR study showed that the binding site on p24 for cyclophilin A (CypA) is located on the exposed flexible loop, which contains the peptide ^{89}GP^{90} [10]. It is known that the interaction of p24 and CypA results in the packaging of about 200 copies of CypA into each HIV-1 virus [19]. Although the precise function of CypA still needs to be determined, the viruses lacking CypA are poorly infectious [20]. CypA may, therefore, play an important role in HIV replication, possibly helping to disassemble the capsid core upon infection [21]. An antibody that has a binding site on p24 that overlaps that of

CypA may interfere with this essential function, thus preventing the progress of the disease.

In order to further define the structure of the epitope on p24 recognized by the monoclonal antibody, 13-102-100, and to provide an alternative method studying this linear epitope, an affinity capillary electrophoresis (ACE) study of this epitope was also undertaken [22]. In the ACE study, a series of synthetic peptides with the amino acid sequence corresponding to the epitope as determined by MS, but with N- or C-terminal truncations, was employed to probe the structure of the antigentic determinant recognized by the antibody, 13-102-100. The results showed that the first amino acid from the C-terminal of the epitope (G) has little effect on the binding of the peptide to the antibody. The antibody was determined by ACE to recognize the peptide ^{83}VHPVHAGPIAP^{93} with the highest affinity. Shorter peptides containing part of the epitope, however, also showed affinity to the antibody to some extent. These results indicated that ACE has the ability to conveniently detect changes in binding caused by the slight change in the structure of a molecule. In addition, the high resolving power, ease of automation and the ability to detect the interaction of the protein in their native states makes ACE very attractive for the study of antibody and antigen interaction [23-25].

In this study, each amino acid in the peptide (^{83}VHPVHAGPIAP^{93}) (except alanines) was substituted with alanine (Ala). The binding of the complete series

of alanine substituted peptides was examined by ACE to further probe the importance of the contribution of the side chain of each amino acid to binding with the antibody. Two approaches were used in the affinity study. One is the peak height change assay and the other is the migration time shift assay [22]. If the binding between a peptide and the antibody is strong, and the complex dissociates slowly in the time scale of the CE separation, the peptide can be incubated with the antibody until the equilibrium is reached. The peak height change as a function of the concentration of peptide can be measured to evaluate of the binding between the peptide and the antibody. If the dissociation rate is fast compared to the separation time scale, The changing migration time of the antibody as a function of the concentration of the peptide added to the electrophoresis buffer allows the measurement of strength of the interaction. Using these two approaches, we determined the importance of each amino acid within the epitope to the binding affinity of the peptide.

MATERIALS AND METHODS

Chemicals: Tricine (N-tris(hydroxymethyl)methylglycine, electrophoresis reagent, 99%) was purchased from Sigma Chemical Co. (St. Louis, MO). Mouse monoclonal antibody (mAb 13-102-100) recognizing HIV-1 capsid protein p24 was obtained from Advanced Biotechnologies (Columbia, MD). The monoclonal antibody was provided in PBS buffer with 0.1% sodium azide at pH 7.4. All peptides were synthesized by Genosys Biotechnologies, Inc. (The Woodlands,

TX). All the solutions were prepared with deionized water purified by a Model RO 40 ultra-pure water system (Hydro Corp., Research Triangle Park, NC).

Capillary Electrophoresis: All CE experiments were performed on a Hewlett Packard ^{3D}Capillary Electrophoresis System (Hewlett Packard, Waldbronn, Germany). Separations were carried out using a 75 μm i.d. × 365 μm o.d. fused silica capillary. All capillaries were purchased from Polymicro Technologies (Tucson, AZ). The electrophoresis buffer was 100 mM Tricine at pH 8.0. The buffer solution was filtered through a 0.45 μM pore size filter from Millipore C0. (Bedford, MA) prior to use. A 30 kV voltage was applied across a 64.5 cm long capillary with an effective length of 56 cm (from the injection end to the detection window). The capillary was maintained at 25°C by Peltier cooling. Samples were introduced into the capillary by pressure injection for 4s at 50 mbar followed by an injection of electrophoresis buffer for 1s at the same pressure. Between each analysis, the capillary was rinsed sequentially with 0.1 N sodium hydroxide, water for 2 min each before being rinsed with running buffer for 5 min. Analytes were detected at 200 nm. Data collection, storage and analysis were performed using the HP Chemstation (Hewlett Packard data system). Data reported here are the means of triplicate analyses.

Peak Height Change Assay: The monoclonal antibody stock solution (6.66 μM) was used as received. Stock solutions (333.3 μM) of peptides were prepared by dissolving the required amount of peptide into the running buffer.

The peptide solutions were prepared by serial dilution of the stock solution with running buffer. All sample solutions were obtained by adding 12 μL of the monoclonal antibody solution at constant concentrations to 12 μL of the peptide solutions of different concentrations. The final concentration of the monoclonal antibody was 1.67 μM. Concentrations of the peptides varied. Each sample was mixed thoroughly and incubated at room temperature for 30 min prior to CE analysis. It has been reported that equilibrium between synthetic peptide (^{83}VHPVHAGPIAP^{93}) and the antibody can be reached in solution within 30 min with no further significant changes in peak areas observed up to 12 hour of incubation at room temperature [22].

Migration Time Shift Assay: Electrophoresis buffers were prepared by serial dilution of the peptide stock solution with 100 mM Tricine at pH 8.0. Final concentrations of the peptide in the buffer varied from 0 μM to 40 μM. The migration time of acetonitrile was used as an electroosmotic flow (EOF) marker, and was measured in the same electrophoresis buffer as that used for the analysis of the migration time shift of the antibody. Subtraction of the EOF from the migration time shift of the antibody in the same electrophoresis buffer (t_R-EOF) corrects for the changes in migration time of the antibody caused by the changes in EOF. The migration time shifts of the antibody used are the EOF corrected migration times.

RESULTS AND DISCUSSION

Peak Height Change Assay: Prior to CE analysis, all the samples were incubated at room temperature for 30 min to ensure that equilibrium was established. Shown in Figure 6-1 are the representative electropherograms used during the peak height change assay for the evaluation of the binding between the antibody and peptide (^{83}VAPVHAGPIAP^{93}, a single site mutation of H^{84} $\rightarrow$ Ala). The small peak that migrates before the EOF can be attributed to the salt from the buffer that comes with the antibody sample. The peak corresponding to the antibody is well shaped with no indication of adsorption. The antibody migrates slower than the EOF which indicates that the antibody carries a net negative charge under the electrophoresis condition. A small peak corresponding to the peptide at the maximum concentration of peptide used in the experiment was also observed (Figure 6-1F). As the molar ratio of peptide:antibody increases, a bigger and broader peak, assigned as peptide/antibody complex peak, appears at the same migration time as does the peptide peak. The height of the antibody peak decreases correspondingly. When the molar ratio of peptide:antibody exceeded 3:1, no further significant decrease in the height of the antibody peak was observed indicating that dissociation of the complex occurs on the separation time scale.

The single site mutation (H84$\rightarrow$ Ala) has little effect on the binding ability of the peptide to the antibody suggesting that the side chain of H84 may not be the part of the binding site [22]. However, deletion of ^{83}VH^{84} greatly reduced binding ability of the peptide to the antibody as showed in the previous ACE

study [22]. This indicates that the ^{83}VH^{84} sequence may be important in maintaining the conformational stability of the peptide.

Figure 6-2 shows the representative electropherograms used in detecting the effect of the single site mutation G89 → Ala on the binding of the peptide to the antibody. Notice that even when the molar ratio of peptide:antibody reaches 20:1, no peak due to the formation of the peptide:antibody complex was observed. This means that substituting G89 by Ala abolished binding between the synthetic peptide and the antibody G89, therefore, is critical to the binding site recognized by the antibody. It has been reported that the binding site of CypA on p24 is located on the flexible loop connecting helices IV and V. Mutation on this loop, including P90 → Ala, G89 → Ala and deletion of ^{90}PIAP^{93} abolished CypA binding *in Vitro* and diminished viral infectivity in culture [10, 20, 26]. This suggests that the anti-p24 antibody has a binding site on p24 similar to the CypA recognition site.

Binding of the antibody to the single site mutation P85 → Ala was decreased considerably, although it was not totally abolished (Figure 6-3). The mutations V83 → Ala or V86 → Ala, however, did not significantly alter the ability of the antibody to recognize the peptides. The relative contributions of each amino acid side chain on binding to the antibody are plotted in Figure 6-4. The percentage of unbound antibody in the sample was calculated by dividing the experimentally observed peak height by the peak height of the same

concentration of antibody under the same electrophoresis condition in the absence of peptide. These results showed that the antibody recognizes a 9-mer proline rich flexible loop ^{85}PVHAGPIAP^{93}, in which the absence of a side chain in G89 is crucial to binding. I91 and H87 are also very important binding residues. The profound effect of the mutation (H87 $\rightarrow$ Ala) on binding to the antibody suggests that the positive charge of H87 may play an important role in the binding. The substitution of any one of the three prolines may result in an improper peptide conformation. It has been reported, however, that P93 is located within the CypA binding loop, and can be mutated to Ala without affecting virus production or infectivity [26]. The results shown in this ACE study also indicate that the substitution (P93 $\rightarrow$ Ala) may not lead to the total destabilization of the conformation of the peptide. The resulting peptide is still recognized by the antibody. The deletion (not substitution) of P93, however, almost completely eliminates the affinity between the antibody and the peptide as reported previously [22]. Both V83 and H84 could be replace by Ala without a loss of antibody recognition suggesting that the side chains of the amino acids at these positions were either not specifically or at least not strongly involved in antigen recognition. Although V86 is located in the antigenic determinant, the affinity of the V86 $\rightarrow$ Ala mutant for the antibody remained the same, indicating that the substitution has little effect on binding which may be due to the similarity of the physical properties of these two amino acids.

It is also interesting to note that NMR studies have shown that in the free monomeric N-terminal domain, P90 could adopt kinetically trapped cis and trans conformations. It was hypothesized that the different loop conformations may serve as a molecular switch for capsid assembly and disassembly or may facilitate distinct intermolecular interactions [10]. Site mutations showed that a single site mutation of P90 to alanine abolished CypA binding and prevented viral replication, indicating that P90 is an essential residue for CypA binding. However, P85 $\rightarrow$ Ala and P93 $\rightarrow$ Ala mutants did not replicate, although they could still bind CypA [27]. The incorporation of ^{87}HAGPIA^{92} loop of HIV-1 into chimeric capsid proteins that of otherwise contain non-binding sequences enables CypA binding. These results showed that there is a significant overlap of the CypA binding site and the binding site recognized by the antibody 13-102-100. This antibody, therefore, may interfere with the binding between p24 and CypA, and, thus, may preventing the progress of the disease.

Migration Time Shift Assay: For peptides that have an equilibrium time faster than the CE separation time scale, evaluation of the binding between the antibody and peptides was achieved by migration time shift assay [22]. In this method, different concentrations of peptide solutions were used as electrophoresis buffers. The changes in the electrophoretic mobility of the antibody using buffers with different peptide concentrations were measured. Acetone was used as a marker for the electroosmotic flow. The electroosmotic flow was subtracted from the experimentally measured mobility of the antibody

before using the mobility of the antibody to determine the changes in mobility caused by the changes in the buffer composition. Shown in Figure 6-5 are the electropherograms used in the migration time shift assay of peptide ^{83}VHPVAAGPIAP^{93} (a single site mutation of H87 $\rightarrow$ Ala). Increasing the concentration of the peptide in the buffer from 1.25 to 40 μM, a 10 s migration time change of the antibody was determined. Significant peak broadening was also observed suggesting that this mutant is still recognized by the antibody.

Increasing the concentration of substitute V83 $\rightarrow$ Ala or V86 $\rightarrow$ Ala in the buffer, the antibody peak is fractionated into interacting and non-interacting peaks indicating that binding between the antibody and these two peptides is very strong, and that the dissociation rate is slow relative to the separation time scale (data not shown). Migration time shift assay, therefore, can not be used in this case. Upon increasing the concentration of the mutant G89 $\rightarrow$ Ala from 0 μM to 20 μM, no change in migration time for the antibody was observed. This is consistent with the results we obtained from the peak height change assay, indicating that this single site mutation totally abolished the binding between the mutant and the antibody (Figure 6-6). The rest of the substitutions were also examined. The antibody peak starts to broaden as the concentration of the peptide in the buffer is increased, and the migration time of the antibody varied from 7 s to 11 s indicating that the substitutes are still recognized by the antibody (Figure 6-6). The initial order is the same as for the peak height change assay except that the order of P90 and P85 are reversed.

CONCLUSIONS

ACE has been used to study the effect of the single site mutations on the binding ability of the epitope on p24 recognized by a commercially-available anti-p24 monoclonal antibody 13-102-100. Each residue of the original epitope determined by the previous MS study was successively substituted by alanine, and the effect of the substitutes on their affinity to the antibody was examined by ACE. We were able to determine that a single site mutation of G89 $\rightarrow$ Ala almost abolished the binding between the synthetic peptide and the antibody. The substitutions I91 $\rightarrow$ Ala, and H87 $\rightarrow$ Ala had significantly lower affinity to the antibody, Replacement of P90 $\rightarrow$ Ala, P85 $\rightarrow$ Ala, or P93 $\rightarrow$ Ala decreased, but did not eliminate the binding ability to the antibody. The affinity for the antibody of the mutants V83$\rightarrow$ Ala, H84 $\rightarrow$ Ala, and V86 $\rightarrow$ Ala, however, remained the same. Increased detailed information or the relative contribution of the side chain of each residue to the affinity of the peptide to the antibody, therefore, was obtained. These results showed that the sequence ^{85}PVHAGPIAP^{93} contained the core epitope. Both V83 and H84 determined previously to be part of the epitope by epitope excision combined with MS, are important for maintaining the conformation of the peptide but the side chains are not involved in the interaction because substitution of these residues with Ala had little effect on the binding ability of the peptides.

The results we obtained from the ACE study showed that the antibody studied has a binding site similar to that of CypA, whose binding to p24 is believed to facilitate viral uncoating. This may provide useful information in the design of synthetic vaccines to induce virus-neutralizing antibodies that interfere with the interaction between p24 and CypA. High separation power and ease of automation of ACE offer an effective and rapid means to study of these types of biological interaction.

ACKNOWLEDGEMENTS

This project is financially supported by Office of the AIDS Research and NIH, for which the authors are grateful.

REFERENCES

1. Lang, J. M. A., Paul, D. A., Huisman, H. G., de Wolf, F., van den Berg, H., Coutinho, R. A., Danner, S. A., van de Noordaa, J., Goudsmit, J. Persistent HIV Antigenaemia and Decline of HIV Core Antibodies Associated with Transition to AIDS. *Br. Med. J.,* **1986,** *293,* 1459-1462.
2. Weber, J. N., Clapham, P. R., Weiss, R. A., Parker, D., Roberts, C., Duncan, J., Weller, I., Carne, C., Tdder, R. S., Pinching, A. J., Cheingsong-Popov, R. Human Immunodeficiency Virus Infection in Two Cohorts of Homosexual Men: Neutralising Sera and Association of Anti-gag Antibody with Prognosis. *Lancet,* **1987,** *1,* 119-122.
3. Broliden, P. A., Morfeldt-Mansson, L., Rosen, J., Jondal, M., Wahren, B. Fine Specificity of IgG Subclass Response to Group Antigens in HIV-1-infected Patients. *Clin. Exp. Immunol.,* **1989,** 76, 216-221.
4. Cunningham, A. L., Dwyer, D. E., Dowton, D. N. Viral Markers in HIV Infection and AIDS. *J. Acquir. Immune Defic. Syndr.,* **1993**, *6 Suppl 1,* S32-35.
5. Saag, M. S. Use of Virologic Markers in Clinical Practice. *J. Acquir. Immune Defic. Synd.r Hum. Retrovirol.,* **1997,***16 Suppl 1,*S3-13.
6. Barin, F. AIDS Vaccine Predictions. *Nature,* **1987,** *328,* 21.
7. Chou, M. J., Lee, T. H., Hatzakis, A., Mandalaki, T., Mclane, M. F., Essex, M. Antibody Response in Early Human Immunodeficiency Virus Type 1 Infection in Hemophiliacs. *J. Infect. Dis.,* **1988,** *157,* 805-811.
8. Lusso, P., Markham, P. D., Ranki, A., Earl, P., Moss, B., Dorner, F., Gallo, R. C., Krohn, K. J. Cell-Mediated Immune Response Toward Viral Envelope and

Core Antigens in Gibbon Apes (Hylobates lar) Chronically Infected with Human Immunodeficiency Virus-1. *J. Immunol.,* **1988,** *141,* 2467-2473.

9. Amit, A. G., Mariuzza, R. A., Phillips, S. E., Poljak, R. J. Three-Dimensional Structure of an Antigen-Antibody Complex at 2.8 A Resolution. *Science,* **1986,** *233,* 747-753.
10. Gitti, R. K., Lee, B. M., Walker, J., Summers, M. F., Yoo, S., Sundquist, W. I. Structure of the Amino-Terminal Core Domain of the HIV-1 Capsid Protein. *Science,* **1996,** *273,* 231-235.
11. Mizukami, T., Fuerst, T. R., Berger, E. A., Moss, B. Binding Region for Human Immunodeficiency Virus (HIV) and Epitopes for HIV-blocking Monoclonal Antibodies of the CD4 Molecule Defined by Site-directed Mutagenesis. *Proc. Natl. Acad. Sci. USA,* **1988**, 85, 9273-9277.
12. Parker, C. E., Papac, D. I., Trojak, S. K., Tomer, K. B. Epitope Mapping by Mass Spectrometry: Determination of an Epitope on HIV-1_{IIIB} p26 Recognized by a Monoclonal Antibody. *J. Immunol.,* **1996,** *157,* 198-206.
13. Jeyarajah, S., Parker, C. E., Summner, M. T., Tomer, K. B. Matrix-Assisted Laser Sesorption Ionization Mass Spectrometry Mapping of Human Immunodeficiency Virus-gp120 Epitopes Recognized by a Limited Polyclonal Antibody. *J. Am. Mass Spectrom.,* **1998,** *9,* 157-165.
14. Langedijk, J. P. M., Schalken, J. J., Tersmette, M., Huisman, J. G., Meloen, R. H. Location of Epitopes on the Major Core Protein p24 of Human Immunodeficiency Virus. *J. Gen. Virol.,* **1990,** *71*, 2609-2614.

15. Cornette, J. L., Margalit, H., DeLisi, C., Berzofsky, J. A. Identification of T-Cell Epitope and use in Construction of Synthetic Vaccine. *Methods Enzymol.,* 178, 611-634.
16. Milich, D. R., Thornton, G. B. use of Synthetic T-Cell Epitopes as Immunogens to Induce Antibodies to Hepatitis B Components. *Methods Enzymol.,* 178, 634-659.
17. Francis M. J., Clarke, B. E. Peptide Vaccines Based on Enhanced Immunogenicity of Peptides Epitopes Presented with T-Cell Determinants or Hepatitis B Core Protein. *Methods Enzymol.,* 178, 659-676.
18. Gnann, J. W. Jr., Smith L., Oldstone, M. B. A. Custom-Designes Synthetic peptide Immunoassays for Distinguishing HIV Type 1 and Type 2 Infections. *Methods Enzymol.,* 178, 693-715.
19. Luban, J., Bossolt, K. L., Franke, E. K., Kalpana, G. V., Goff, S. P. Human Immunodeficiency Virus Type 1 Gag Protein Binds to Cyclophilins A and B. *Cell,* **1993,** *73*, 1067-1078.
20. Thali, M., Bukovsky, A., Kondo, E., Rosenwirth, B., Walsh, C. T., Sodroski, J., Gottlinger, H. G. Functional Association of Cyclophilin A with HIV-1 Virions. *Nature,* **1994**, *372*, 363-365.
21. Gamble, T. R., Vajdos, F. F., Yoo, S., Worthylake, D. K., Houseweart, M., Sundquist, W. I., Hill, C. P. Crystal Structure of Human Cyclophilin A Bound to the Amino-Terminal Domain of HIV-1 Capsid. *Cell,* **87**, 1285-1294.

22. Qian, X. H., Tomer, K. B. Affinity Capillary Electrophoresis Investigation of an Epitope on Human Immunodeficiency Virus Recognized by a Monoclonal Antibody. *Electrophoresis,* **1998,** *19,* 415-419.
23. Heegard, N. H. H. Determination of Antigen-Antibody Affinity by Immuno-Capillary Electrophoresis. *J. Chromatogr.,* **1994**, *680*, 405-412.
24. Schmalzing, D., Nashabeh, W. Capillary Electrophoresis Based Immunoassays: a Critical Review. *Electrophoresis*, **1997**, *18*, 2184-2193.
25. Chu, Y. H., Dunayevskiy, Y. M., Kirby, D. P., Vouros, P., Karger, B. L. Affinity Capillary Electrophoresis-Mass Spectrometry for Screening Combinatorial Libraries. *J. Am. Chem. Soc.,* **1996,** *118,* 7827-7835.
26. Franke, E. K., Yuan, H. E., Luban, J. Specific Incorporation of Cyclophilin A into HIV-1 Virions. *Nature,* **1994**, *372*, 359-362.
27. Momany, C., Kovari, l. C., Prongay, A. J., keller, W., Gitti, R. K., Lee, B. M., Gorbalenya, A. E., Tong, L., Rossmann, M. G. Crystal Structure of Dimeric HIV-1 Capsid Protein. *Nat. Struct. Biol.,* **1996,** 3, 763-770.

Figure 6-1. Electropherograms used for the evaluation of the binding between the antibody 13-102-100 and the peptide ^{83}VAPVHAGPIAP^{93} in the peak height change assay. All samples contained 1.67 μM antibody. The molar ratios of antibody:peptide in the samples were: (A) 1:0 (B) 1:1 (C) 1:2 (D) 1:3 (E) 1:5 (F) 0:5. Buffer: 100 mM Tricine at pH 8.0. Applied voltage: 30 kV. Capillary: 64.5 cm (56 cm effective separation length) × 75 μm I. D.

Figure 6-2. Electropherograms used for the evaluation of the binding between the antibody 13-102-100 and the peptide ^{83}VHPVHAAPIAP^{93} in the peak height change assay. All samples contained 1.67 μM antibody. The molar ratios of antibody:peptide in the sample were: (A) 1:0 (B) 1:3 (C) 1:5 (D) 1:10 (E) 1:20 (F) 0:20. Electrophoresis conditions are as described in Figure 6-1.

Figure 6-3. Electropherograms used for the evaluation of the binding between the antibody 13-102-100 and the peptide ^{83}VHAVHAGPIAP^{93} in peak height change assay. All samples contained 1.67 μM antibody. The molar ratios of antibody:peptide in the sample were: (A) 1:0 (B) 1:1 (C) 1:3 (D) 1:5 (E) 1:10 (F) 0:10. Electrophoresis conditions are as described in Figure 6-1.

Figure 6-4. Binding profile between the mAb (13-102-100) and the alanine substitutions for the peptide ^{83}VHPVHAGPIAP^{93}. The y-axis represents the percent of the peak height of the antibody compared to the original peptide. The molar ratio of the antibody:peptide was 1:5 for all substitutions.

Figure 6-5. Electropherograms used for the evaluation of the binding between the antibody 13-102-100 and the peptide ^{83}VHAVHAGPIAP^{93} in the migration time shift assay. The concentration of the antibody was 1.67 μM. The buffer was 100 mM Tricine at pH=8.0 with the addition of (A) 1.25 μM (B) 2.5 μM (C) 5 μM (D) 10 μM (E) 20 μM (F) 40 μM of the peptide. Electrophoresis conditions are as described in Figure 6-1.

Figure 6-6. Relative migration time change (t_R-EOF) assay for the interaction of mAb (13-102-100) and the alanine substitutions for the peptide ^{83}VHPVHAGPIAP^{93}. Relative migration time change is the function of the concentration of peptides added to the electrophoresis buffer.

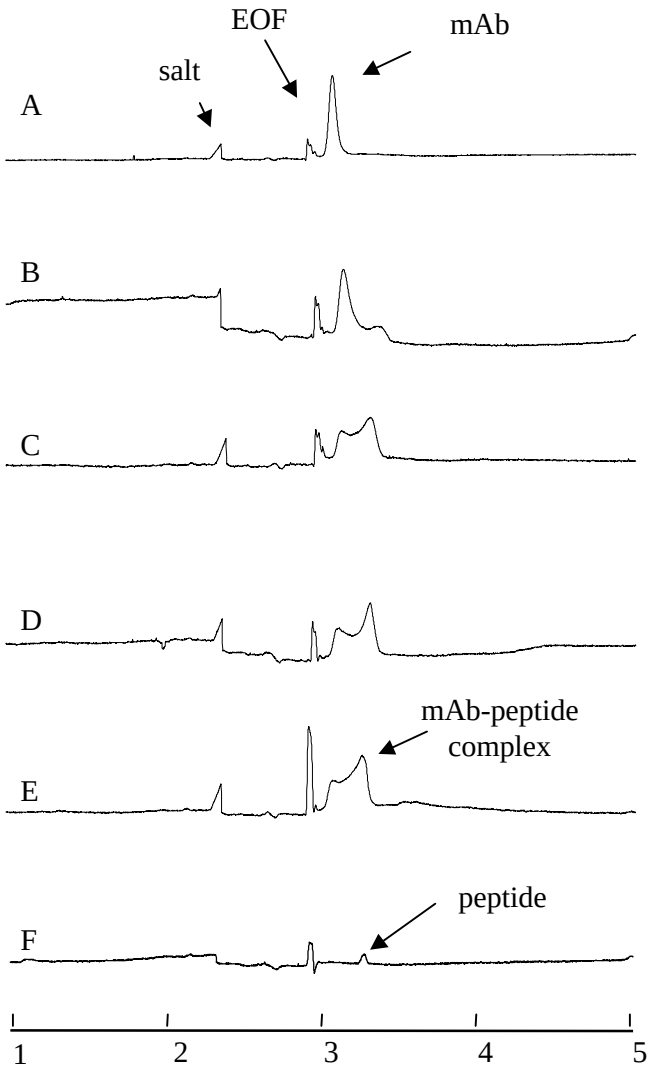
EOF
mAb
salt
A
B
C
D
mAb-peptide
complex
E
peptide
F
1
2
3
4
5
Time (min)

Figure 6-1

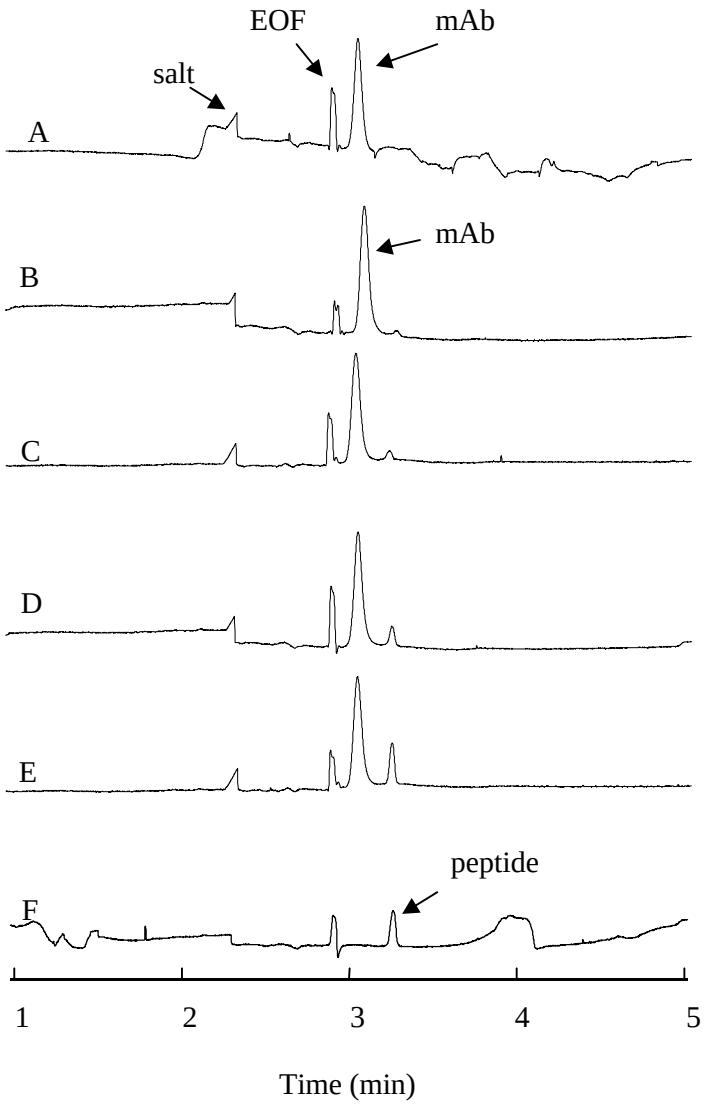

Figure 6-2

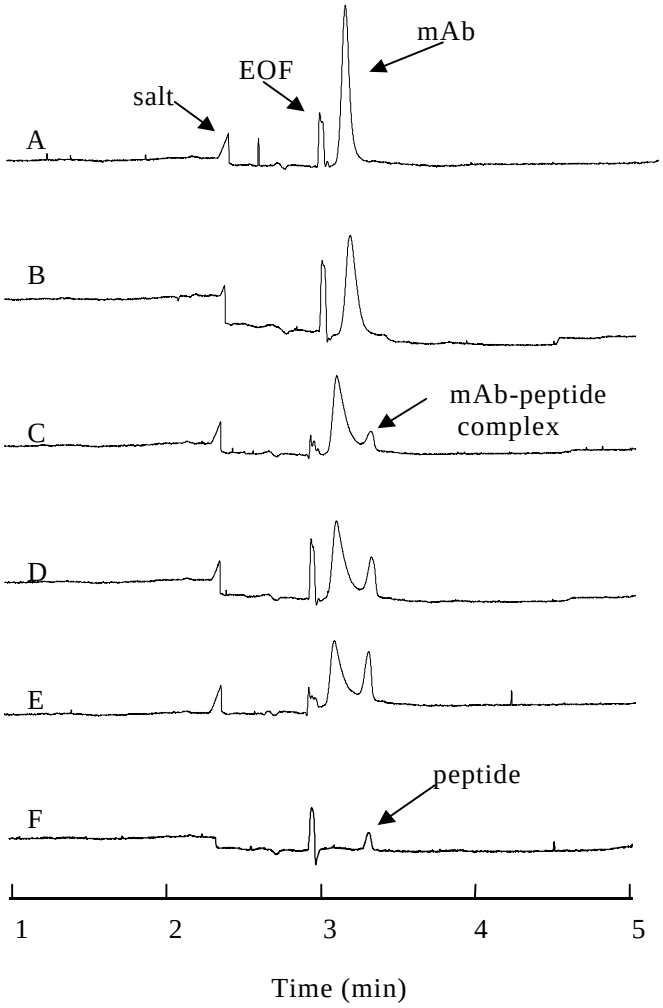
mAb
EOF
salt
A
B
mAb-peptide
complex
C
D
E
peptide
F
1
2
3
4
5
Time (min)

Figure 6-3

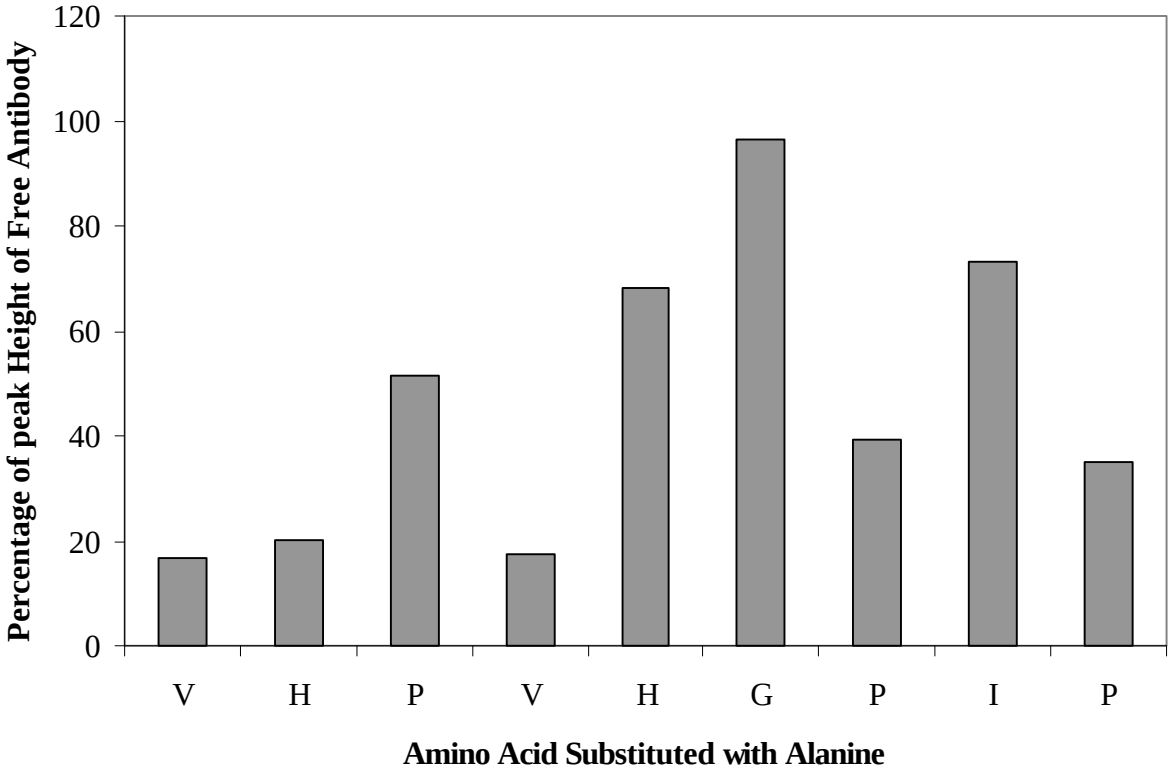
120
100
80
60
40
20
0
Percentage of peak Height of Free Antibody
V
H
P
V
H
G
P
I
P
Amino Acid Substituted with Alanine

Figure 6-4

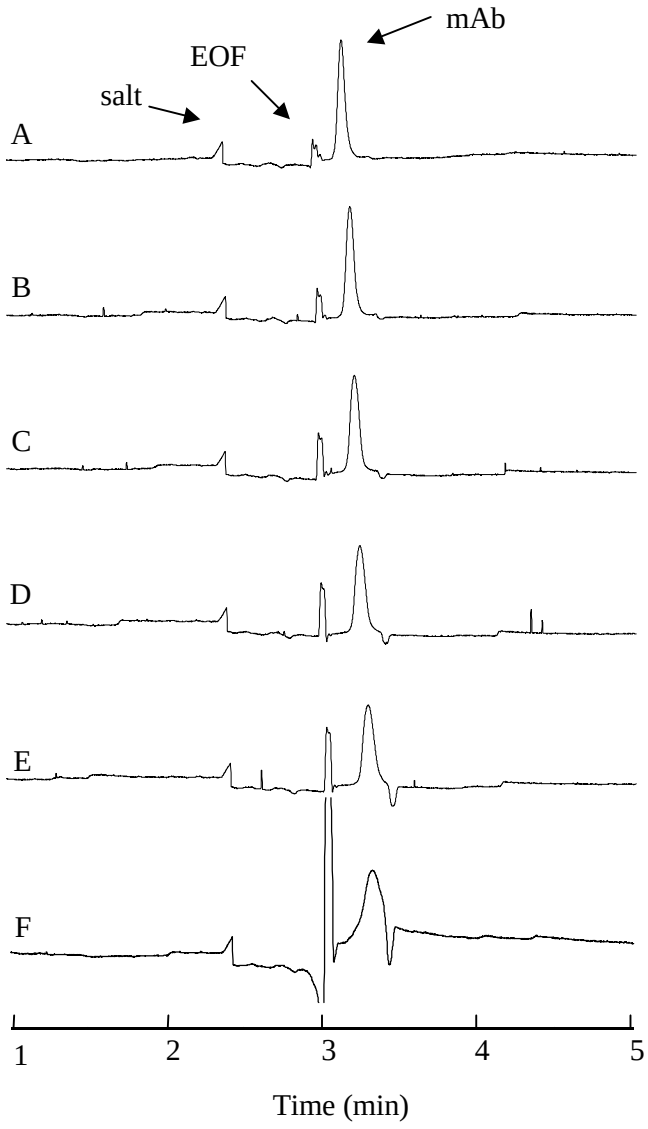

Figure 6-5

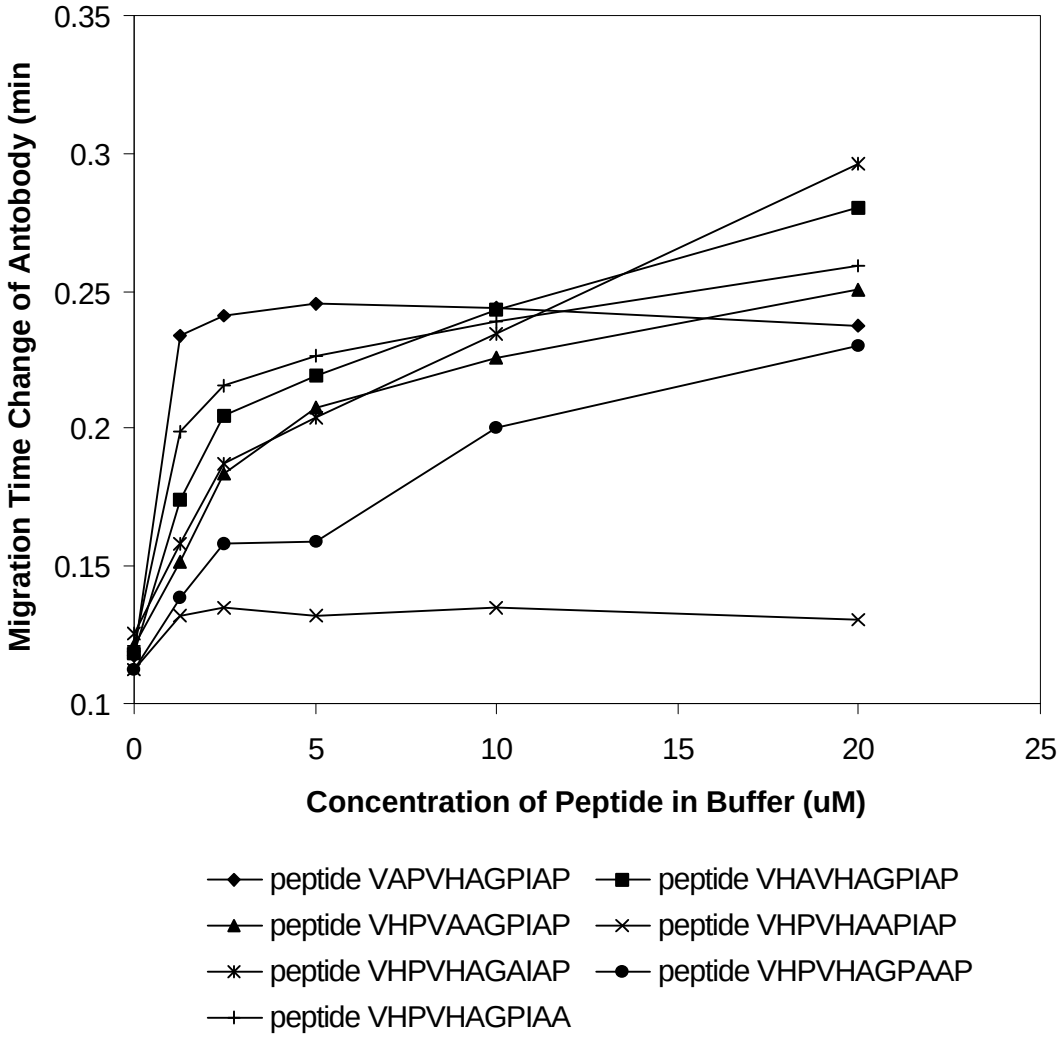
0.35
0.3
0.25
0.2
0.15
0.1
Migration Time Change of Antobody (min
0
5
10
15
20
25
Concentration of Peptide in Buffer (uM)
peptide VAPVHAGPIAP
peptide VHAVHAGPIAP
peptide VHPVAAGPIAP
peptide VHPVHAAPIAP
peptide VHPVHAGAIAP
peptide VHPVHAGPAAP
peptide VHPVHAGPIAA

Figure 6-6

Appendix:

Separation of Synthetic Polymers by Capillary Electrochromatography and Capillary Electrophoresis

Wei Zhou, Leesa J. Deterding, Kenneth B. Tomer, Morteza, G. Khaledi

ABSTRACT

Despite the explosive growth of reports on the applications of capillary electrophoresis (CE) and capillary electrochromatography (CEC) for the separations of small molecules or large biological molecules, the separation of synthetic polymers of industrial significance has been largely ignored. This has been mainly due to the difficulties associated with the separation of synthetic polymers, such as the lack of charge and chromophore in most of the synthetic polymers. In this study, the separation of synthetic polymers by both CE and CEC was attempted. The successful application of size exclusion CEC for the separation of uncharged synthetic macromolecules has been achieved. In addition, separations of non-ionic surfactants by CE were obtained. The profound effects of an organic modifier as well as ionic strength on the separation selectivity are discussed.

INTRODUCTION

Capillary electrophoresis (CE) [1,2] has gained enormous popularity in the past years due to a combination of high efficiency, short analysis time and small sample size requirement. In addition, the flexibility of incorporating various separation mechanisms greatly extends the range of application of CE to separation of various charged and uncharged compounds. For example, in micellar electrokinetic chromatography (MEKC) [3,4], micelles can be used as pseudo-stationary phases to facilitate the separation of uncharged compounds. But in some cases, binding to the micelle is often so strong that it is difficult to achieve any degree of selectivity using micelles alone. As a result, organic modifiers have been added to the buffers to adjust the degree of interaction between solute and micelle [5,6]. A number of reports have also been made on the use of polymeric additives in CE [7,8]. By incorporating a sieving media, the separation of macromolecules by CE based on the size difference also becomes possible.

Capillary electrochromatography (CEC) has attracted much interest recently [9-13]. In CEC, a mobile phase is driven through a stationary phase in a packed capillary column by electroosmotic flow (EOF) generated by an electric field. In contrast to the parabolic flow profile of pressure driven systems, the almost perfect plug flow profile of CEC reduces band broadening, thus higher efficiency is expected. In addition, EOF allows the solute to partition between the mobile and stationary phases. Therefore, CEC becomes an alternative to MEKC

for the separation of neutral molecules, especially polycyclic aromatic hydrocarbons (PAHs) [14] and stereoisomers [15].

So far, most of the applications of CE and CEC have been focused on separations of small molecules or large biological molecules. The separation of synthetic polymers of industrial significance has been largely ignored for several reasons, such as the lack of charge and chromophore in most of the synthetic polymers together with poor aqueous solubility making the separation and detection of synthetic polymers more difficult.

In spite of the difficulties described above, there are several papers demonstrating the potential of using CE to separate synthetic polymers [16,17]. Polymer separations by electrophoretic methods fall into two broad classes: high molecular weight polymers (MW>10,000), where the sieving mechanism of molecular size separation could be effective, and oligomers in the low molecular weight range, where the high peak capacity of CE could offer an advantage over liquid chromatography. Bullock [18] reported the characterization of the oligomeric distribution of different kinds of synthetic polymers with molecular weights up to 4000 by CE. Several different separation and detection strategies were used including indirect detection, MEKC and derivatization. Poli and Schure [19] studied the separation of polystyrene sulfonates by CE using polymeric additives. By incorporating sieving media, the separation range of molecular weight of polymers extended to 1,200,000.

In this work, the separation of synthetic polymers by both CE and CEC was performed. CE separations of two kinds of non-ionic surfactants with molecular weights up to 2000 were obtained by derivatizing oligomers with phthalic anhydride. For polymers with high molecular weight, electrophoretic separation mechanism based only on the differences in charge to size ratio of oligomers was insufficient for separation. To improve the separation, size exclusion packing material was used to pack the capillary column. By incorporating size exclusion media, CEC separations of polystyrenes (PS) with molecular weight up to 641,000 were obtained. As expected, the high efficiency of CEC enables excellent separation of uncharged macromolecules, suggesting that size exclusion in CEC is potentially more desirable for neutral macromolecule separations. The effects of an organic modifier and variations in the buffer's ionic strength on the separation were examined.

MATERIALS AND METHODS

Chemicals

Brijs, Igepals, phthalic anhydride, citric acid were purchased from Aldrich (Milwaukee, WI). N,N-dimethylformamide (DMF) and acetonitrile (ACN) were purchased from Fisher Scientific (Fair Lawn, NJ). All the polystyrene (PS) standards were from Aldrich. The concentration of each PS standard is 2 mg/ml in DMF. Tris (hydroxymethyl) aminomethane (Tris) was purchased from Schwarz/Mann Biotech (Cleveland, OH).

Derivatization of Brij and Igepal Series Compounds

Brij or Igepal series compound (1.0 g) was dissolved in 2 mL acetonitrile. An amount of phthalic anhydride equivalent to 600/(average molecular weight of polymer) g was added into the solution. The hydroxyl groups were esterified at a temperature of 100 °C for 15 hours. Samples were then diluted with a mixture of acetonitrile-5 mM borate buffer (30:70) at pH=8.5 before analysis.

Preparation of Capillary Columns for CEC

A piece of fused silica capillary 42 cm l (total length) × 50 μm i.d., 375 μm o.d. was used for column packing. The first frit was made by tapping the end of the capillary into a pile of 5 μm irregular shape silica particles several times. A few silica particles were therefore forced into the column. This end of the capillary was then mounted onto a micro electric arc device [20] with the section containing the silica particles between the electrodes. The silica was sintered by a 2s discharge generated by the variable transformer. The frit was tested by flushing with methanol from both directions under 300 psi before packing. The slurry of 1 mg of 5 μm, 300 Å silica stationary phase (YMC Co., Ltd. Wimington, NC) in 1 ml methanol was sonicated before use. The column was packed in the manner similar to that used for preparing packed capillaries reported by Tomer and co-workers [21]. After the column has been packed to the desired length, the second frit at the front of the column was made using the same arcing device while keeping the pressure on. The pressure was released slowly before the

column was taken off the packing device so that the packing bed would not be disturbed. Methanol was used to flush the column from both directions to remove all the extra stationary phase inside the column. The detection window was then created adjacent to the second frit to avoid extra band broadening. The finished column was equilibrated with the running buffer for at least two hours before use.

INSTRUMENTATION

Experiments were carried out on a home-built system which consisted of a box equipped with safety interlock, a UV-visible detector (model 500 Scientific Systems Incorporated, State College, PA) and a 30 kV high voltage power supply (Spellman, Plainview, NY). All capillaries (50 μm i.d. × 375 μm o.d.) were from Polymicro Technologies (Phoenix, AZ). For the derivatized oligomer separations, the total length of the capillary used was 60 cm with a 49 cm separation distance. The detection wavelength was 205 nm for Brij series oligomers and 200 nm for Igepal series oligomers. Samples were hydrodynamically injected and separated at 25 kV. The total length of the capillary for the polystyrene standards separation is 42 cm with 31 cm packing length. The detection wavelength was set at 269 nm. Sample introduction was conducted electrokinetically.

RESULTS AND DISCUSSION

CE Analysis of Non-Ionic Surfactants:

Hydroxyl-terminated polyethers have been used intensively as non-ionic detergents and lubricants in pharmaceutical industries as well as in other fields

[22,23]. There are two major kinds of non-ionic surfactants. One is alcohol polyethoxylates (AE) and the other is alkylphenol polyethoxylates (APE), shown in Figure 1. The AE are the most important non-ionic surfactants. The hydrophilic moiety of AE is typically composed of 1 to 25 ethoxy units with an average ethoxylation number of 6-11. Because of poor degradability as well as persistent metabolites, the use of APE in household detergents has been almost entirely replaced by AE [24]. However, the low cost of APE makes it still useful in industrial applications. Since the chronic toxicity and the biodegradation rate of non-ionic surfactants depend on the length of both alkyl and polyethoxylic chains, the development of separation methods in order to obtain more insight into oligomeric distribution would be of great interest.

Non-ionic surfactants could not be separated directly by CE due to the lack of charge. In addition, the lack of chromophores for AE makes the detection even more difficult. In order to add both characteristics onto the surfactants, derivatizaton was performed using the same method as Bullock's [18]. Figure 2 shows a CE separation of a mixture of a series of derivatized Brij oligomers with molecular weight up to 2000 as a function of acetonitrile concentration in the buffer. The electropherograms show that the percentage of acetonitrile has a profound effect on the separation, mainly due to reduced EOF. The higher the percentage of acetonitrile, the slower the EOF, which results in better resolution of individual oligomers. The maximum acetonitrile composition examined was 75% (data not shown) because the electrolyte constituents were not soluble at

higher acetonitrile content. In order to further systematically study the effect of the percentage of acetonitrile on the EOF, the change of EOF under different percentages of acetonitrile was plotted as shown in Figure 3. A very steep decrease in the electroosmotic flow with increasing acetonitrile content up to 40% was observed. Further addition of organic modifier leads to a continuous, but much slower, decrease in EOF. The reason behind this observation is postulated as due to the ratio of ε/η of the running buffer in dependence with the percentage of acetonitrile. According to Schwer and Kenndlers's papers [25], there was a decrease in the ratio ε/η with increasing percentage of acetonitrile. After passing through a minimum, the curve rises again. However, different observations were reported by other groups. For example, Rozing et al [26] observed an increase in mobility with increasing ACN content using Tris, HCl 5 mM pH8 buffer. Yan et al [13] observed a decrease of mobility with increasing ACN content in a 4 mM pH9 tetraborate buffer. The real reason of these contradictory observations is still unknown.

The separation of Brij series oligomers was also studied in both phosphate and borate buffers. Interestingly, the borate buffer could reduce the EOF further than phosphate buffer even at the same ionic strength as shown in Figure 4. This is probably due to the change of the ξ potential of the capillary surface with borate buffer.

Different buffers have been used to probe the separation of Igepal series oligomers. Since these non-ionic surfactants bear UV chromophores, the detection of them are expected to be easier. However, a different separation method MEKC had been tried without any luck. At a low concentration of organic modifier (0-10% acetonitrile), the selectivity of SDS micelles is not sufficient to separate the oligomers. When the concentration of acetonitrile is increased above 30%, SDS micelles may be broken down. The SDS monomer, however, still has a strong hydrophobic interaction with the Igepal oligomers. Theoretically, the charge could be added to the Igepal oligomers through this interaction. Separation of individual oligomers is therefore predicted. Suprisingly, the results showed that the binding between solute and SDS monomer was too strong to provide any degree of selectivity with only a broad peak being observed (data not shown). The separation of Igepal oligomers was achieved, however by derivatizing the sample with phthalic anhydride and analyzing them using the same condition as that used for Brij derivatization. Figure 5 shows the separation obtained for the oligomers in Igepal CO-520 and CO-720. About 20 oligomers were observed.

CEC Separation of Polystyrene Standards:

PS has more diverse uses than any other polymers because of its excellent physical properties, ease of fabrication and low cost. The principal applications of PS include packing, appliances, construction and electronic equipment. The molecular weight of PS greatly influences its thermal,

mechanical and rheological properties. Over the past years, size exclusion chromatography (SEC) [26] has been one of the most important methods in molecular weight determination. However, the traditional pressure driven SEC suffers from a number of disadvantages, including low efficiency and large sample size requirement. In this study, the capillary was packed with a rigid packing material, 300 Å pore silica. PS were separated based on the size difference while moving through the column by EOF. In other words, the separation mechanism of size exclusion in CEC is the same as that of high performance liquid chromatography except that the propulsion power is electric field instead of pressure. Higher efficiency is expected in size exclusion in CEC due to a flat flow profile and the possibility of using longer columns.

PS is a nonpolar polymer and it is only soluble in nonpolar organic solvents. Therefore, DMF was chosen as solvent for the CEC separation. Figure 6 shows the CEC separations of five PS standards under different ionic strength (buffer indicated in figure legend). Excellent separation was achieved. The results also showed that ionic strength has a significant effect on the separation. Very poor peak shape was observed when the total ionic strength increased from 3 mM to 30 mM. The strict requirement for use of low ionic strength buffer in CEC separations is mainly to overcome bubble formation which causes the poor efficiency and unstable of CEC performance. As has been reported, bubble formation has been a notorious problem in CEC separation. It is believed that bubble formation maybe related to the joule heating generated by electrolytes

and the quality of the frits [9]. Although the formation of bubbles could be minimized [29,30] by pressuring both buffer reservoirs, the buffer is still limited to the low ionic strength.

The packed column provided an excellent calibration curve shown in Figure 7. Note that the largest PS studied 641000 g/mol was almost totally excluded from the 300 Å pores. Resolution was lost in the molecular weight range above 641,000. Toluene was the totally permeating solute.

The efficiency test of packed column shows an interesting result. For a general discussion of the effect of flow rate on plate height in SEC, the van Deemter equation can be represented by:

$$H = A + B/v + Cv$$

where v is the flow velocity. A, B, C are associated with the plate height term due to eddy diffusion, logitudinal diffusion and mass transfer respectively. Band broadening in SEC separation is controlled by the mass transfer (C term) since longitudinal effect (B term) is insignificant except for very small molecules which have very large diffusion coefficient. Therefore, instead of getting a typical van Deemter plot, the increase in plate with increasing flow rate for large molecules was observed in SEC. In the open tube CE separation, Jorgenson and Lukacs [1,31] derived the efficiency of electrophoretic system from basic principles using the assumption that diffusion is the only source of band broadening. As a result, the use of high voltage gives the high efficiency until the point where heat

dissipation is inadequate since the separation proceeds rapidly, the effect of diffusion is minimized. However, the test solute with low diffusion coefficient as PS will has little effect with the change of voltage. Taking these two factors into account, in size exclusion CEC, increase in plate height as increasing in voltage when use PS as test solutes was observed as expected. Decrease in the plate height with increasing the voltage when use toluene as a test solute in size exclusion in CEC indicates that diffusion plays an important role in the efficiency test of small molecule.

CONCLUSIONS

This research demonstrated the CE and CEC separation of uncharged macromolecules. It was found that the efficiency test of the size exclusion in CEC is a combination of CE and HPLC. The excellent separation shows that size exclusion in CEC can be applied in the analysis of neutral macromolecules. Separations are efficient and fast.

ACKNOLEDGEMENT

Funding by the National Institutes of Health (GM 38738) is gratefully acknowledged.

REFERENCES

1. Jorgenson, J. W., Lukacs, K. D. Zone Electrophoresis in Open-Tubular Galss Capillaries. *Anal. Chem*., **1981,** *53,* 1298-1302.
2. Monning, C. A., Kennedy, R. T. Capillary Electrophoresis. *Anal. Chem*., **1994,** *66*, 280R-314R.
3. Terabe, S., Otsuka, K., Ichikawa, K., Tsuchiya, A., Ando, T. Electrokinetic Separation with Micellar Solutions and Open-Tubular Capillaries. *Anal. Chem*., **1984,** *56*, 111-113.
4. Khaledi, M. G. Micelles as Separation Media in High-Performance Liquid Chromatography and High-Performance Capillary Electrophoresis: Overview and Perspective. *J. Chromatogr*., **1997,** *780,* 3-40.
5. Janini, G. M., Issaq, H. J. Micellar Electrokinetic Capillary Chromatography - Basic Considerations and Current Trends. *J. Liq. Chromatogr*., **1992,** *15*, 927-960.
6. Terabe, S., Miyashita, Y., Shibata, O., Barnhart, E. R., Alexander, L. R., Patterson, D. G., Karger, B. L., Hosoya, K., Tanaka, N. Separation of Highly Hydrophobic Compounds by Cyclodextrin-Modified Micellar Electrokinetic Chromatography. *J. Chromatogr*., **1990,** *516*, 23-31.
7. Grossman, P. D., Soane, D. S. Capillary Electrophoresis of DNA in Entangled Polymer Solutions. *J. Chromatogr*., **1991,** *559*, 257-266.
8. Strege, M., Lagu, A. Separation of DNA Restriction Fragments by Capillary Electrophoresis using Coated Fused Silica Capillaries. *Anal. Chem*., **1991,** *63*, 1233-1236.

9. Knox, J. H., Grant, I. H. Electrochromatography in Packed Tubes using 1.5 to 50 μm Silica Gels and ODS Bonded Silica Gels. *Chromatographia*, **1991,** *32*, 317-328.
10. Lloyd, D. K., Li, S., Ryan, P. Protein Chiral Selectors in Free-Solution Capillary Electrophoresis and Packed-Capillary Electrochromatography. *J. Chromatogr*., **1995,** *737,* 285-296.
11. Rebscher, H., Pyell, U. In-Column Versus On-Column Fluorescence Detection in Capillary Electrochromatography. *J. Chromatogr*., **1996,** *737,* 171-180.
12. Ding, J., Vouros, P. Capillary Electrochromatography and Capillary Electrochrormatography-Mass Spectrometry for the Analysis of DNA Adduct Mixtures. *Anal. Chem*., **1997,** *69*, 379-384.
13. Yan, C., Schaufelberger, D., Erni, F. Electrochromatography and Micro High-Performance Liquid Chromatography with 320 μm I.D. Packed Columns. *J. Chromatogr*., **1994,** *670*, 15-23.
14. Yan, C., Dadoo, R., Zhao, H., Zare, R. N. Capillary Electrochromatography: Analysis of Polycyclic Aromatic Hydrocarbons. *Anal. Chem*., **1995,** *67*, 2026-2029.
15. Lelievre, F., Yan, C., Zare, R. N., Gareil, P. Capillary Electrochromatography: Operating Characteristics and Enantiomeric Separation. *J. Chromatogr*., **1996,** *723*, 145-156.

16. Ryder, D. S. Determination of Sodium Vinyl Sulphonate in Water-Soluble Polymers using Capillary Zone Electrophoresis. *J. Chromatogr*., **1992,** *605*, 143-147.
17. Jones, H. K., Ballou, N. E. Separation of Chemically Different Particles by Capillary Electrophoresis. *Anal. Chem*., **1990,** *62*, 2484-2490.
18. Bullock, J. Application of Capillary Electrophoresis to the Analysis of the Oligomeric Distribution of Ploydisperse Polymers. *J. Chromatogr*., **1993,** *645*, 169-177.
19. Poli, J. B., Schure, M. R. Separation of Poly(styrenesulfonates) by Capillary Electrophoresis with Polymeric Additives. *Anal. Chem*., **1992,** *64*, 896-904.
20. Hoyt, A. M. Jr., Beale, S. C., Larmann, J. P. Jr., Jorgenson, J. M. Preparation and Evaluation of an Online Preconcentrator for Capillary Electrophoresis. *J. Microcol.,* **1993,** *5*, 325-330.
21. Moseley, M. A., Deterding, L. J., Tomer, K. B. Nanoscale Packed-Capillary Liquid Chromatography Coupled with Mass Spectrometry using a Coaxial Continuous-Flow Fast Atom Bombardment Interface. *Anal. Chem.,* **1991, *63,*** 1467-1473.
22. Marcomini, A., Zanette, M. Chromatographic Determination of Non-Ionic Aliphatic Surfactants of the Alcohol Polyethoxylate Type in the Environment. *J. Chromatogr*., **1996,** *733*, 193-206.
23. Garti, N., Kaufman, V. R., Aserin, A. *Nonionic surfactants: Chemical analysis. Marcel Dekker. New York*, *NY***. 1987,** Ch. 7.

24. Kiewiet, A. T., Voogt, P. de. Chromatographic Tools for Analyzing and Tracking Non-Ionic Surfactants in Aquatic Environment. *J. Chromatogr*., **1996,** 733, 185-192.

25. Schwer, C., Kenndler, E. Electrophoresis in Fused Silica Capillary-The Influence of Organic Solvents on the Electroosmotic Velocity and the Zeta-Potential. *Anal. Chem*., **1991,** *64*, 1801-1807.

26. Dittman, M. M., Rozing, G. P. Capillary Electrochromatography - a High-Efficiency Micro-Separation Techniques. *J. Chromatogr*., **1996,** *744*, 63-74.

27. Smith, C. G., Smith, P. B., Pasztor, A. J. Jr., Mckelvy, M. L., Meunier, D. M., Froelicher, S. M. Analysis of Synthetic Polymers and Rubbers. *Anal. Chem*., **1995,** *67*, 97R-126R.

28. Renn, C. N., Synovec, R. E. High-Speed and Super-Speed Size Exclusion Chromatography of Polymers for Process Analysis. *Anal. Chem*., **1988,** *60*, 200-204.

29. Smith, N. W., Evans, M. B. The Analysis of Pharmaceutical Compounds using Electrochromatography. *Chromatographia,* **1994,** *38*, 649-657.

30. Behnke, B., Grom, E., Bayer, E. Evaluation of the Parameters Determining the Performance of Electrochromatography in Packed Capillary Columns. *J. Chromatogr*., **1995,** *716*, 207-213.

31. Jorgenson, J. W., Lukacs, K. D. Free-Zone Electrophoresis in Glass Capillaries. *Clin. Chem*., **1981,** *27*, 1551-1553.

Figure1. Structures of polymeric compounds analyzed in this work.

Figure 2. Effect of the addition of acetonitrile on the CE separation of Brij series oligomers. Buffer: (A) 0%, (B) 30%, (C) 50% (v/v) acetonitrile in 60 mM, pH=9.5 borate; detection at 205 nm; 63 cm capillary (50 μm i.d.) with injection to detection length of 51.5 cm; separation voltage: 25 kV; hydrodynamic injection time: 7 s.

Figure 3. Effect of the percentage of acetonitrile on the electroosmotic flow.
Experimental conditions as in Figure 2.

Figure 4. Effect of the ionic strength on the electroosmotic flow.
50% (v/v) acetonitrile in pH=8.5 borate and phosphate buffers. Other experimental conditions as in Figure 2.

Figure 5. CE separation of Igepal CO-520 and CO-720 oligomers.
Buffer: 50% (v/v) acetonitrile in 60 mM, pH=9.5 borate; detection at 200 nm; 63 cm capillary (50 μm i.d.) with injection to detection length of 51.5 cm; separation voltage: 25 kV; hydrodynamic injection time: 10 s.

Figure 6. The effect of ionic strength on the CEC separation of polystyrene standards.

Buffer: (A) 2mM Tris, 1 mM citric acid, (B) 10 mM Tris, 5 mM Citric acid (C) 20 mM Tris 10 mM Citric acid in DMF; detection at 269 nm; 42 cm capillary (50 μm i.d.) with packed injection to detection length of 31 cm; separation voltage 20 kV; electrokinetic injection at 20 kV for 3 s. Peak number is as follows: 1 = 641,000, 2 = 212,000, 3 = 44,000, 4 = 18,000, 5 = 3700, 6 = toluene.

Figure 7. Calibration curve for polystyrene standards.

Buffer: 2 mM Tris, 1 mM citric acid in DMF; separation voltage 20 kV. Other experimental conditions as in Figure 5.

Figure 8. The effect of voltage on the efficiency of the packed column.

Buffer: 2 mM Tris, 1 mM citric acid in DMF. Other experimental conditions as in Figure 5.

1. Brij Series Oligomers (AE)

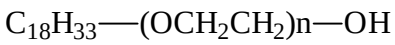

2. Igepal Series Oligomers (APE)

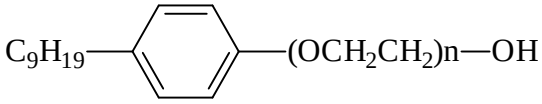

3. Polystyrene

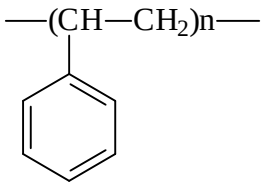

Figure 1

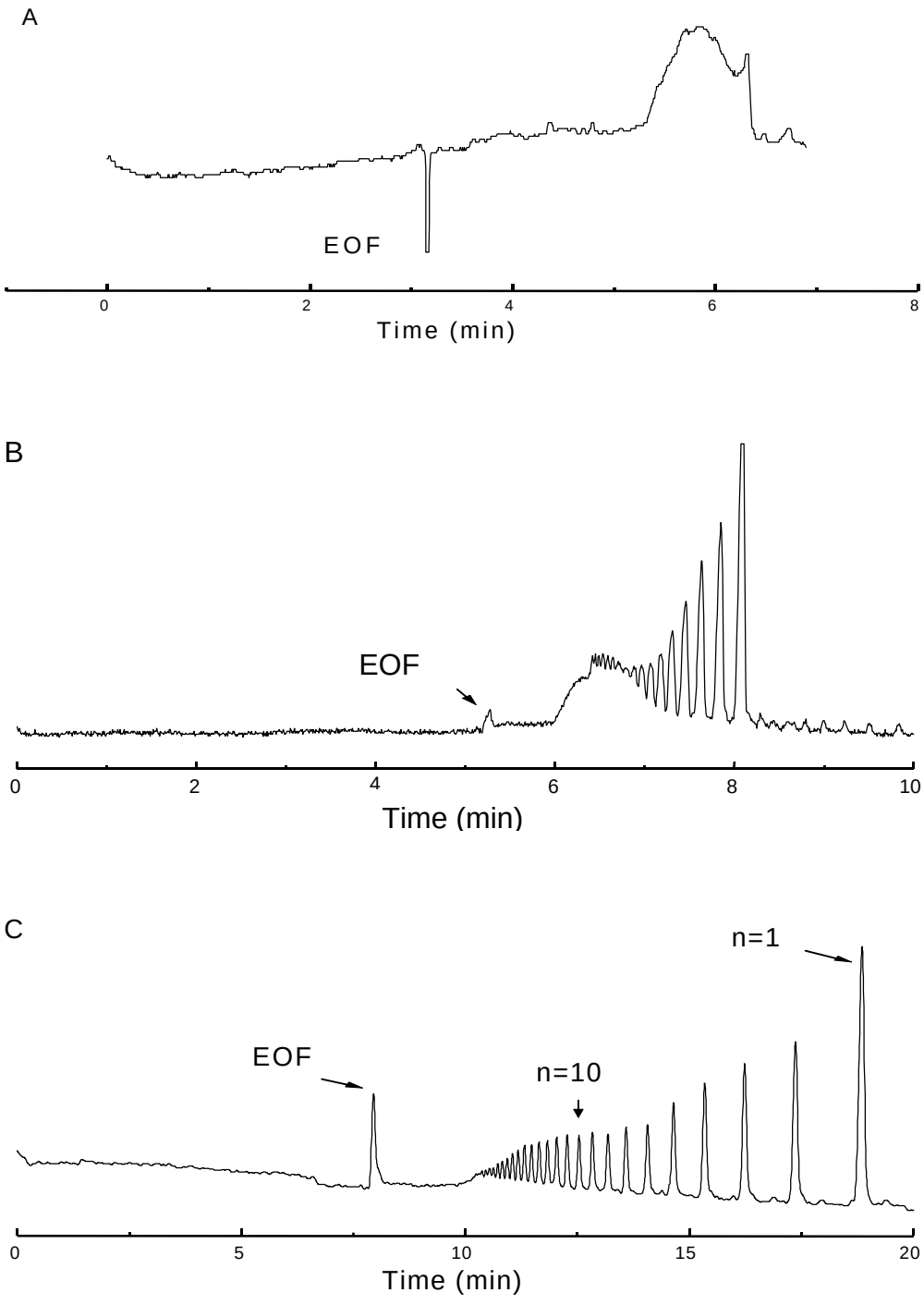
A
EOF
0
2
4
6
8
Time (min)
B
EOF
0
2
4
6
8
10
Time (min)
C
n=1
EOF
n=10
0
5
10
15
20
Time (min)

Figure 2

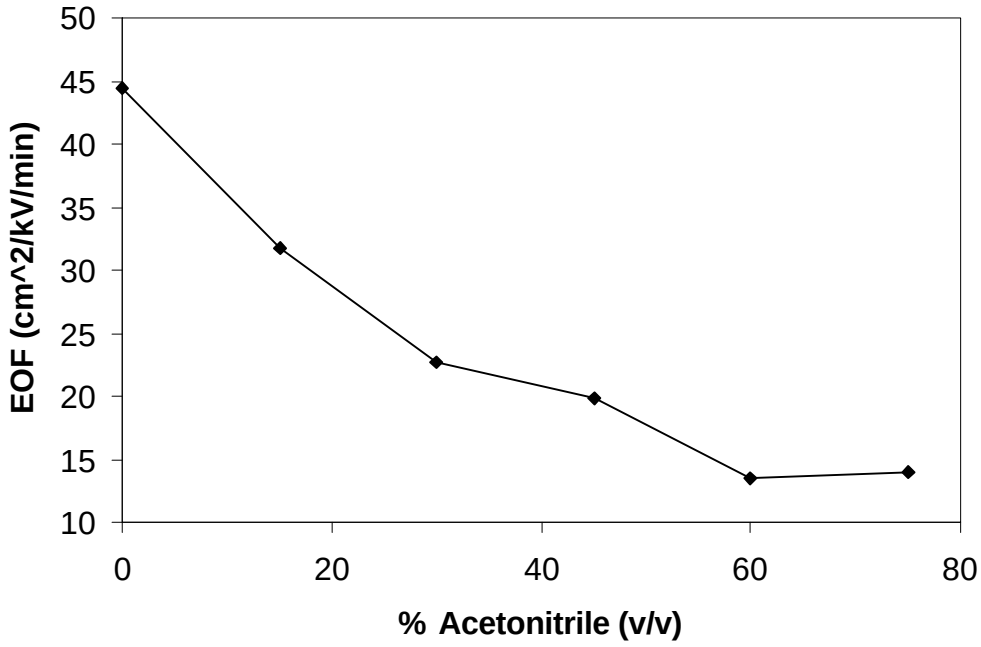
50
45
40
35
30
25
20
15
10
EOF (cm^2/kV/min)
0
20
40
60
80
% Acetonitrile (v/v)

Figure 3

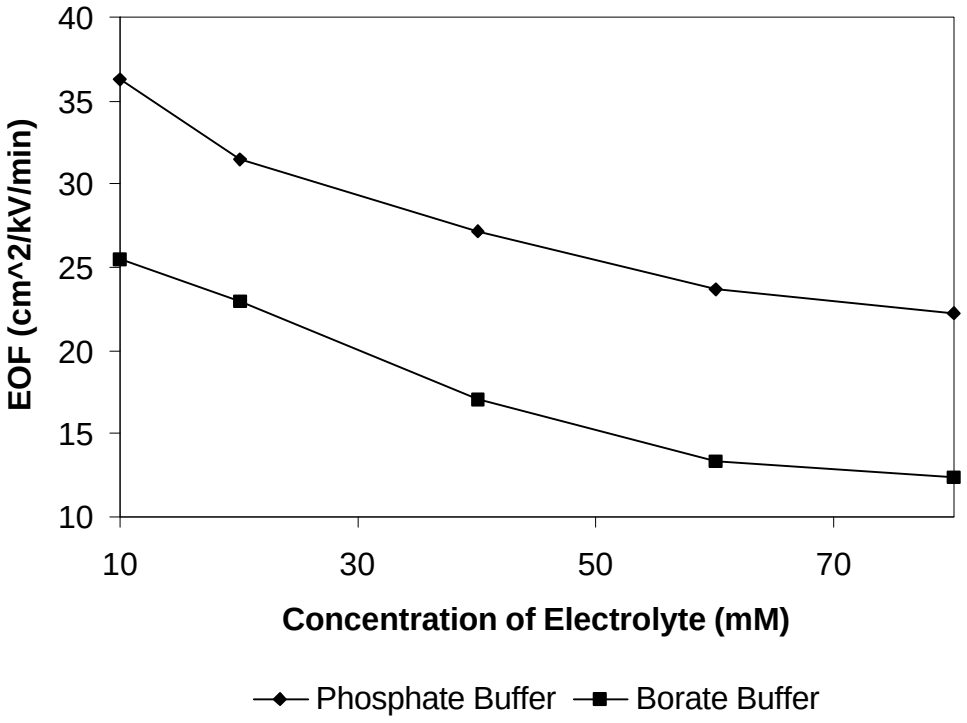
40
35
30
25
20
15
10
EOF (cm^2/kV/min)
10
30
50
70
Concentration of Electrolyte (mM)
Phosphate Buffer
Borate Buffer

Figure 4

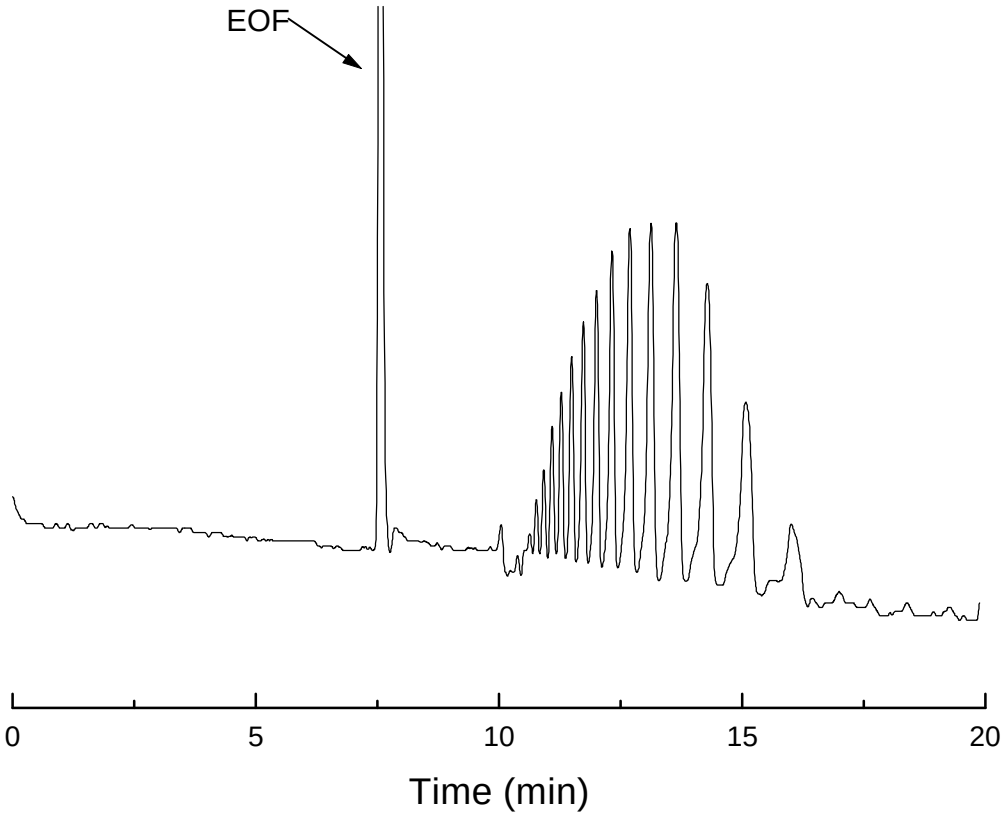

Figure 5

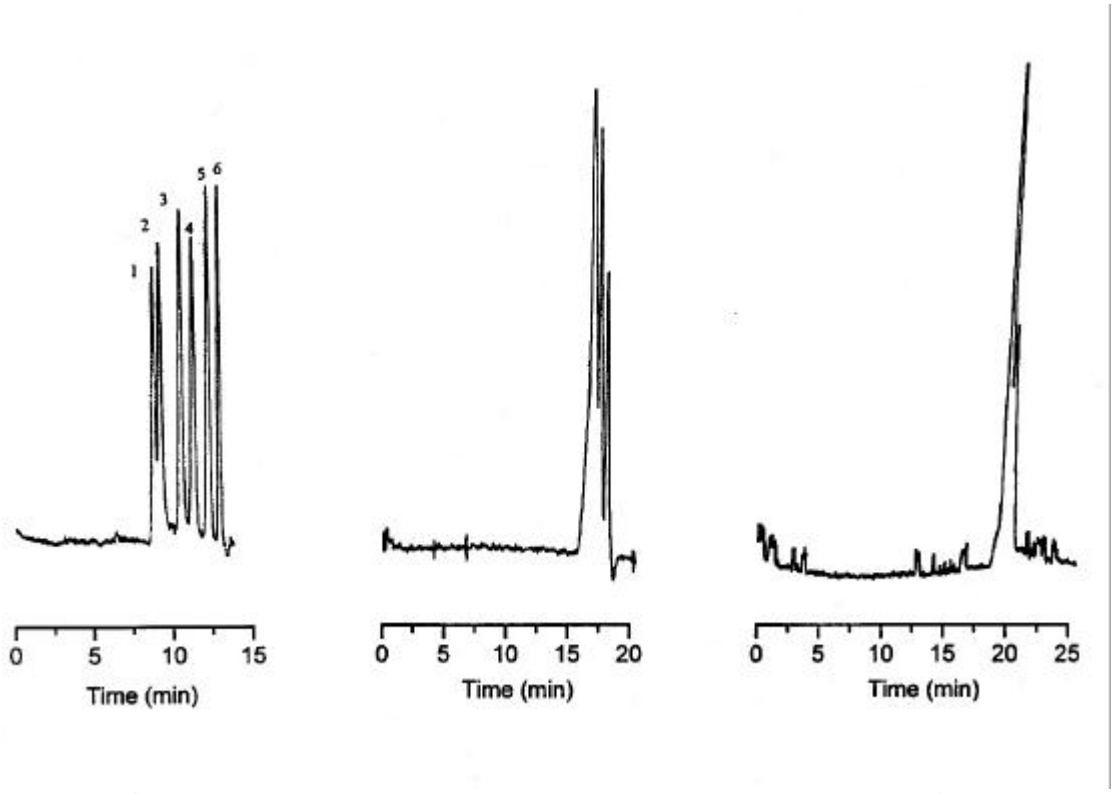
1
2
3
4
5
6
0 5 10 15
Time (min)
0 5 10 15 20
Time (min)
0 5 10 15 20 25
Time (min)

A B C

Figure 6

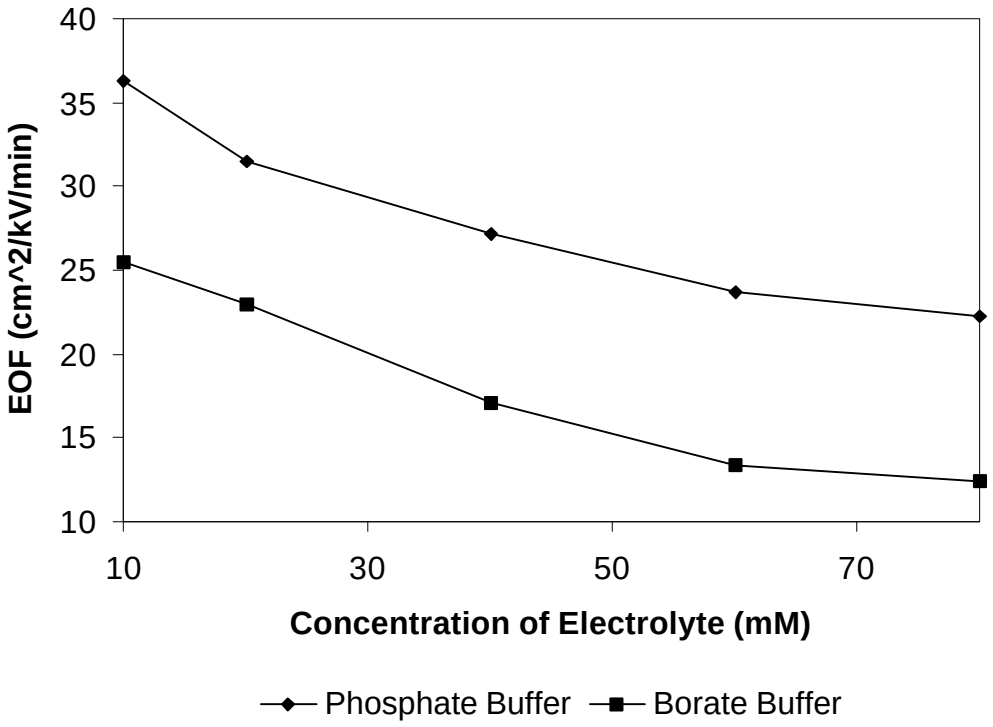
40
35
30
25
20
15
10
EOF (cm^2/kV/min)
10
30
50
70
Concentration of Electrolyte (mM)
Phosphate Buffer
Borate Buffer

Figure 7

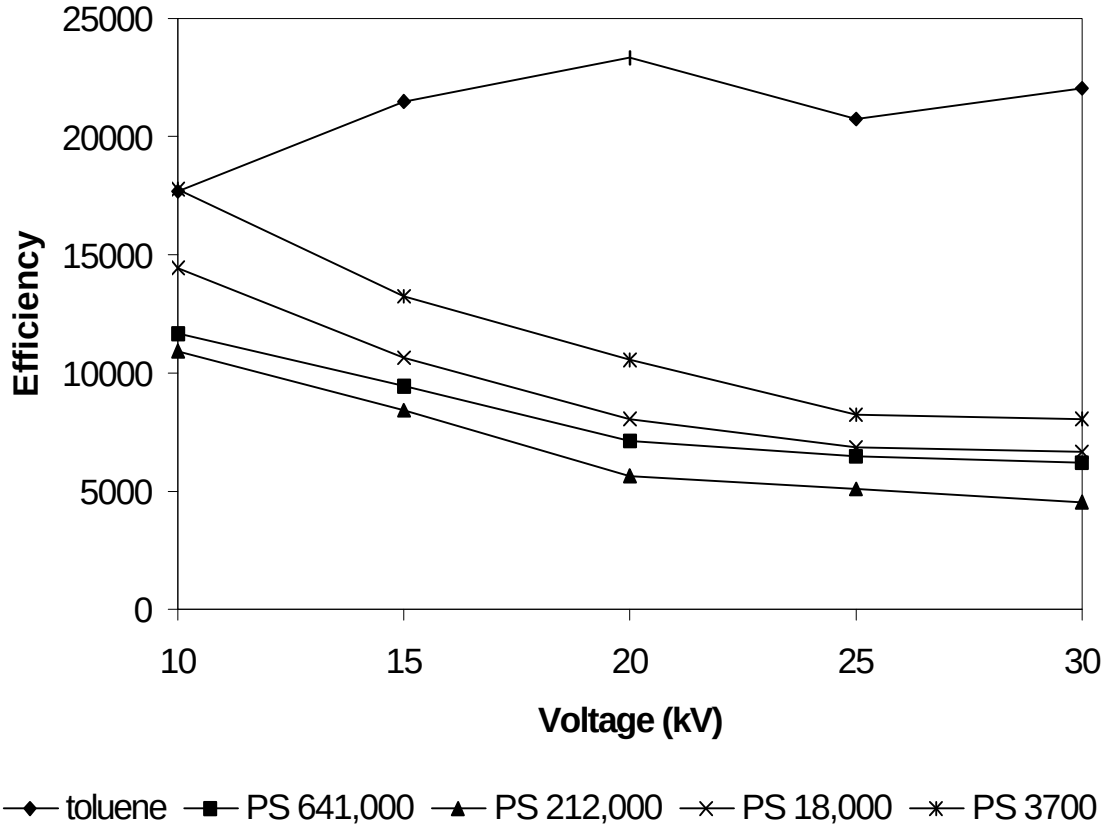
25000
20000
15000
10000
5000
0
Efficiency
10
15
20
25
30
Voltage (kV)
toluene
PS 641,000
PS 212,000
PS 18,000
PS 3700

Figure 8